NTNU
Innovation and Creativity

Advanced leak detection in oil and gas pipelines using a nonlinear observer and OLGA models

Espen Hauge

Master of Science in Engineering Cybernetics
Submission date: June 2007
Supervisor: Ole Morten Aamo, ITK

Norwegian University of Science and Technology
Department of Engineering Cybernetics

Problem Description

The subject originates from the requirement of monitoring pipelines carrying oil and gas. Statoil operates several pipelines, for instance between Kollsnes and Mongstad. A system for supervision of these pipelines is imposed by the authorities. This system must incorporate a thorough model, enabling among others Mongstad to predict the production rate and detect leakages. The thesis is based on earlier submitted projects and theses where methods of detecting leaks have been tested under nominal conditions with a simplified model. That is why this thesis shall focus on proper modelling and robustness with regard to modelling error and biased measurements. The thesis is performed in collaboration with Statoil's R&D center at Rotvoll. The following subjects are to be considered:

1. Outline earlier work done in the special field of leak detection and motivate for further work.
2. Define a one-phase flow in a straight, horizontal pipeline (should be a fairly simple case to ease debugging), and implement with OLGA. The earlier constructed Matlab observer should be tested with data from OLGA and compared with an observer designed in OLGA. Cases with both stationary and non-stationary flow should be tested.
3. Document the procedure of setting up an OLGA observer.
4. Test the leak detection system constructed with OLGA with data produced with OLGA and where there are no modelling errors. (The observer should be an exact copy of the model.) Performance with both stationary and non-stationary flow should be examined. How does this compare to earlier results?
5. Design an OLGA observer for a pipeline with varying altitude and commit similar tests as above.
6. Define and carry out a systematic study of robustness with regard to modelling errors and biased measurements with stationary boundary conditions.
a. The modelling error should originate from a set of chosen parameters, and the observer should consist of fewer segments than the model.
b. Details regarding biased measurements are provided by Statoil.
7. Make suggestions for further work – consider the possibility of developing a leak detection system for two-phase flow.
8. Write a conference article to NOLCOS 2007 (7th IFAC Symposium on Nonlinear Control Systems)
9. Write a journal article to SPE Journal.

Assignment given: 08. January 2007
Supervisor: Ole Morten Aamo, ITK

Summary

An adaptive Luenberger-type observer with the purpose of locating and quantifying leakages is presented. The observer only needs measurements of velocity and temperature at the inlet and pressure at the outlet to function. The beneficial effect of output injection in form of boundary conditions is utilized to ensure fast convergence of the observer error. This approach is different from the usual practice where output injection might appear as a part of the PDE's. This makes it possible to employ OLGA, which is a state of the art computational fluid dynamics simulator, to govern the one-phase fluid flow of the observer. Using OLGA as a base for the simulations introduces the possibility to incorporate temperature dynamics in the simulations which in previous work was impossible. The observer is tested with both a straight, horizontal pipeline and an actual, long pipeline with difference in altitude. Both simulations with oil and gas are carried out and verification of the robustness of the observer is emphasized. In order to cope with modelling errors and biased measurements, estimation of roughness in the monitored pipeline is introduced.

Preface

This work is the result of the Master of Science thesis performed at the department of engineering cybernetics at the Norwegian University of Science and Technology (NTNU) during the period from January '07 until June '07. The thesis is a collaboration between NTNU and Statoil R&D, department of process control, at Rotvoll, Trondheim.

I would like to thank my advisor at Statoil, John-Morten Godhavn, and especially my advisor at NTNU, Ole Morten Aamo.

Contents

List of Figures

List of Tables

Chapter 1

Introduction

Leak detection based on dynamic modelling is a propitious approach in the special field of leak quantification and location. This report documents one of the first real steps toward a new method of pipeline monitoring. A state of the art multiphase simulator is manipulated through Matlab to work as an adaptive Luenberger-type observer which uses measurements from the supervised pipeline as well as internal measurements. This observer is capable of handling modelling errors and disturbances, as opposed to open-loop observers, due to the use of output injection and estimation of friction. Since the only measurements fed into the observer are pressure and velocity measurements from the inlet and outlet, which in most cases already are available, the method can be used with most existing pipelines without extra instrumentation. Also, the computational fluid dynamics simulator, which is the backbone of the observer, is a widely used one, namely OLGA.[1] Many of the existing pipelines have already been modeled in OLGA which can be exploited in the construction of the observer.

The benefits of a leak detection system able of locating the position of the leak within a quantified tolerance are obviously of an environmental kind. But the economical aspect of it is also important since it may be the determining factor when new technology is taken into practice. Another advantage of this kind of method would be that it under some circumstances can be used after a leak has been detected and the pipeline has been shut down. This is possible by logging the relevant measurements and running simulations with the observer with the stored model data. It is also be possible to have multiple observers with different tuning and starting point monitoring a pipeline during operation.

The work done in this thesis is based on the previous work done in (Hauge, 2006) where the pipeline flow was simulated by a Matlab model based on two coupled one dimensional first order nonlinear hyperbolic partial differential equations. This model is recapitulated in the theory section, and also mentioned in the method section for the

[1] OLGA is developed by IFE, Sintef, Statoil and Scandpower Petroleum Technology

sake of the reader. The update laws of the observer are based on this model and are strictly heuristic.

Whereas the previous computational fluid dynamics simulator written in Matlab did not incorporate an energy equation or support pipelines with difference in altitude, OLGA is thoroughly tested for one-, two- and three-phase flow in pipeline with altitude differences. This adds a new dimension to the simulations which can be conducted more realistically than before. An example of this is the observer designed and tested for the Tor 1 pipeline, which is an existing pipeline in the North Sea carrying oil. Also, an observer is constructed and tested for a horizontal pipeline with one-phase flow of oil and gas.

The estimates of leak magnitude and location are based on measurements from the inlet and outlet of the monitored model as well as internal measurements. This makes the observer prone to errors such as drifting, noise and biases. And, as with all observers, there will always be some sort of modelling error. In order to cope with these problems, adaption of the roughness in the pipeline is carried out, and the effects of some of the possible errors in the observers are presented in a robustness study.

The body of the report is of the conservative type where a short study of relevant previous work is presented in the next chapter and then followed by a short introduction of the fundamental theory. The chapter concerning the methods applied, includes information on the Matlab observer, how to construct an OLGA observer and the necessary explanation for the reader to examine the results. The succeeding chapter deals with the results which are discussed in detail in its own chapter. The thesis is rounded off by suggestions for further work and conclusions.

Chapter 2

Previous work

Over the last forty years a lot of effort has been put into the special field of leak detection. Many different approaches has been taken and lately the most popular one has been software based where acquisition and advanced processing of measurements along the pipeline helps identify and classify a leak. These methods often incorporates mass balances, momentum balances, pressure signatures of transitions from no-leak to leak and dynamic modelling. The better part of the research concerning leak detection involves pressure signatures in some way. In (Ming and Wei-qiang, 2006) a wavelet algorithm is used to detect pressure waves caused by the transition from the state of no-leak to leak and the registered time instances is used to compute the position of the leak. A more sophisticated approach is taken in (Feng et al., 2004) where both pressure gradients and negative pressure waves are combined with fuzzy logic to detects faults. A different scheme of identifying leaks can be seen in (Hu et al., 2004) where principal component analysis, which is a technique used in computerized image recognition, is applied to filter out negative pressure waves caused by a bursted pipeline. The research done in (Emara-Shabaik et al., 2002) focuses on using a modified extended Kalman filter in conjunction with feed forward computations to anticipate the leak magnitude. A bank of leak mode filters is established and decision logic is introduced to isolate the leak. This method is somewhat similar to the one introduced in (Verde, 2001) where N discretized models of the pipeline consisting of N nodes makes up a bank of observers. In case of a leak all but one observer will react and this single observer yields the position of the leak. In (Billmann and Isermann, 1987) a dynamic model is used as a observer with friction adaption. When a leak occurs the observer differs from the process and a correlation technique is applied to detect, quantify and locate the leak.

The work done in (Hauge, 2006) was founded on previous work from (Aamo et al., 2005) and (Nilssen, 2006) and treats the performance of leak detection with time varying boundary conditions. A model and an adaptive Luenberger observer based on a set of two coupled one dimensional first order nonlinear hyperbolic partial differential equations were implemented in Matlab and leak detection during cases such as shut

down were tested with satisfying results. This motivated for further work with a more exact computational fluid dynamics simulator which is obtained by using OLGA as both model and observer.

Chapter 3

Theory

This chapter is meant as a brief introduction. For a more thorough discussion regarding the mathematical model, it is recommended to consult (Aamo et al., 2005) and (Nilssen, 2006) which contains the derivation of the physical model, the characteristic model and the observer. (Aamo et al., 2005) also contains a Lyapunov analysis of a linearized version of the observer error, proving it to be exponentially stable at the origin. Some of the following equations were first presented in (Aamo et al., 2005) and were recited in (Hauge, 2006). They are also given in this report, some slightly modified, for the sake of completeness. There has been added sections on adaption of friction coefficients and OLGA related material.

3.1 Mathematical Model used in Matlab

The model is a set of two coupled one-dimensional first order nonlinear hyperbolic partial differential equations which are valid for isothermal pipeline flow of a Newtonian fluid. The physical model is based on conservation laws and can be transformed into a characteristic form which simplifies the numerical solution of the PDE.

3.1.1 Physical Model

For liquid flow in a pipe the mass conservation is

$$\frac{\partial p}{\partial t} + u\frac{\partial p}{\partial x} + \rho c^2 \frac{\partial u}{\partial x} = 0, \tag{3.1}$$

and the momentum conservation is

$$\frac{\partial u}{\partial t} + u\frac{\partial u}{\partial x} + \frac{1}{\rho}\frac{\partial p}{\partial x} = 0, \tag{3.2}$$

for $(x,t) \in [0,\, L] \times [0,\, \infty)$, and where $u(x,t)$ is flow velocity and $p(x,t)$ is pressure. The density $\rho(x,t)$ is modeled as

$$\rho = \rho_{ref} + \frac{p - p_{ref}}{c^2}. \tag{3.3}$$

This can be written in a more compact form by using the matrix

$$\bar{A}(p,u) = \begin{bmatrix} u & k+p \\ \frac{c^2}{k+p} & u \end{bmatrix}, \tag{3.4}$$

where c is the speed of sound, $k = c^2\rho_{ref} - p_{ref}$. p_{ref} and ρ_{ref} are reference pressure and the density at this pressure respectively. It must be emphasized that c is a constant depending on the fluid in the pipeline. The system can now be written more conveniently as

$$\frac{\partial}{\partial t}\begin{bmatrix} p \\ u \end{bmatrix} + \bar{A}(p,u)\frac{\partial}{\partial x}\begin{bmatrix} p \\ u \end{bmatrix} = 0. \tag{3.5}$$

The boundary conditions of the pipe are

$$u(0,t) = u_0(t) \tag{3.6}$$

$$p(L,t) = p_L(t) \tag{3.7}$$

and in (Aamo et al., 2005) found to yield $p_L = \bar{p}$ and $u_0 = \bar{u}$ where $(\bar{p}, \bar{u})$ are the steady state solution of (3.5). Also the eigenvalues of $\bar{A}$ were found to be

$$\lambda_1 = u - c,\ \lambda_2 = u + c, \tag{3.8}$$

which under the assumption $u \ll c$, are distinct and satisfy

$$\lambda_1 < 0 < \lambda_2. \tag{3.9}$$

The system is therefore strictly hyperbolic.

3.1.2 Characteristic Form

Transformation of the physical model over to characteristic form is done by applying a change of coordinates given by

$$\alpha(p,u) = c\ln\left(\frac{k+p}{k+\bar{p}}\right) + u - \bar{u}, \tag{3.10}$$

$$\beta(p,u) = -c\ln\left(\frac{k+p}{k+\bar{p}}\right) + u - \bar{u}, \tag{3.11}$$

which is defined for all physical feasible p and u. The inverse transformation is given by

$$p(\alpha,\beta) = (k+p)\exp\left(\frac{\alpha-\beta}{2c}\right) - k, \tag{3.12}$$

$$u(\alpha,\beta) = \bar{u} + \left(\frac{\alpha+\beta}{2}\right). \tag{3.13}$$

Notice that the fixed point $(\bar{p}, \bar{u})$ corresponds to $(0, 0)$ in the new coordinates. The time derivative of (3.10)-(3.11) is

$$\frac{\partial \alpha}{\partial t} = c\frac{\frac{\partial p}{\partial t}}{k+p} + \frac{\partial u}{\partial t}, \tag{3.14}$$

$$\frac{\partial \beta}{\partial t} = -c\frac{\frac{\partial p}{\partial t}}{k+p} + \frac{\partial u}{\partial t}. \tag{3.15}$$

Replacing $\frac{\partial p}{\partial t}$ and $\frac{\partial u}{\partial t}$ from (3.5) yields

$$\frac{\partial \alpha}{\partial t} = -(u+c)\frac{\partial \alpha}{\partial t}, \tag{3.16}$$

$$\frac{\partial \beta}{\partial t} = -(u-c)\frac{\partial \beta}{\partial t}. \tag{3.17}$$

By using (3.13), this can be written as

$$\frac{\partial \alpha}{\partial t} + \left(\bar{u} + c + \frac{\alpha+\beta}{2}\right)\frac{\partial \alpha}{\partial x} = 0, \tag{3.18}$$

$$\frac{\partial \beta}{\partial t} + \left(\bar{u} - c + \frac{\alpha+\beta}{2}\right)\frac{\partial \beta}{\partial x} = 0. \tag{3.19}$$

The boundary conditions in the characteristic form are obtained from (3.12)-(3.13), which give

$$\alpha(0,t) + \beta(0,t) = 0, \tag{3.20}$$

$$\alpha(L,t) - \beta(L,t) = 0. \tag{3.21}$$

3.1.3 Observer Design

For the physical model mentioned in the above section, the input signals to the pipeline is $u_0(t)$ and $p_L(t)$ and not the usual choke openings. For the observer design a copy of the plant is needed and (3.5) provides the dynamics

$$\frac{\partial}{\partial t}\begin{bmatrix}\hat{p}\\ \hat{u}\end{bmatrix} + \bar{A}(\hat{p},\hat{u})\frac{\partial}{\partial x}\begin{bmatrix}\hat{p}\\ \hat{u}\end{bmatrix} = 0 \tag{3.22}$$

with boundary conditions

$$\hat{u}(0,t) = u_0(t), \tag{3.23}$$

$$\hat{p}(L,t) = p_L(t). \tag{3.24}$$

In (Aamo et al., 2005) output injection is proposed as a method to get better convergence properties for this Luenberger-type observer. Without applying output injection, convergence is already guaranteed when the process is operated at asymptotically stable

fixed points. But by choosing different boundary conditions for the observer, represented in transformed coordinates as

$$\frac{\partial\hat{\alpha}}{\partial t}+\left(\bar{u}+c+\frac{\hat{\alpha}+\hat{\beta}}{2}\right)\frac{\partial\hat{\alpha}}{\partial x}=0, \tag{3.25}$$

$$\frac{\partial\hat{\beta}}{\partial t}+\left(\bar{u}-c+\frac{\hat{\alpha}+\hat{\beta}}{2}\right)\frac{\partial\hat{\beta}}{\partial x}=0, \tag{3.26}$$

it is possible to get faster convergence. Using output injection is done by changing the boundary conditions so that they incorporate measurements of its own boundaries as well as the ones of the model. In (Aamo et al., 2005) the following boundary conditions were proven to give faster convergence.

$$\hat{\alpha}(0,t)=\alpha(0,t)-k_0\big(\beta(0,t)-\hat{\beta}(0,t)\big), \tag{3.27}$$

$$\hat{\beta}(L,t)=\beta(L,t)-k_L\big(\alpha(L,t)-\hat{\alpha}(L,t)\big), \tag{3.28}$$

where

$$|k_0|\leq 1 \quad \text{and} \quad |k_L|<1. \tag{3.29}$$

By defining the observer error as $\tilde{\alpha}=\alpha-\hat{\alpha}$ and $\tilde{\beta}=\beta-\hat{\beta}$ and the boundary conditions can be rewritten as

$$\tilde{\alpha}(0,t)=k_0\tilde{\beta}(0,t), \tag{3.30}$$

$$\tilde{\beta}(L,t)=k_L\tilde{\alpha}(L,t). \tag{3.31}$$

In physical coordinates, the observer can be summed up as

$$\frac{\partial\hat{p}}{\partial t}+\hat{u}\frac{\partial\hat{p}}{\partial x}+(k+\hat{p})\frac{\partial\hat{u}}{\partial x}=0, \tag{3.32}$$

$$\frac{\partial\hat{u}}{\partial t}+\frac{c}{k+\hat{p}}\frac{\partial\hat{p}}{\partial x}+\hat{u}\frac{\partial\hat{u}}{\partial x}=0, \tag{3.33}$$

with boundary conditions

$$\hat{u}(0,t)=u(0,t)+c\frac{1-k_0}{1+k_0}\ln\left(\frac{k+p(0,t)}{k+\hat{p}(0,t)}\right), \tag{3.34}$$

$$\hat{p}(L,t)=(k+p(L,t))\times\exp\left(\frac{k_L-1}{c(1+k_L)}\big(u(L,t)-\hat{u}(L,t)\big)\right)-k. \tag{3.35}$$

Later in this thesis, the boundary conditions mentioned above will be applied to an observer based on a different mathematical model, namely the one used in OLGA. Details regarding the modelling of this computational fluid dynamics simulator are unknown, but it is expected that it is far more complicated. It also incorporates an energy equation and takes into account the effect of gravity. Due to this difference in modelling, it is not guaranteed that the OLGA observer will inherit the beneficial effect the boundary conditions (3.34)-(3.35) involve.

3.1.4 Adaption of friction coefficient

A friction coefficient can be added to the physical model (3.1)-(3.2) by introducing f which in (Schetz and Fuhs, 1996) is given by

$$\frac{1}{\sqrt{f}} = 1.8 \log_{10} \left[\left(\frac{\epsilon/D}{3.7} \right)^{1.11} + \frac{6.9}{\mathrm{Re}_d} \right], \tag{3.36}$$

where ϵ/D represents the relative roughness and Re_d is the Reynolds number defined as

$$\mathrm{Re}_d = \frac{\rho u D}{\mu}, \tag{3.37}$$

where μ is fluid viscosity. An uncertainty in the friction coefficient can be counted for by introducing a constant Δ. The mass balance would now be the same as earlier, namely

$$\frac{\partial p}{\partial t} + u\frac{\partial p}{\partial x} + \rho c^2 \frac{\partial u}{\partial x} = 0, \tag{3.38}$$

and the momentum conservation is changed to

$$\frac{\partial u}{\partial t} + u\frac{\partial u}{\partial x} + \frac{1}{\rho}\frac{\partial p}{\partial x} = -(1+\Delta)\frac{f}{2}\frac{|u|u}{D}, \tag{3.39}$$

where D is the diameter of the pipe. The observer with output injection and adaption of the constant Δ is then

$$\frac{\partial \hat{p}}{\partial t} + \hat{u}\frac{\partial \hat{p}}{\partial x} + (k+\hat{p})\frac{\partial \hat{u}}{\partial x} = 0, \tag{3.40}$$

$$\frac{\partial \hat{u}}{\partial t} + \frac{c}{k+\hat{p}}\frac{\partial \hat{p}}{\partial x} + \hat{u}\frac{\partial \hat{u}}{\partial x} = -(1+\hat{\Delta})\frac{\hat{f}}{2}\frac{|\hat{u}|\hat{u}}{D}, \tag{3.41}$$

with boundary conditions (3.34)-(3.35). The parameter update law from (Aamo et al., 2005) is heuristic and chosen as

$$\dot{\hat{\Delta}}(t) = -\kappa_\Delta \big(\tilde{\alpha}(L,t) + \tilde{\beta}(0,t) \big), \tag{3.42}$$

where κ_Δ is a strictly positive constant.

3.1.5 Leak Detection

By adding friction and a leak to the physical model (3.1)-(3.2) and setting $\Delta = 0$, the following equations are obtained. The mass balance

$$\frac{\partial p}{\partial t} + u\frac{\partial p}{\partial x} + (k+p)\frac{\partial u}{\partial x} = -\frac{c^2}{A} f_l(x,t), \tag{3.43}$$

and the momentum conservation

$$\frac{\partial u}{\partial t} + u\frac{\partial u}{\partial x} + \frac{c^2}{(k+p)}\frac{\partial p}{\partial x} = -\frac{f}{2}\frac{|u|u}{D} + \frac{1}{A}\frac{c^2 u}{(k+p)}f_l(x,t). \tag{3.44}$$

The leak $f_l(x,t)$ is a point leak and is selected as

$$f_l(x,t) = w_l\delta(x - x_l)H(t - t_l), \tag{3.45}$$

where w_l is the magnitude of the leak, x_l the position of the leak and t_l is the time instance when the leak occurs. δ denotes the Dirac distribution

$$\delta(x) = \begin{cases} \infty & \text{if} \quad x = 0 \\ 0 & \text{if} \quad x \neq 0 \end{cases} \tag{3.46}$$

$H(t)$ denotes the Heaviside step function

$$H(t) = \int_0^t \delta(\tau)\,\mathrm{d}\tau. \tag{3.47}$$

The observer can now be written as

$$\frac{\partial \hat{p}}{\partial t} + \hat{u}\frac{\partial \hat{p}}{\partial \hat{x}} + (k+\hat{p})\frac{\partial \hat{u}}{\partial \hat{x}} = -\frac{c^2}{A}\hat{w}_l\delta(x - \hat{x}_l), \tag{3.48}$$

$$\frac{\partial \hat{u}}{\partial t} + \hat{u}\frac{\partial \hat{u}}{\partial \hat{x}} + \frac{c^2}{(k+\hat{p})}\frac{\partial \hat{p}}{\partial \hat{x}} = -\frac{f}{2}\frac{|\hat{u}|\hat{u}}{D} + \frac{1}{A}\frac{c^2\hat{u}}{(k+\hat{p})}\hat{w}_l\delta(x - \hat{x}_l), \tag{3.49}$$

which incorporates estimates of the leak magnitude and position, $\hat{w}_l$ and $\hat{x}_l$. Notice that the Dirac distribution δ, in this case is only dependent on x since $\hat{w}_l$ is to be adapted. The parameter update laws are heuristic and are in (Aamo et al., 2005) chosen as

$$\dot{\hat{w}}_l(t) = \kappa_w\left(\tilde{\beta}(0,t) - \tilde{\alpha}(L,t)\right), \tag{3.50}$$

$$\dot{\hat{x}}_l(t) = -\kappa_x\varphi_{\alpha\beta}|\varphi_{\alpha\beta}|^{\frac{1}{\gamma}-1}, \tag{3.51}$$

where

$$\varphi_{\alpha\beta}(t) = \tilde{\alpha}(L,t) + \tilde{\beta}(0,t) \tag{3.52}$$

and κ_w, κ_x and γ are strictly positive constants.

3.1.6 Remodelling the leak

In the simulations discussed in (Aamo et al., 2005) and (Nilssen, 2006), the leak magnitude is assumed to be constant. This is a valid approximation under the assumption that the system is in a steady state and that the leak has been present long enough to stabilize. But this approximation will not hold at the time the leak occurs since the

pressure will start varying as well as the mass rate going out at the point of the leak. During a shut-down the pressure at the leak will eventually converge to the ambient pressure as the mass flow through the pipeline stops and the system reaches an equilibrium. To cope with this, the leak is remodeled as a pressure- and density-dependent function. This approach makes it possible to estimate a constant rather than a time varying function. This will be further explained in the following.

Instead of estimating the mass rate, the leak is modeled as a valve with a $C_d A_{opening}$-term which is the target of the estimation. The valve equation from (White, 2003, page 13) yields

$$q(p_l, \rho_l) = C_d A_{opening} \sqrt{\frac{(p_l - p_l^{\text{amb}})}{\rho_l}}, \tag{3.53}$$

where q is the volume rate in m^3/s, C_d is the discharge coefficient, $A_{opening}$ is the area of the hole in the pipeline, ρ_l is the density of oil or gas found from (3.3), p_l is the pressure inside the pipeline at the point of the leak and p_l^{amb} is the pressure of the surroundings of the pipeline at the leakage. Multiplying (3.53) with ρ_l the following equation for mass rate in kg/s is obtained

$$w_l(p_l, \rho_l) = C_d A_{opening} \sqrt{(p_l - p_l^{\text{amb}})\rho_l}. \tag{3.54}$$

For simplicity's sake, lets define $C_v = C_d A_{opening}$ so that the target of estimation now is C_v instead and use (3.3) to get rid of ρ_l. This yields

$$w_l(p_l) = \frac{C_v}{c} \sqrt{(k + p_l)(p_l - p_l^{\text{amb}})}, \tag{3.55}$$

and similarly for the observer

$$\hat{w}_l(\hat{C}_v, \hat{p}_l, \hat{p}_l^{\text{amb}}) = \frac{\hat{C}_v}{c} \sqrt{(k + \hat{p}_l)(\hat{p}_l - \hat{p}_l^{\text{amb}})}. \tag{3.56}$$

Notice that (3.56) is dependent on $\hat{p}_l^{\text{amb}}$ since the ambient pressure along the pipeline may change with the position of the estimated leak when there is a difference in altitude along the pipeline, whereas p_l^{amb} on the other hand, is constant.

Since the update laws proposed in (Aamo et al., 2005) are heuristic and estimating leak magnitude and C_v has a similar physical effect on the system, the same update law used for $\dot{\hat{w}}_l$ in (3.50) can be re-used for $\dot{\hat{C}}_v$. That is,

$$\dot{\hat{C}}_v(t) = \kappa_C \left(\tilde{\beta}(0, t) - \tilde{\alpha}(L, t) \right), \tag{3.57}$$

where κ_C is a strictly positive constant.

3.1.7 Summary

The equations for the Matlab model can be summed up by the mass balance

$$\frac{\partial p}{\partial t} + u\frac{\partial p}{\partial x} + (k+p)\frac{\partial u}{\partial x} = -\frac{cC_v}{A}\sqrt{(k+p_l)(p_l - p_l^{\text{amb}})}\delta(x-x_l)H(t-t_l), \tag{3.58}$$

and the momentum conservation

$$\begin{aligned}\frac{\partial u}{\partial t} + u\frac{\partial u}{\partial x} + \frac{c^2}{(k+p)}\frac{\partial p}{\partial x} &= -(1+\Delta)\frac{f}{2}\frac{|u|u}{D} \\ &\quad + \frac{cC_v u}{A(k+p)}\sqrt{(k+p_l)(p_l - p_l^{\text{amb}})}\delta(x-x_l)H(t-t_l),\end{aligned} \tag{3.59}$$

with boundary conditions

$$\begin{aligned}u(0,t) &= u_0(t), \\ p(L,t) &= p_L(t).\end{aligned}$$

And the Matlab observer is described by

$$\frac{\partial \hat{p}}{\partial t} + \hat{u}\frac{\partial \hat{p}}{\partial \hat{x}} + (k+\hat{p})\frac{\partial \hat{u}}{\partial \hat{x}} = -\frac{c\hat{C}_v}{A}\sqrt{(k+\hat{p}_l)(\hat{p}_l - \hat{p}_l^{\text{amb}})}\delta(x-\hat{x}_l), \tag{3.60}$$

$$\begin{aligned}\frac{\partial \hat{u}}{\partial t} + \hat{u}\frac{\partial \hat{u}}{\partial \hat{x}} + \frac{c^2}{(k+\hat{p})}\frac{\partial \hat{p}}{\partial \hat{x}} &= -(1+\hat{\Delta})\frac{f}{2}\frac{|\hat{u}|\hat{u}}{D} \\ &\quad + \frac{c\hat{C}_v\hat{u}}{A(k+\hat{p})}\sqrt{(k+\hat{p}_l)(\hat{p}_l - \hat{p}_l^{\text{amb}})}\delta(x-\hat{x}_l),\end{aligned} \tag{3.61}$$

with the boundary conditions

$$\begin{aligned}\hat{u}(0,t) &= u(0,t) + c\frac{1-k_0}{1+k_0}\ln\left(\frac{k+p(0,t)}{k+\hat{p}(0,t)}\right), \\ \hat{p}(L,t) &= (k+p(L,t)) \times \exp\left(\frac{k_L - 1}{c(1+k_L)}\big(u(L,t) - \hat{u}(L,t)\big)\right) - k,\end{aligned}$$

where $|k_0| \leq 1$ and $|k_L| < 1$. And the heuristic update laws

$$\dot{\hat{\Delta}}(t) = -\kappa_\Delta(\varphi_1 + \varphi_2), \tag{3.62}$$

$$\dot{\hat{C}}_v(t) = \kappa_C(\varphi_1 - \varphi_2), \tag{3.63}$$

$$\dot{\hat{x}}_l(t) = -\kappa_x(\varphi_1 + \varphi_2)|\varphi_1 + \varphi_2|^{\frac{1}{\gamma}-1}, \tag{3.64}$$

where

$$\varphi_1 = u(0,t) - \hat{u}(0,t) + c\ln\left(\frac{k+\hat{p}(0,t)}{k+p(0,t)}\right), \tag{3.65}$$

$$\varphi_2 = u(L,t) - \hat{u}(0,t) + c\ln\left(\frac{k+p(L,t)}{k+\hat{p}(L,t)}\right), \tag{3.66}$$

and κ_C, κ_x and κ_Δ are all strictly positive constants.

3.2 The OLGA simulator

OLGA is a dynamic simulator for multiphase flow which is developed by IFE, Statoil, SINTEF and lately Scandpower Petroleum Technology. It is capable of simulating transient flow in networks of pipelines with process equipment such as valves, pumps, heat exchangers, controllers etc. The fundamentals of OLGA consist of three continuity equations: one for gas, one for the liquid bulk and one for liquid droplets; two momentum equations, one for the continuous liquid phase and one for the combination of gas and possible liquid droplets; one mixture energy equations for both phases. The velocity of possible entrained liquid droplets in the gas phase is given by a slip relation.

The OLGA model is far more complicated than the Matlab model mentioned in the section above, and does not put any restrictions on inclinations of the pipeline or temperature of the fluid. Leaving OLGA in charge of the computational fluid dynamics simplifies the detection of leaks a since the main focus can be conducted to the method of finding leaks instead of the simulation of fluid flow.

OLGA models are often used to model pipelines during construction and to monitor existing pipelines. These models are typically made up by coupled pipes which are divided into segments of possibly different length. Various process equipments can be added to the segments and controlled during simulations. The input to the pipeline can be modeled as a well or a plain source, the outlet is often defined as a pressure node. Acquisition of data is done by specifying a trend variable to be logged in a segment. These trend variables can for instance be density, temperature, pressure, velocity of liquid phase and many more. A complete list is given in (Sca, a). Fluid properties can be described in a separate file which is used by OLGA as a look-up table or computed internally.

3.2.1 The connection between OLGA and Matlab

The OLGAMatlabToolbox makes it possible to run and control OLGA simulations in Matlab. It is also possible to retrieve trend variables from OLGA and store them in Matlab. This enables the possibility of applying output injection in form of boundary conditions to the OLGA observer and controlling the simulations in general. A thorough introduction to the OLGAMatlabToolbox and some practical examples can be found in (Sca, b).

3.2.2 Friction adaption with OLGA

In a OLGA model one can specify the roughness for of each of the pipes making up the pipeline. With the OLGAMatlabToolbox these parameters are available for tuning. This is done by introducing a tuning factor ζ which initially has the value 1 and using the same update law as (3.42). The tuning factor is multiplied with each pipes specified

roughness and thereby affecting the friction in the pipeline. The update law in physical coordinates takes the form

$$\dot{\zeta}(t) = -\kappa_f(\varphi_1 + \varphi_2) \tag{3.67}$$

where φ_1 and φ_2 are defined in (3.65) and (3.66), and κ_f is a strictly positive constant.

3.2.3 Estimation of leak parameters with OLGA

The magnitude of the leakages in the OLGA observer is adjusted by controlling the opening of the leaks. This is done by setting a control signal $\hat{u}_s$ which can take a value between 0 and 1. $\hat{u}_s$ is assumed to appear in the expression for $\hat{C}_v$ in the following manner

$$\hat{C}_v = \hat{C}_d \hat{u}_s \frac{\pi}{4} \hat{D}_l, \tag{3.68}$$

where $\hat{C}_d$ is the discharge coefficient and $\hat{D}_l$ is the diameter of the opening of the leakage. $\hat{C}_d$ and $\hat{D}_l$ are constants which must be specified in the OLGA observer prior to simulations. The update law for the control signal is similar to the update law of $\hat{C}_v$ in the Matlab observer and takes the form

$$\dot{\hat{u}}_s(t) = \kappa_u \left(\varphi_1 - \varphi_2\right), \tag{3.69}$$

where κ_u is a positive constant and φ_1 and φ_2 are defined in (3.65) and (3.66). Further explanation regarding estimation of $\hat{C}_v$ are presented in Section 4.4. The estimation of position is done as with the Matlab observer with (3.64).

Chapter 4

Method

The purpose of this chapter is to give the reader a close insight into some of the practical issues which arises when constructing an OLGA or Matlab observer. There will also be given pointers on how to interpret the results.

Simulations are performed in Mathworks Matlab version 7.2.0.232 (R2006a), and OLGA 5.1 with OLGAMatlabToolbox version 1.1.

Some of the material in this chapter have been presented earlier in (Hauge, 2006) but is added in this chapter for the sake of the reader. The simulator constructed in Matlab is based on the code used in (Hauge, 2006) with added functionality for adaption of friction.

4.1 Numerical solution in Matlab

The numerical solution is based on the characteristic form (3.25)-(3.26). This transformation of coordinates decouples the PDE's and divides the flow of information into two separate directions. (3.25) carries information in the same direction as the velocity of the fluid, while (3.26) carries information the opposite way.

In order to simulate the leak detection system, a discretization of the pipeline and a numerical solver is needed. The pipeline is divided into by $N-1$ sections and N nodes where each section has a uniform length Δx. This is illustrated in Figure 4.1.

Due to the separate direction of the flow of information, a finite difference method can be used to calculate values for the spatial derivatives. For the α-equation, a first order backwards difference scheme is suitable

$$\frac{\partial \alpha_i^n}{\partial x} = \frac{\alpha_i^n - \alpha_{i-1}^n}{x_i - x_{i-1}}, \qquad i = 2, \cdots, N-1 \tag{4.1}$$

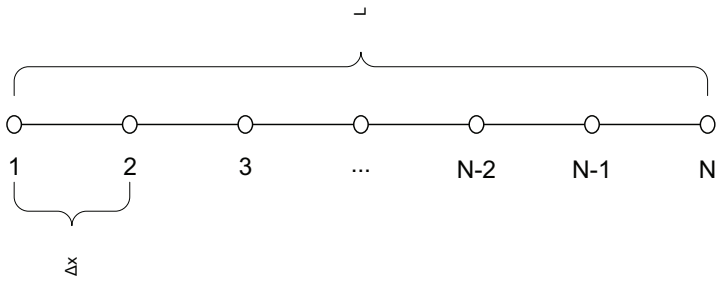

Figure 4.1: Discretization of the pipeline.

where $i \in [1, N]$ indicates the number of the node and $n \in [0, \infty)$ the time step. Note that the numbering of the nodes imply that α_1^n corresponds to $\alpha(0, n \cdot \Delta t)$ and α_N^n corresponds to $\alpha(L, n \cdot \Delta t)$.

In a similar manner as above, the β-equation describes information flowing in the opposite direction, and a first order forward difference scheme is used

$$\frac{\partial \beta_i^n}{\partial x} = \frac{\beta_i^n - \beta_{i+1}^n}{x_{i+1} - x_i}, \qquad i = 2, \cdots, N-1 \tag{4.2}$$

The two equations above is used in (3.18)-(3.19) at each time step which gives the partial derivative of α and β with respect to t. Now the value of α and β for the next time step can be computed.

$$\alpha_i^{n+1} = \alpha_i^n + \frac{\partial \alpha_i^n}{\partial t}\Delta t, \qquad i = 2, \cdots, N-1 \tag{4.3}$$

$$\beta_i^{n+1} = \beta_i^n + \frac{\partial \beta_i^n}{\partial t}\Delta t, \qquad i = 2, \cdots, N-1. \tag{4.4}$$

where Δt is the length of the time step. The values for α_i^n and β_i^n for $i = 1$ and $i = N$ is given by the boundary values in (3.20)-(3.21) and by extrapolation. Extrapolation is used to determine α_1^n and β_N^n since these to values can not be computed accurately with the finite difference scheme. The second order extrapolation scheme from (Nilssen, 2006) is used. That is

$$\beta_1^n = 3\beta_2^n - 3\beta_3^n + \beta_4^n \tag{4.5}$$

$$\alpha_N^n = 3\alpha_{N-1}^n - 3\alpha_{N-2}^n + \alpha_{N-3}^n. \tag{4.6}$$

The values obtained from the extrapolation is applied to the boundary conditions (3.20)-(3.21) to determine the value of α_1^n and β_N^n. A similar approach is used for the endpoints in the observer, but due to application of output injection the boundary values from (3.30)-(3.31) are utilized.

4.2 Distributing the leak over two nodes

Modelling and discretizing the leak in the right manner is crucial to for the convergence of the estimated values. Ideally the grid size should not have any effect on the convergence properties of the estimated leak magnitude and position. Unfortunately this will never be the case, but if there exists a sufficiently small Δx_s such that all $\Delta x < \Delta x_s$ yield approximately the same convergence properties, then the leak is well modeled and discretized. In other words, when the pipeline is divided by sufficiently many nodes, further refinement will not improve the convergence properties of the estimates concerning the leak.

In (Hauge, 2006) it was shown that the method of discretizing the leak presented below, exhibited good performance regarding the criterion mentioned above.

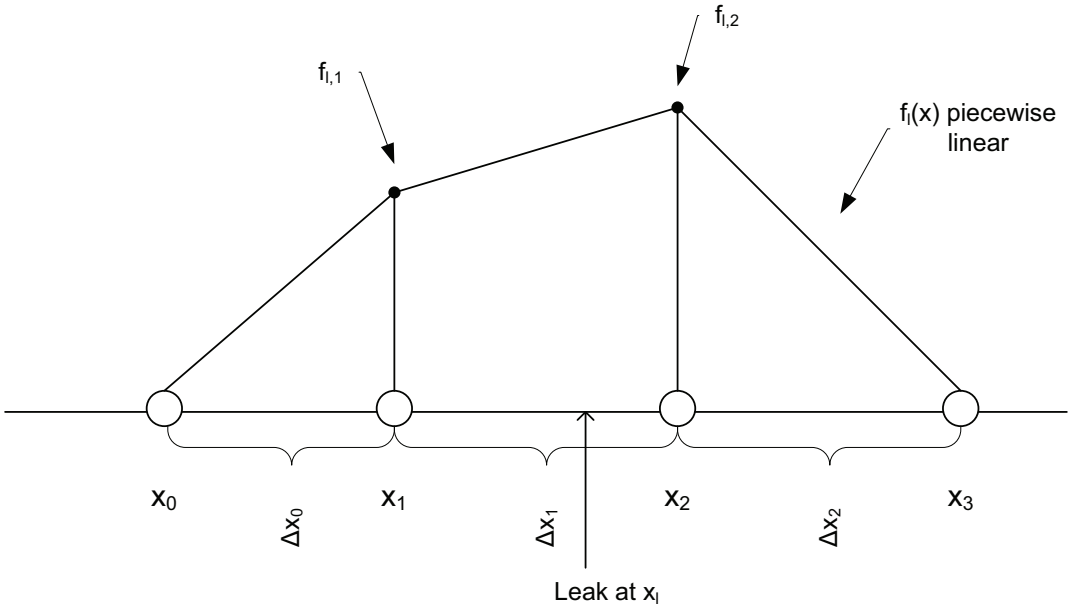

Figure 4.2: Sketch of the distribution of the leak.

Considering that the leak can occur between two nodes, a way of distributing the leak to these two nodes is needed. Discretizing the leak w_l at x_l between the nodes x_1 and x_2 can be done in the following manner

$$f_{l,1} = f_l(x_1), \tag{4.7}$$
$$f_{l,2} = f_l(x_2), \tag{4.8}$$

which means that the leak is distributed over two nodes. This is shown in Figure 4.2. The values of the functions $f_{l,1}$ and $f_{l,2}$ are decided by the position of x_l relatively to x_1 and x_2, and of course w_l. The integral of $f_l(x)$ over the pipeline must correspond to the

magnitude of the leak, that is

$$w_l = \int_0^L f_l(x)\,\mathrm{d}x \tag{4.9}$$

The mass of the leak is equally proportioned on each side of the point of leak

$$\frac{w_l}{2} = \int_{x_0}^{x_l} f_l(x)\,\mathrm{d}x, \tag{4.10}$$

$$\frac{w_l}{2} = \int_{x_l}^{x_3} f_l(x)\,\mathrm{d}x. \tag{4.11}$$

Consider the following

$$f_l(x_l) = f_{l,1} + \frac{f_{l,2} - f_{l,1}}{\Delta x_1}(x_l - x_1) \tag{4.12}$$

$$= \left(1 - \frac{x_l - x_1}{\Delta x_1}\right) f_{l,1} + \frac{x_l - x_1}{\Delta x_1} f_{l,2}, \tag{4.13}$$

and

$$w_l = \Delta x_0 \frac{f_{l,1}}{2} + \Delta x_1 \frac{f_{l,1} + f_{l,2}}{2} + \Delta x_2 \frac{f_{l,2}}{2}, \tag{4.14}$$

which corresponds to the total area of w_l in Figure 4.2, and

$$\frac{w_l}{2} = \frac{\Delta x_0 f_{l,1}}{2} + \frac{(x_l - x_1)\big(f_{l,1} + f_l(x_l)\big)}{2}. \tag{4.15}$$

which corresponds to half the area of w_l in Figure 4.2. This gives two linearly independent equations for w_l, namely

$$w_l = \Delta x_0 \frac{f_{l,1}}{2} + \Delta x_1 \frac{f_{l,1} + f_{l,2}}{2} + \Delta x_2 \frac{f_{l,2}}{2} \tag{4.16}$$

$$= \frac{\Delta x_0 + \Delta x_1}{2} f_{l,1} + \frac{\Delta x_1 + \Delta x_2}{2} f_{l,2}. \tag{4.17}$$

and

$$w_l = \Delta x_0 f_{l,1} + (x_l - x_1)\big(f_{l,1} + f_l(x_l)\big) \tag{4.18}$$

$$= \left(\Delta x_0 + 2(x_l - x_1) - \frac{(x_l - x_1)^2}{\Delta x_1}\right) f_{l,1} + \frac{(x_l - x_1)^2}{\Delta x_1} f_{l,2}. \tag{4.19}$$

The results above can be rewritten in a more compact form

$$\begin{bmatrix} f_{l,1} \\ f_{l,2} \end{bmatrix} = G_l^{-1} \begin{bmatrix} w_l \\ w_l \end{bmatrix}, \tag{4.20}$$

where

$$G_l = \begin{bmatrix} \frac{\Delta x_0+\Delta x_1}{2} & \frac{\Delta x_1+\Delta x_2}{2} \\ \Delta x_0 + 2(x_l - x_1) - \frac{(x_l-x_1)^2}{\Delta x_1} & \frac{(x_l-x_1)^2}{\Delta x_1} \end{bmatrix}. \tag{4.21}$$

In (Hauge, 2006) it was stated that this method of discretizing the leak did not pose any restrictions on the section lengths Δx_i for $i = 0,\ 1,\ 2$. This is true if the signs of $f_{l,1}$ and $f_{l,2}$ are not relevant. A negative value for either $f_{l,1}$ or $f_{l,2}$ implies that there should be a injection into the pipeline in the given node. Theoretically this is possible in the Matlab observer, but for the OLGA observer it is not. In order to overcome this problem, logic statements are introduced in the code which governs the leak openings in the OLGA observer. This logic will be further explained in Section 4.4.3.

The need of a uniform grid can be proven with a simple chain of reasoning.

1. Let $w_l > 0$.
2. If $\Delta x_1 > \Delta x_0$ and $x_l = x_1$, then $f_{l,2} < 0$ in order for (4.11) to be satisfied. Thus $\Delta x_0 \geq \Delta x_1$.
3. Due to symmetry $\Delta x_2 \geq \Delta x_1$.
4. If x_l moves along the pipeline, for instance to a point between x_2 and x_3, then $\Delta x_1 \geq \Delta x_2$ and $\Delta x_3 \geq \Delta x_2$ due to the same reasoning as above.
5. Thus all Δx_i, $i = 1,\ 2,\ \cdots,\ N$ must be of equal length.

A more formal proof can be found in Appendix C.1.

Notice that $f_{l,1}$ and $f_{l,2}$ have the denomination $\frac{\text{kg}}{\text{sm}}$ and must be multiplied with a length to represent a mass rate. By inspecting (4.17) one can see that

$$\begin{aligned} w_l &= F_{l,1} + F_{l,2} \\ &= \frac{\Delta x_0 + \Delta x_1}{2} f_{l,1} + \frac{\Delta x_1 + \Delta x_2}{2} f_{l,2} \end{aligned} \tag{4.22}$$

thus

$$F_{l,1} = \frac{\Delta x_0 + \Delta x_1}{2} f_{l,1} \tag{4.23}$$

$$F_{l,2} = \frac{\Delta x_1 + \Delta x_2}{2} f_{l,2}. \tag{4.24}$$

4.3 Computing pressures and density at point of leak

Since the leak can appear between two nodes, estimates of the pressure inside the pipe and the ambient pressure at the point of leak are necessary. This can be solved by applying a simple interpolation scheme, assuming that the pressures are linearly dependent on the distance between two nodes. If the leak is somewhere between two nodes, say x_i

and x_{i+1} with the respective pressures p_i and p_{i+1}, an approximation of the derivative of the pressure can be found by computing

$$\frac{\Delta\hat{p}}{\Delta x} = \frac{\hat{p}_{i+1} - \hat{p}_i}{x_{i+1} - x_i}. \tag{4.25}$$

The interpolated value for $\hat{p}_l$ is now

$$\hat{p}_l = \hat{p}_i + (x_l - x_i)\frac{\Delta\hat{p}}{\Delta x}. \tag{4.26}$$

For pipelines with difference in altitude, estimation of the ambient pressure at the leak is done in the same manner, i.e.

$$\hat{p}_l^{\text{amb}} = \hat{p}_i^{\text{amb}} + (x_l - x_i)\frac{\Delta\hat{p}^{\text{amb}}}{\Delta x}. \tag{4.27}$$

For the OLGA observer an interpolated value for the density at the point of leak must be found. This is done similarly as above, i.e.

$$\hat{\rho}_l = \hat{\rho}_i + (x_l - x_i)\frac{\Delta\hat{\rho}}{\Delta x}. \tag{4.28}$$

4.4 Setting up an OLGA observer

The satisfactory results in (Hauge, 2006) set out the grounds for using OLGA as an observer in the same manner as the Matlab observer. The easiest way to do this is to duplicate an existing OLGA model and modifying it into a observer with controllable leaks at each segment of the pipeline. Issues that arise when doing this are discussed in the following.

4.4.1 Obtaining correct measurements

In order to apply output injection the pressures (p_0, p_L) and velocities (u_0, u_L) at the inlet and outlet of the model are needed. Since OLGA differentiates between boundary variables and volume variables, it is necessary to extrapolate the values for p_L. This is illustrated in Figure 4.3 where the measuring points in OLGA are located. Notice that the last available measurement of pressure available is p_N. The measurement of the velocity at the inlet, u_0, is available and extrapolation is not needed.

Velocities is defined as a boundary variable in OLGA which means that it is computed at the boundaries between segments. Pressure is a volume variable and is computed at the middle of each segment. Since the source is located at the middle of a segment, it is not necessary to extrapolate values for pressure at this point. Neither is it necessary to extrapolate the values for the velocity at the outlet. But the measurements p_{N-2}, p_{N-1}, p_N and Δx_{N-2}, Δx_{N-1}, Δx_N must be used in a cubic extrapolation scheme in order to compute an approximation of p_L.

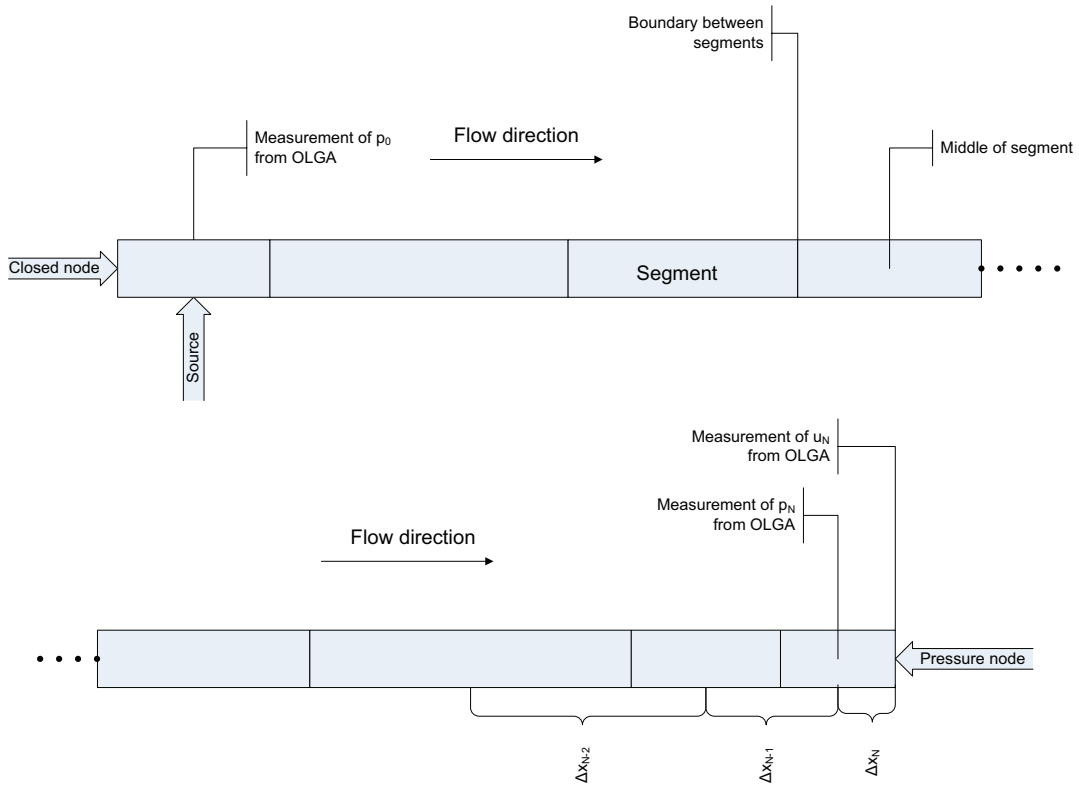

Figure 4.3: The situation of source and pressure node relative to measurements of p and u.

4.4.2 Controlling the boundaries

It is not unusual that OLGA models have chokes at the inlet and outlet in order to control the inflow and outflow of the pipe. In an observer it is more appropriate to use a source and a pressure node since both guarantee instantaneous response of the manipulated variable, whereas controlling a valve or a choke would impose a delay. This method of ensuring tight control of the input and output of the pipeline is crucial when utilizing output injection in form of boundary conditions.

4.4.3 Controlling the leakages

In the Matlab observer a leakage is simulated by estimating a C_v which is used in the valve equation (3.56) to compute the leak magnitude at the point of leak. Since the estimate of the leak position is continuous, the leak in the observer must be able to seemingly occur between two nodes. In the Matlab observer, this is solved by distributing the leak magnitude over two nodes according to (4.20). With the OLGA observer the same technique is applied with a modification to overcome the problem with negative leakage mentioned in Section 4.2. This modification ensures that the possible negative leak is reset to zero and that the other is set to the estimated leak rate.

A leak in OLGA is a process equipment which can be added to a segment of the pipeline. The leak is modeled as a negative mass source and is always situated at the middle of the segment. The main parameters of a leak must be specified in the OLGA input file and are:

- p^{amb} - the ambient pressure (backpressure) at the point of leak.
- C_d - Discharge coefficient.
- D_l - Maximum diameter of the leak.
- Controller - A controller dedicated to govern the leak opening.

The opening of the leak is decided from

$$A_l = \frac{\pi}{4} u_s D_l^2, \quad 0 \leq u_s \leq 1 \tag{4.29}$$

where u_s is a signal from a controller. The maximum diameter and discharge coefficient must be chosen as reasonable values compared to the diameter of the pipeline and its material. In this work the parameters for all of the leaks in the all of the observer have been chosen as: $\hat{D}_l = 0.05$ m and $\hat{C}_d = 0.84$, which are the same values that are set in every model used for testing.

The exact equation for the mass rate at the point of leak implemented in OLGA is not available, but is assumed to resemble the valve equation (3.54). Incorporating the

diameter and control signal into this equation yields

$$w_l(u_s, p_l, p_l^{\text{amb}}, \rho_l) = C_d \frac{\pi}{4} u_s D_l^2 \sqrt{(p_l - p_l^{\text{amb}})\rho_l}. \tag{4.30}$$

If the assumption about this equation is correct, then the term $C_d \frac{\pi}{4} u_s D_l$ can be combined to a uncertain parameter C_v which would be the target of estimation. Since all of the terms making up C_v except u_s are constants, the fact that only $\hat{u}_s$, in the corresponding valve equation in the observer, can be manipulated during simulations should not have any major effect as long as $\hat{C}_d \hat{D}_l > C_d D_l$.

In the OLGA observer a leak is added at every segment along the pipeline and assigned a controller, where each of the controller signals can be manipulated with the OLGAMatlabToolbox. The OLGA observer must also be able to seemingly have a leak between two segments. As with the Matlab observer this is solved by using the distribution from (4.20). But where $f_{l,1}$ and $f_{l,2}$ were incorporated directly in the numerical solution of the partial differential equations in Matlab, the following steps must be taken with the OLGA observer to achieve similar effect:

1. Compute the estimate of $\hat{u}_s$.
2. Compute the leak magnitude with (4.31).
3. Distribute the leak with (4.20) which gives $\hat{f}_{l,1}$ and $\hat{f}_{l,2}$ and then compute $F_{l,1}$ and $F_{l,2}$ with (4.23) and (4.24).
4. Compute the signals, $\hat{u}_{s,1},\ \hat{u}_{s,2}$, to be set by the two controllers corresponding with each of the leaks by rearranging (4.31) and using necessary measurements at each of the leaks.

$$\hat{w}_l(\hat{u}_s, \hat{p}_l, \hat{p}_l^{\text{amb}}, \hat{\rho}_l) = \hat{C}_d \frac{\pi}{4} \hat{u}_s \hat{D}_l^2 \sqrt{(\hat{p}_l - \hat{p}_l^{\text{amb}})\hat{\rho}_l}. \tag{4.31}$$

4.4.4 Adjusting the time step

OLGA is capable of dynamically adjusting the time step during simulations making sure that the duration of the simulations are kept at a minimum. But with boundary control and estimation of parameters through Matlab, the simulations with the OLGA observer are interrupted periodically in order to read measurements such as pressure and fluid velocity, compute control signals and set these back to the observer. This period is denoted Δt_{obs} and must not be confused with Δt which occurred in the numerical solution with the Matlab model. Δt_{obs} must be set sufficiently small so that the boundaries does not fluctuate unnecessarily and thereby corrupting the estimates of x_l and C_v. On the other hand, choosing the time step to small could drastically prolong the duration of the simulations, making the observer unfit for real-time monitoring.

4.5 Verification test of the valve equation

The valve equation (4.30) is derived from Bernoulli's law and only holds for incompressible, inviscid and irrotational fluids. It is therefore not likely that this equation is used in OLGA to model a leak. By running simulations with the OLGA model and storing the variables p_l, p_l^{amb}, ρ_l, w_l, it is possible to compute the expected observer control signal $\hat{u}_{s,\text{exp}}$ by evaluating

$$\hat{u}_{s,\text{exp}} = \frac{w_l}{C_d \frac{\pi}{4} D_l^2 \sqrt{(p_l - p_l^{\text{amb}})\rho_l}}. \tag{4.32}$$

This value can be compared to the actual control signal u_s, which is a constant, to verify the valve equation.

4.6 Estimating mass rate of leak

In earlier work such as (Aamo et al., 2005) and (Nilssen, 2006) the leak magnitude, w_l, was an estimated parameter. But this approach was in (Hauge, 2006) presumed to induce unfavorable convergence properties when the leak magnitude was not constant. This presumption was based on the fact that the convergence proofs for parameter estimation only holds for estimation of constants.

When the current leak estimation scheme is applied to a pipeline with inclinations, the backpressure at the point of leak might change with the location of the leak. And when adapting a leakage with the OLGA observer during stationary flow, the position of the leak in the observer is moving along the pipeline through a distance with a possible height difference. If there is a difference in altitude along the path of the moving leak, the backpressure at the leak will change, and so will $\hat{C}_v$ in order to compensate for the varying differential pressure over the leak. This means that even though the target of estimation, i.e. C_v, is a constant, the corresponding parameter in the observer could vary vastly during simulations.

By going back to the method of estimating the leak mass rate directly, the problem mentioned above might be eliminated for cases with stationary flow in inclined pipelines. With the OLGA observer this is possible by estimating the leak magnitude directly with the update law

$$\dot{\hat{w}}_l = \kappa_w(\varphi_1 - \varphi_2) \tag{4.33}$$

where φ_1 and φ_2 is given by (3.65) and (3.66), and κ_w is strictly positive. In order to control the mass rate out of each of the valves simulating a leak, a controller is needed. The task of this controller is to assure that the values computed by the leak distribution (4.20) are obtained at the respective leaks. Therefore a controller, consisting of two PI controllers and some logic that deals with handling the integral part for the moving

leaks, was made in Matlab. This method of estimating leak magnitude can be summed up with

1. Estimate leak magnitude with (4.33).
2. Distribute the leak with (4.20) and compute the mass rate at each leak with (4.23) and (4.24).
3. Compute error at each of the leaks and use this as input to the controller.
4. Set the control signals from the controller to the respective leaks.

4.7 Adaption of friction coefficients

Schemes for adapting friction coefficients have been implemented for both the Matlab and OLGA observer. There is a principal difference in the influence these coefficients have on each of their models. While the tuning factor ζ affects the roughness in the OLGA observer, the friction coefficient $\hat{\Delta}$ is incorporated in the PDE concerning momentum conservation in the Matlab observer where it affects the friction $\hat{f}$. From (3.36) it is clear that the friction is dependent on the Reynolds number, which again is dependent on the fluid density and velocity, among others. Simulations showed that when using the Matlab observer with data from the OLGA model, $\hat{\Delta}$ was affected by the fluid velocity, making the Matlab observer unfit for leak detection with time-varying boundaries. To overcome this problem estimates of $\hat{\Delta}$ were stored during simulations with non-stationary flow and no leak. These stored estimates were later used as a look-up table for simulations with a leak and similar boundary conditions.

As for the OLGA observer, ζ was estimated during the first period of the simulations were no leak was present and set constant by resetting κ_f to 0 in the code. The same procedure was followed for the Matlab observer with stationary flow, where $\hat{\Delta}$ was estimated for a short period of time prior to the leakage.

4.8 Tuning of update laws

The estimates of the leak magnitude and position are based on information from the end points of the pipeline and the κ-values are therefore dependent on the time the information needs to propagate through the pipeline. This implies that the speed of sound and length of the pipeline have to be taken into consideration when tuning. Also, the mutual effect between the estimate of magnitude and position must be accounted for. For example the effect of a fast converging magnitude may slow down the convergence of the position. And if the magnitude is far from converging when the estimate of the position passes by actual point of the leak, the estimated position will continue in the wrong direction.

For pipelines with varying height, the tuning is more complicated since the slope of the inclinations vary through the pipeline, which again affect the pressure inside the pipeline as well as the ambient pressure. This can be coped with by using multiple observers with different starting points and tuning which will be discussed in the next section.

The observer can be used to locate leaks after a pipeline has been shut down due to a leakage if the sufficient amount of data have been logged. In such cases it is possible to run simulations over and over again to tune the update laws. It is also possible to choose different starting point for the point of leak in the observer if there is a suspicion of where the actual leak might have occurred.

4.9 Multiple observers

If this kind of leak detection method should ever be applied real-time with an actual pipeline, it would be advisable to run multiple observers initialized with the different tunings and starting points of the leak. With this approach it would be possible to increase the accuracy of the estimates, and if multiple observers show similar results, greater confidence regarding the estimates is induced.

4.10 Computing mean values

The mean values of the deviation in the estimates of the leak magnitude and position is found by evaluating the following integrals:

$$\bar{x}_{l,\text{dev}} = \frac{1}{T} \int_{t-T}^{t} \hat{x}_l(\tau) - x_l \, \mathrm{d}\tau \tag{4.34}$$

for the position, and

$$\bar{w}_{l,\text{dev}} = \frac{1}{T} \int_{t-T}^{t} \hat{w}_l(\tau) - w_l(\tau) \, \mathrm{d}\tau \tag{4.35}$$

for the magnitude. T indicates the period of time the mean value is calculated for.

4.11 Computing time of convergence

In order to measure when the estimated position of the leak has been sufficiently close to the actual leak for a period of time, consider the following

$$\frac{1}{T} \int_{t-T}^{t} |\hat{x}_l(\tau) - x_l| \, \mathrm{d}\tau \leq M \tag{4.36}$$

where T is the length of the period and M is the maximum allowed mean deviation from the actual position. Let t_c denote the first time instance when the inequality (4.36) is satisfied for all succeeding $t \in [t_c, t_{end}]$ where t_{end} is the duration of the simulation. By evaluating this integral, the time instance when the estimated position is sufficiently close to actual position can be determined. Note that the evaluation of (4.36) starts at $t = t_l$ so t_c denotes the period of time it takes from the leak occurs to $\hat{x}_l$ stays sufficiently close.

Since the time of convergence is calculated by integrating the absolute value of the deviation in position, it is possible that $\bar{x}_l \leq M$, where $\bar{x}_l$ is computed from (4.34), while t_c does not exist.

4.12 Computing the $\mathcal{L}_2$ norm of the observer error

Convergence properties for the observer error in terms of p and u can be described by computing the $\mathcal{L}_2$ norm. The following equation describes how this is done.

$$e_{\mathcal{L}_2}(v, n) = \left[\sum_{i=1}^{N} \| v_i^n - \hat{v}_i^n \| \right]^{\frac{1}{2}}, \qquad n = 0, 1, \cdots, \frac{t_{end}}{\Delta t} \tag{4.37}$$

where i denotes the node in the pipeline and n denotes the time step. The variable v is arbitrary and will take the form of u and p.

Chapter 5

Results

This chapter presents the relevant results obtained during the phases of development and testing. The test data are produced by running simulations with a model of a pipeline constructed with OLGA. The data obtained are stored as mat-files in Matlab and used as input to the observer. Both an observer made in Matlab and one made in OLGA are treated in this chapter. The results also include simulations with data produced by a model of an actual pipeline, namely Tor 1.

First off, the effect of output injection with the OLGA observer is showed. Then simulations regarding estimation of friction is presented. The proceeding section treats the verification of the valve equation. Then a comparison of the Matlab and OLGA observer points out the advantages of the new computational fluid dynamics simulator for both oil and gas in a horizontal pipeline. Important results obtained for a straight pipe carrying gas with temperature dynamics turned on are showed in its own section before the section dedicated to multiple observers supervising the Tor 1 pipeline. A robustness study with and without adaption of roughness is given attention in Section 5.7 and are followed by a section concerning time-varying boundary conditions with the Tor 1 pipeline. A short section on estimation of mass rate illustrates the benefits of estimating C_v instead of w_l for a case with difference in altitude through the pipeline. The presentation of the simulations are finished off by a case with Tor 1 carrying gas.

Results and relations that might not be apparent to the reader are commented during the presentation of the results. The last section in this chapter contains a discussion that treats all of the presented material and their aspects.

5.1 Output injection

The effect of output injection for the observer is crucial for the convergence of the magnitude and position estimates. This technique of controlling the boundaries ensures

fast convergence in terms of p and u for the observer. In Figure 5.1 the $\mathcal{L}_2$ norm of the observer error is presented for a case with a straight pipeline carrying oil without inclinations matching the specifications in TableA.3. In this case the flow is stationary and the temperature dynamics is turned on. The observer is initialized with $k_0 = k_L = 0$ which means that the observer gain is at is maximum. The model was initialized with the inlet mass rate and output pressure as specified in Table A.3. The observer was initialized with the same values as the model except for the mass rate at the inlet, which was 100 kg/s, and the pressure at the outlet, which was 70 bara. There is neither adaption of roughness or leak magnitude and position, and Δt_{obs} is 0.05 s.

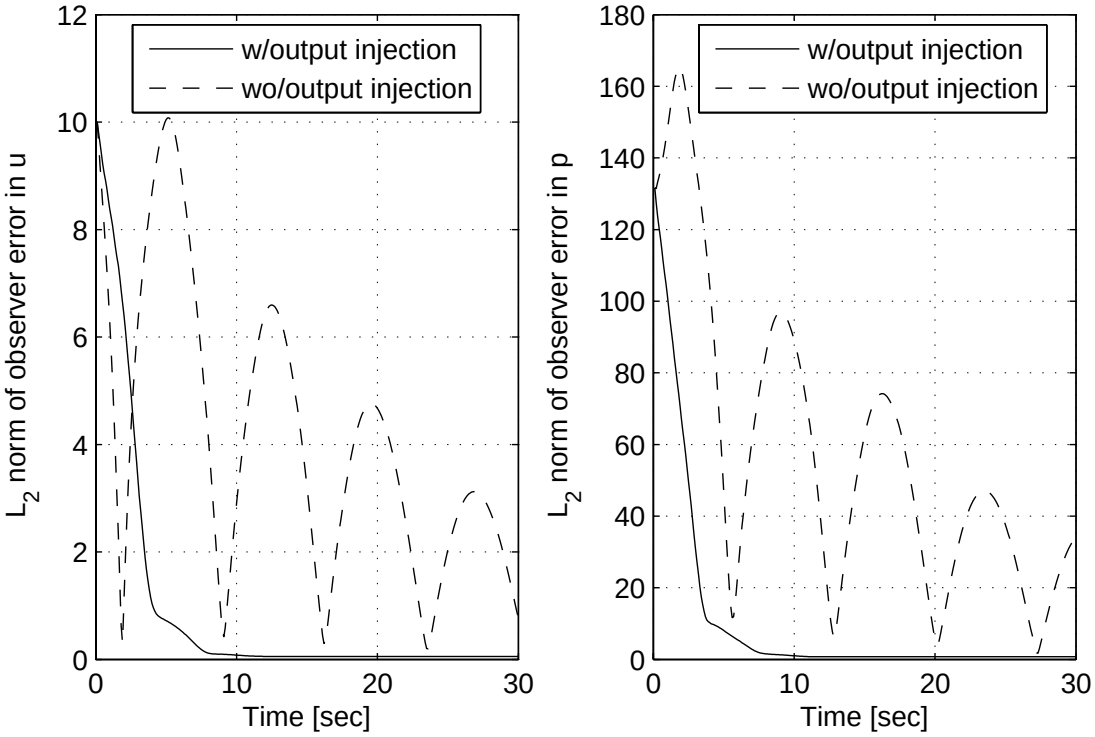

Figure 5.1: **Oil, stationary.** The effect of output injection.

Comments

Neither the observer error in u or p in Figure 5.1 converges exactly to zero. This is due to the difference in mass rate at the inlets at the time of initialization combined with temperature dynamics being turned on. Since the steady state flow in the observer is considerably less than in the model at $t = 0$, the temperature of the fluid in the observer is lower, which again affects the pressure and velocity through the pipeline. This would even out after some time.

5.2 Friction adaption with OLGA

The Figures 5.2-5.3 show the roughness adapted by the OLGA observer in case of oil and gas flow, with and without temperature dynamics turned on. The models are as specified in Table A.3 and the observers are exact copies. Both the observers and models were initialized with the values from Table A.3. During the simulations $\kappa_f = 100$ for oil and $\kappa_f = 0.2$ for gas. There are no leaks present and the observer gain is at its maximum.

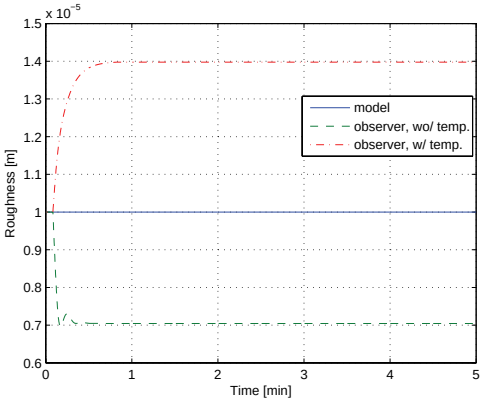

Figure 5.2: **Oil, stationary.** Friction adaption with the OLGA observer with and without temperature dynamics.

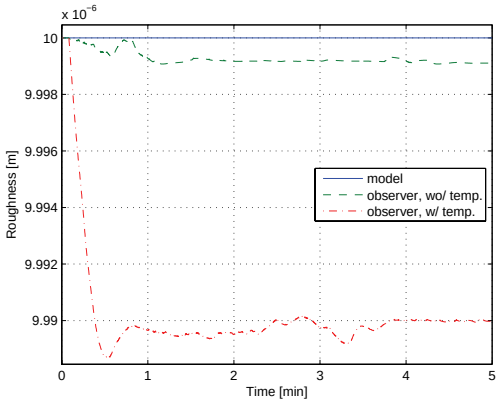

Figure 5.3: **Gas, stationary.** Friction adaption with the OLGA observer with and without temperature dynamics.

Comments

It is alarming that the estimated roughness, in the case with oil, deviates with up to 40 %. This might have been caused by a numerical error during the conversion from mass rate to fluid velocity performed in the code controlling the simulations. Or maybe the extrapolation scheme used to obtain the pressure from the model introduces an unwanted error.

5.3 Verification of the valve equation

In section 4.5, a way of verifying the assumed valve equation were presented. Figure 5.4 shows the computations of $\hat{u}_{s,\text{exp}}/u_s$ for two cases. One where the flow is stationary and one during a shut down. The shut down is similar to the one presented later in Figure 5.13 and the initial values and pipe parameters corresponds to the those given in Table A.3. The control signal u_s for the valve in the model is zero the first minute of the simulations and then held constantly at 0.02.

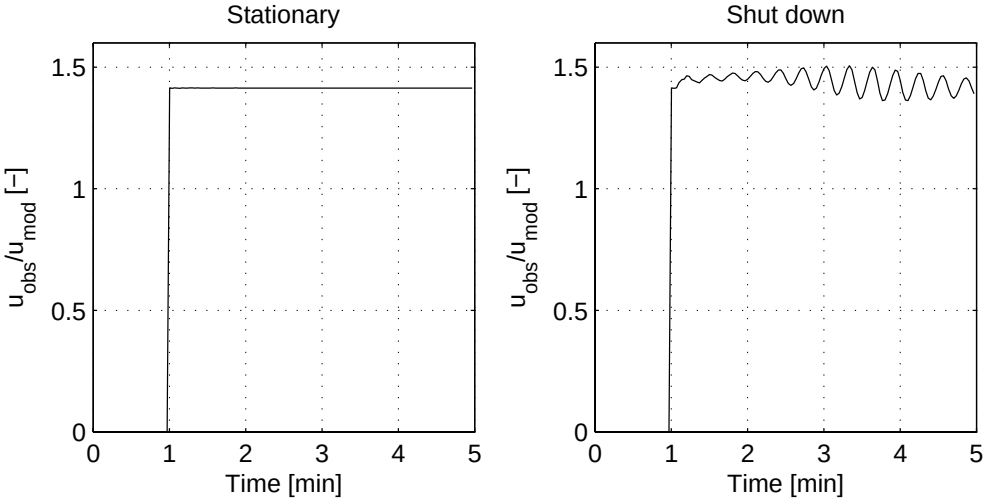

Figure 5.4: The ratio between computed control signal and the actual control signal.

Tests with gas showed the same tendency as Figure 5.4 but with a ratio of 0.04.

5.4 Comparison of the Matlab and OLGA observer

A modified version of the observer made in Matlab in (Hauge, 2006) is in this section compared with the OLGA observer presented in this thesis. The modified Matlab observer is an exact copy of the previous version with added functionality to handle

adaption of friction. The model data is produced by an OLGA model as specified in Table A.3. The pipe and fluid parameters for the Matlab observer can be found in Table A.1 and the tuning parameters in Table A.2. Parameters for the OLGA observer is presented in Table A.3 and the tuning parameters can be seen in Table A.5.

For both of the cases with stationary flow, the adaption of the friction coefficient, $\hat{\Delta}$, is done prior to the occurrence of the leak and then turned off. For the two simulations with non-stationary flow, the adaption of $\hat{\Delta}$ were done without a leak present as described in Section 4.7. The adaption of roughness for the OLGA observer had the same outcome for every case and is shown in Figure 5.2.

The temperature dynamics is turned off for all of the simulations since the Matlab observer does not support this feature. The time step Δt, used in the Matlab observer, is 0.02 s. Δt_{obs} used by the OLGA observer is also 0.02 s. The starting point of the observer is at the middle of the pipeline, namely 2500 m.

5.4.1 Stationary flow

In this subsection two cases with stationary flow is treated. The magnitude of the leaks are presented in Table 5.1. The estimated leak parameters are plotted in Figure 5.5-5.8. Plots of the estimated friction coefficients for each of the cases are put in the appendix in Figure B.1 and B.2.

Position	**Oil**	**Gas**
850	2.24 %	1.03 %
4650	2.19 %	1.02 %

Table 5.1: Maximum leak magnitude in percent of initial mass rate at inlet.

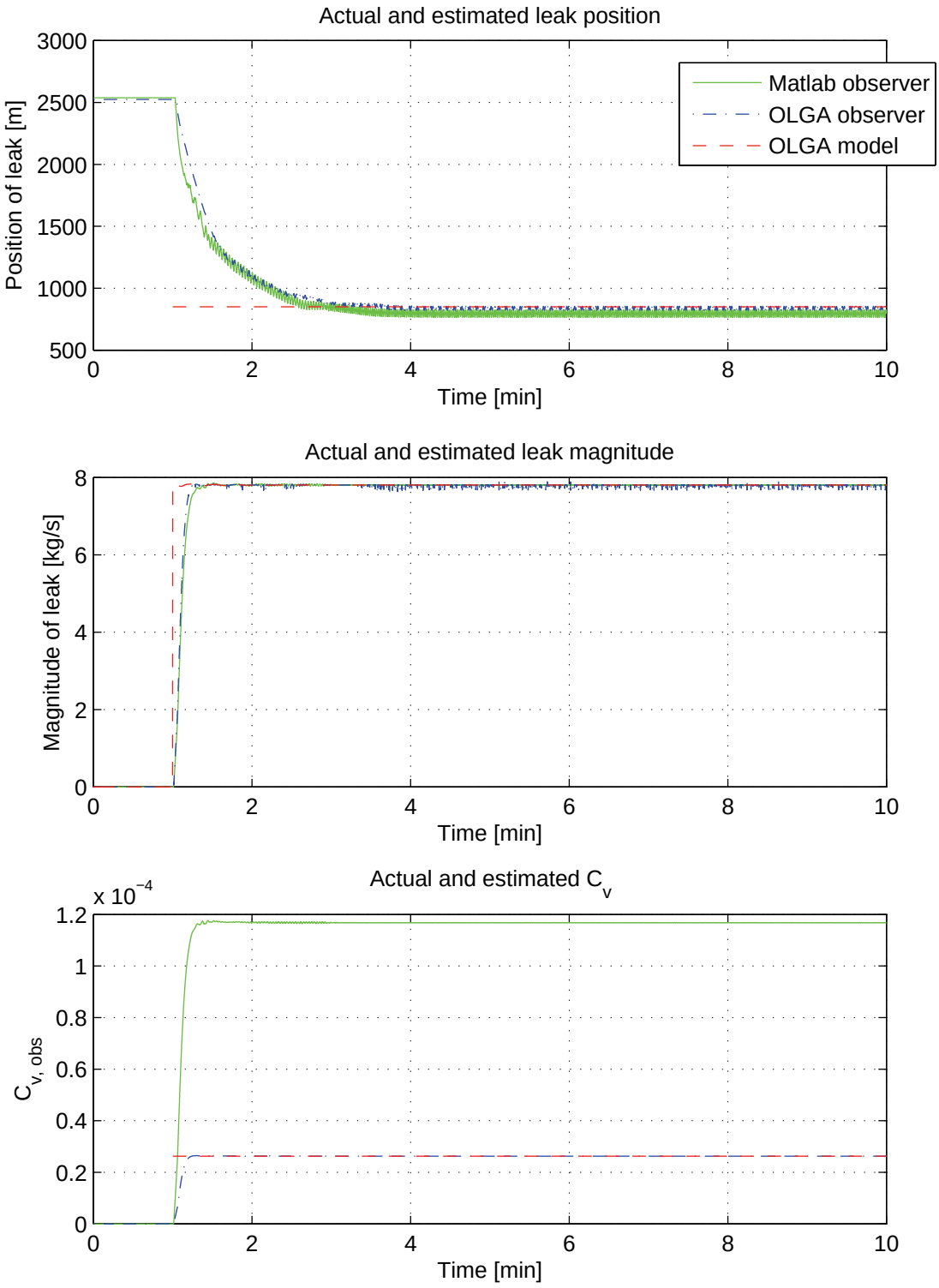

Figure 5.5: **Oil, stationary.** Estimates for a leak at 850 m.

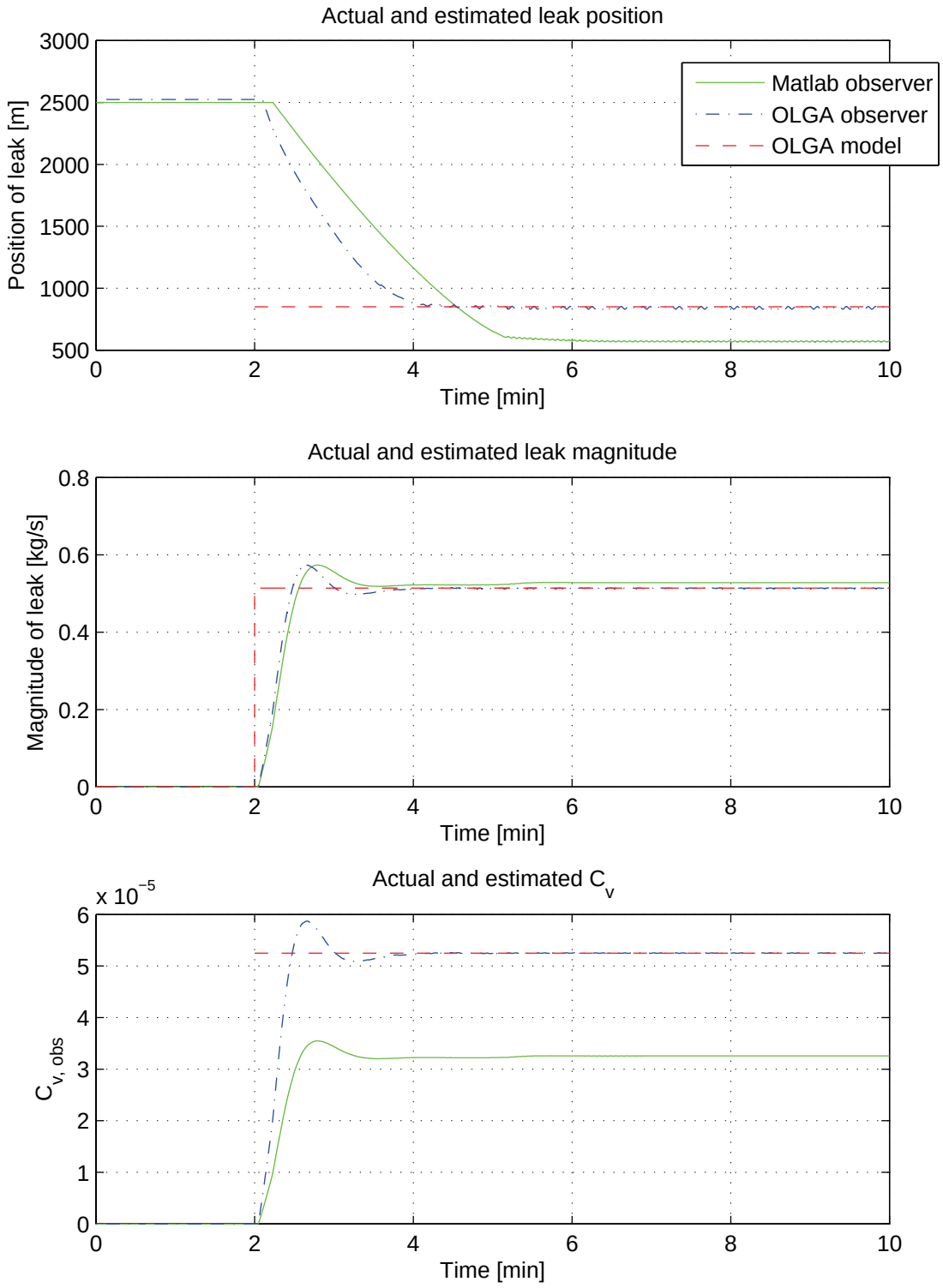

Figure 5.6: **Gas, stationary.** Estimates for a leak at 850 m.

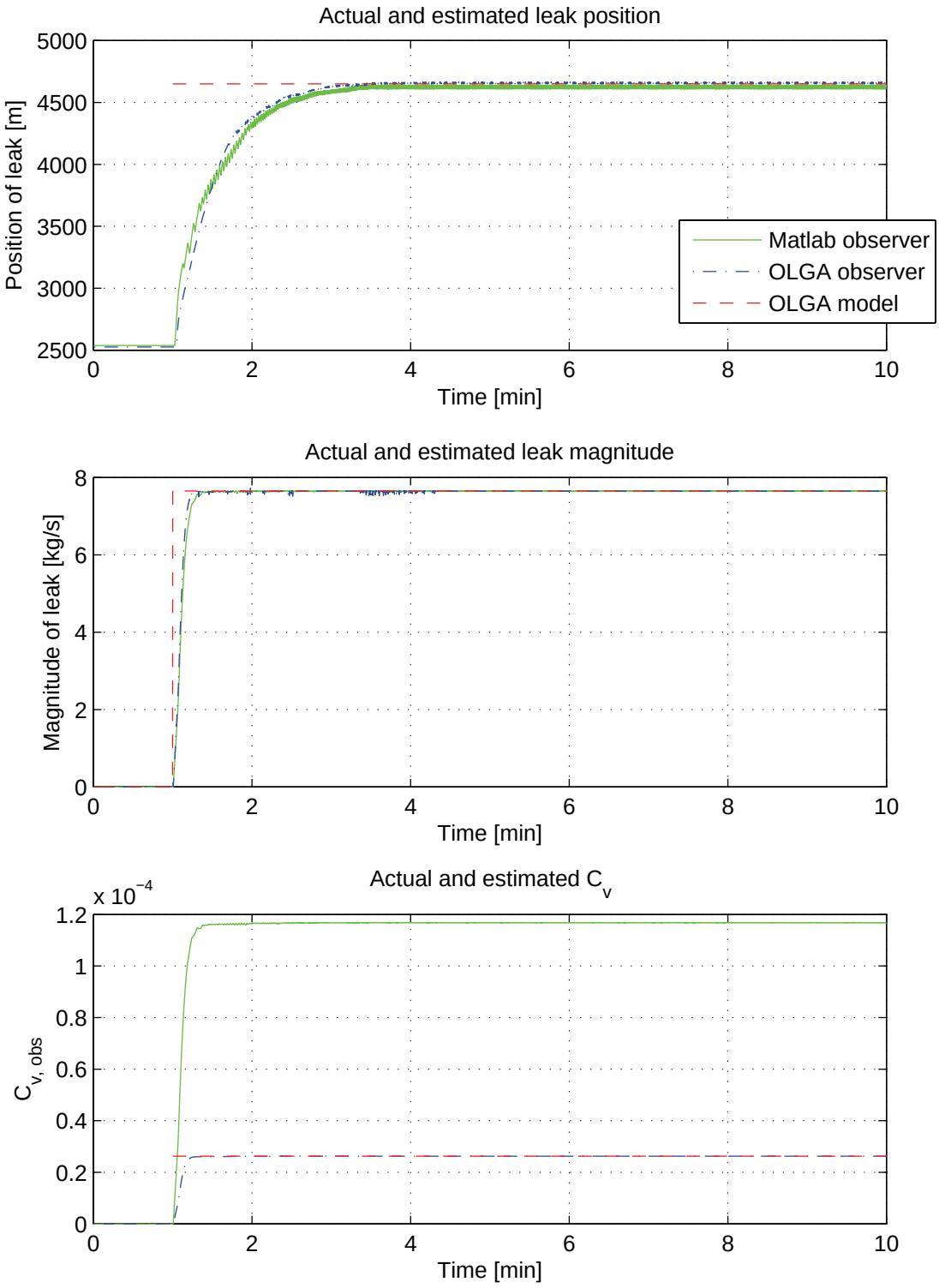

Figure 5.7: **Oil, stationary.** Estimates for a leak at 4650 m.

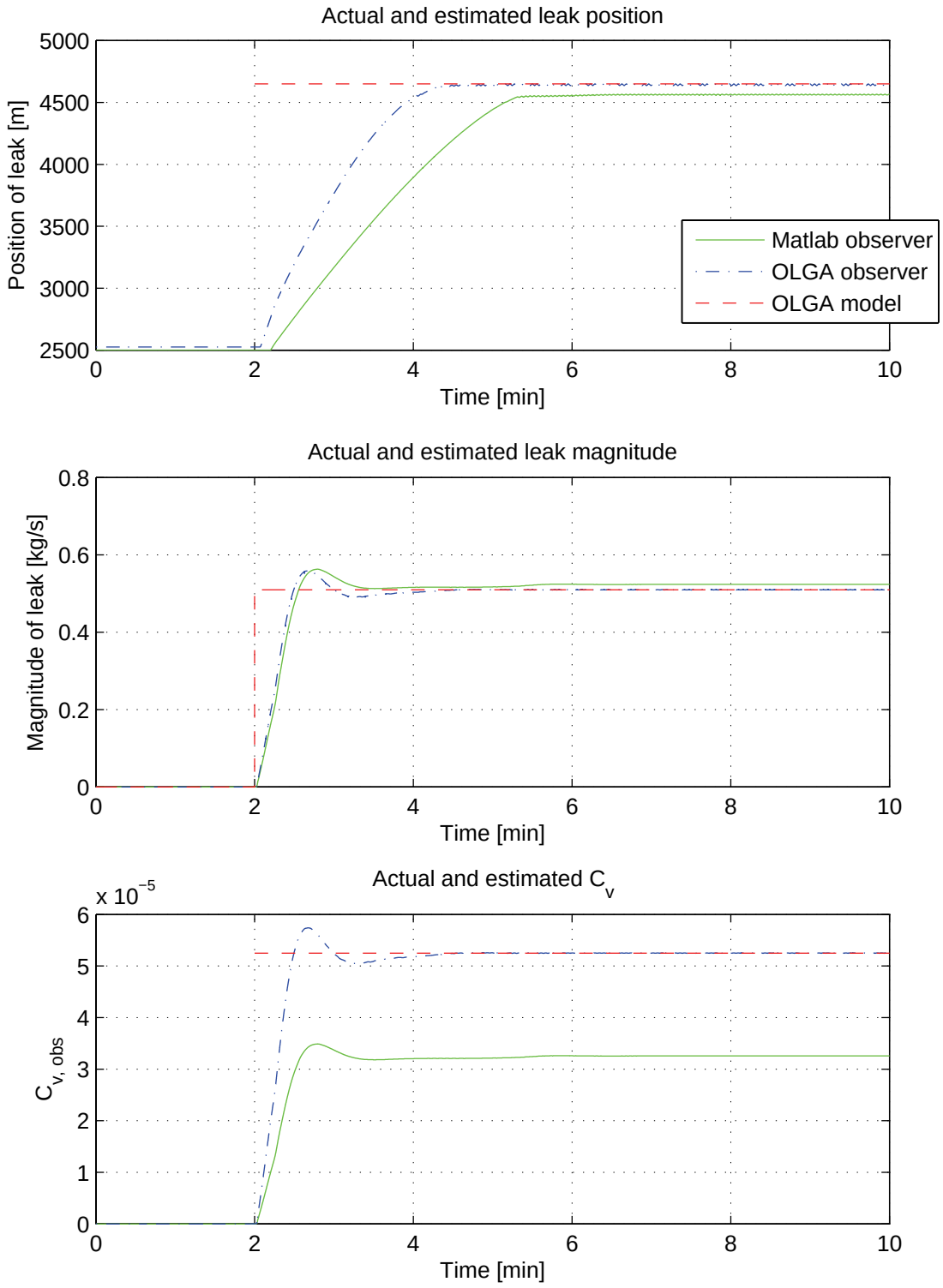

Figure 5.8: **Gas, stationary.** Estimates for a leak at 4650 m.

5.4.2 Sinusoidal varying boundaries

The sinusoidal varying boundaries are meant to represent a change in production rate due to manipulation of chokes at the inlet and outlet. The leak magnitudes are presented in Table 5.2 and the estimated leak parameters can be seen in Figure 5.9-5.12. The estimated friction coefficient for each case can be seen in Figure B.3 and B.4.

Position	Oil	Gas
3450	0.93 %	1.03%

Table 5.2: Maximum leak magnitude in percent of initial mass rate at inlet.

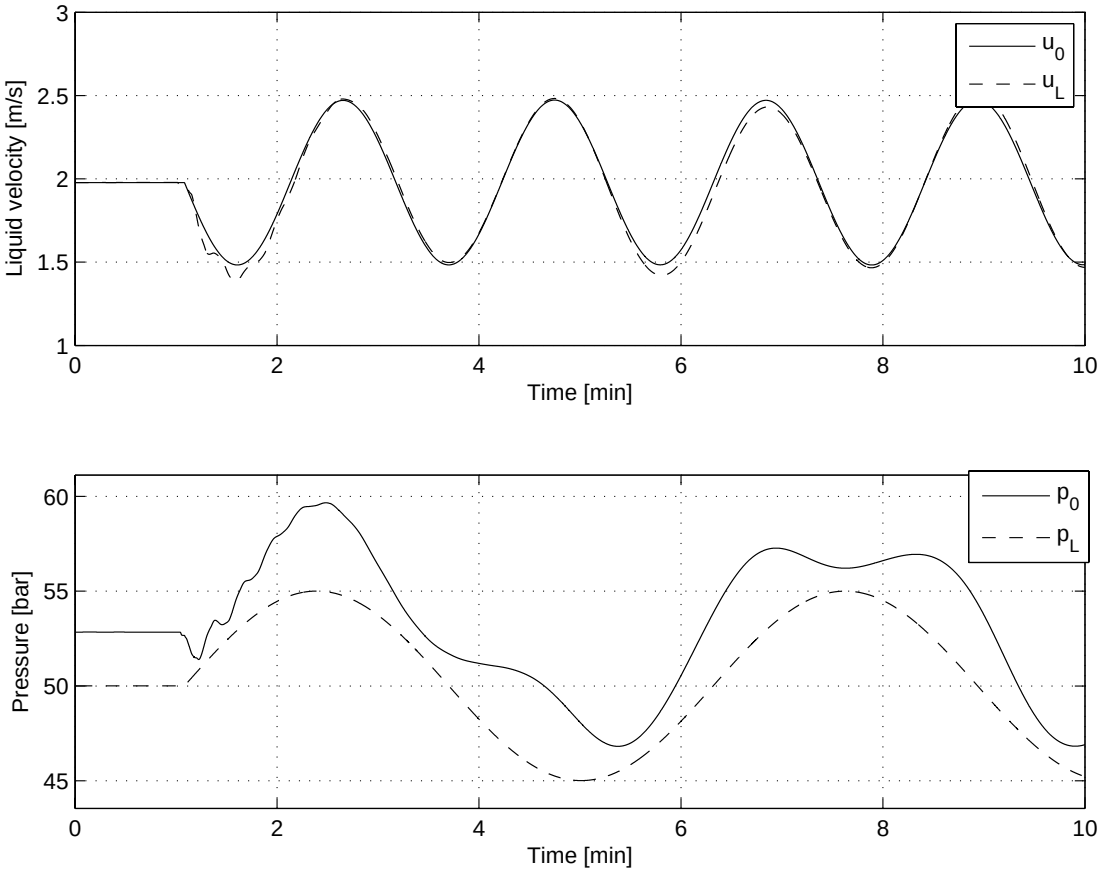

Figure 5.9: **Oil, sinusoid.** Measurements from OLGA of the boundaries with a leak at 3450 m.

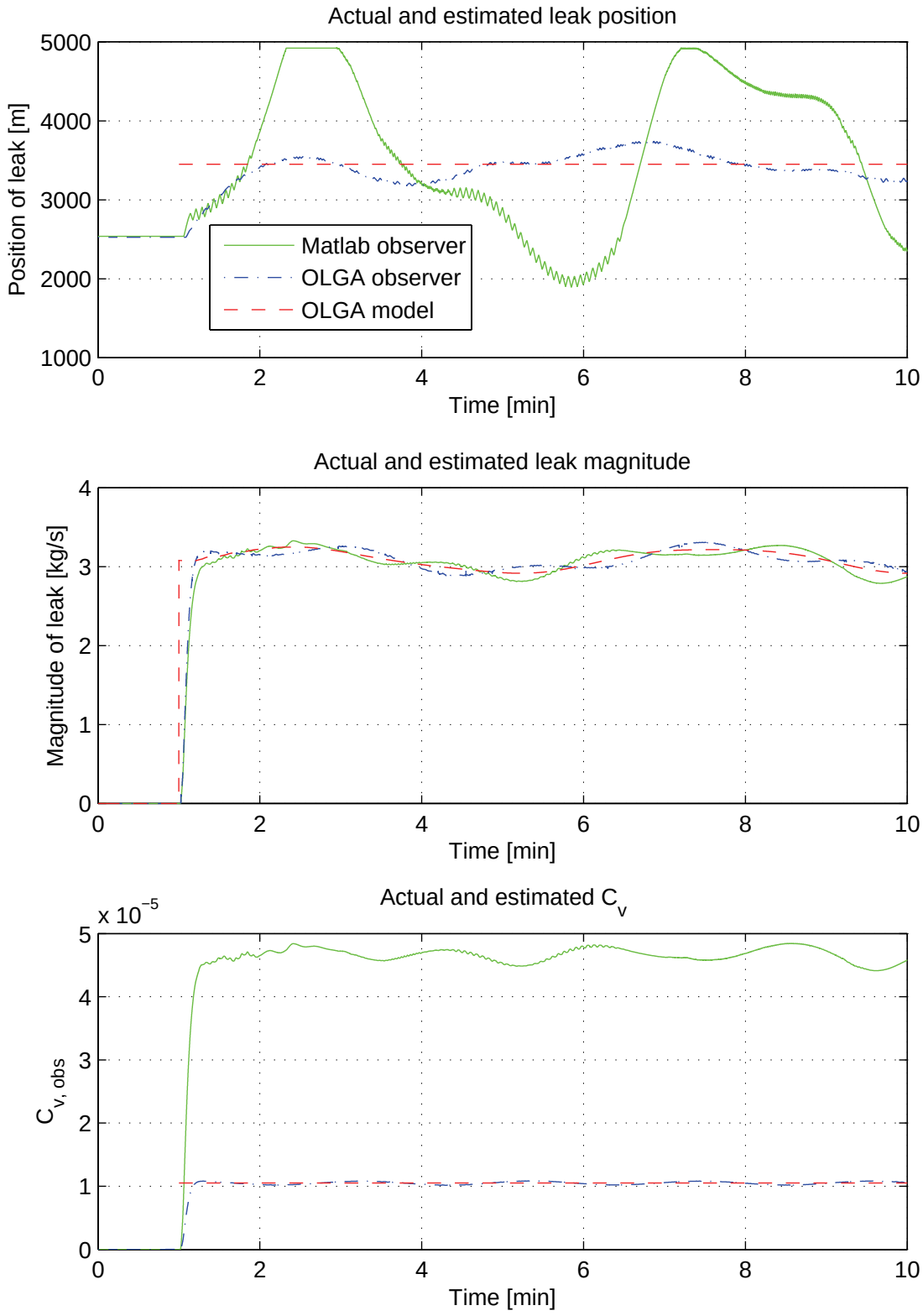

Figure 5.10: **Oil, sinusoid.** Estimates for a leak at 3450 m.

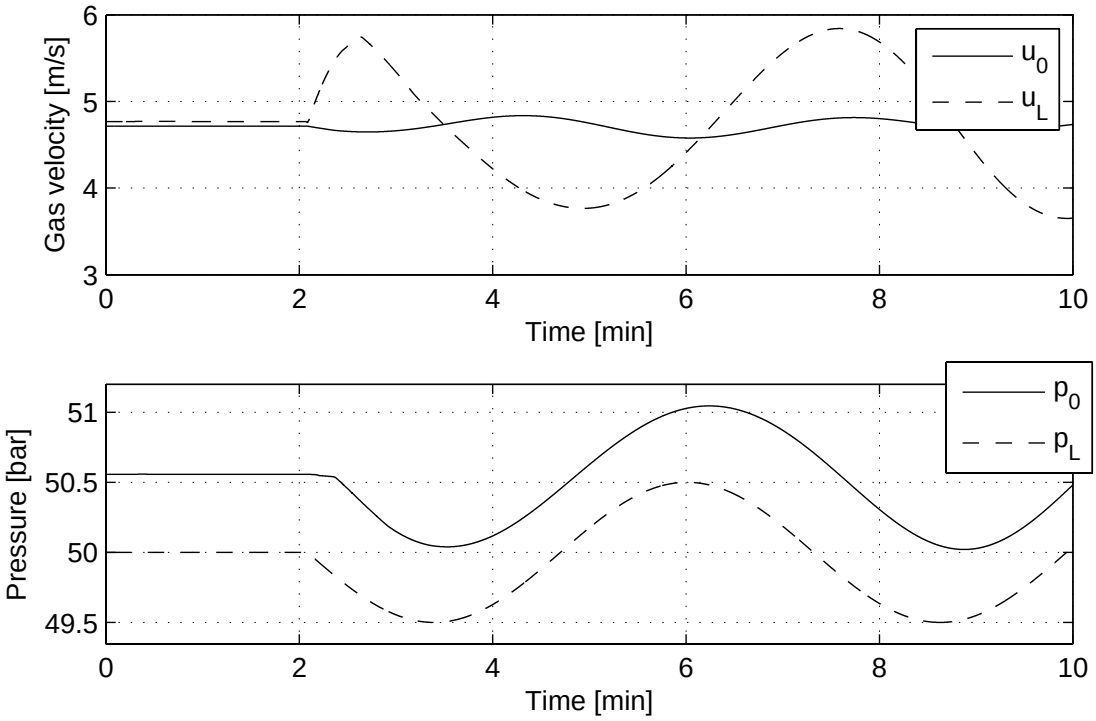

Figure 5.11: **Gas, sinusoid.** Measurements from OLGA of the boundaries with a leak at 3450 m.

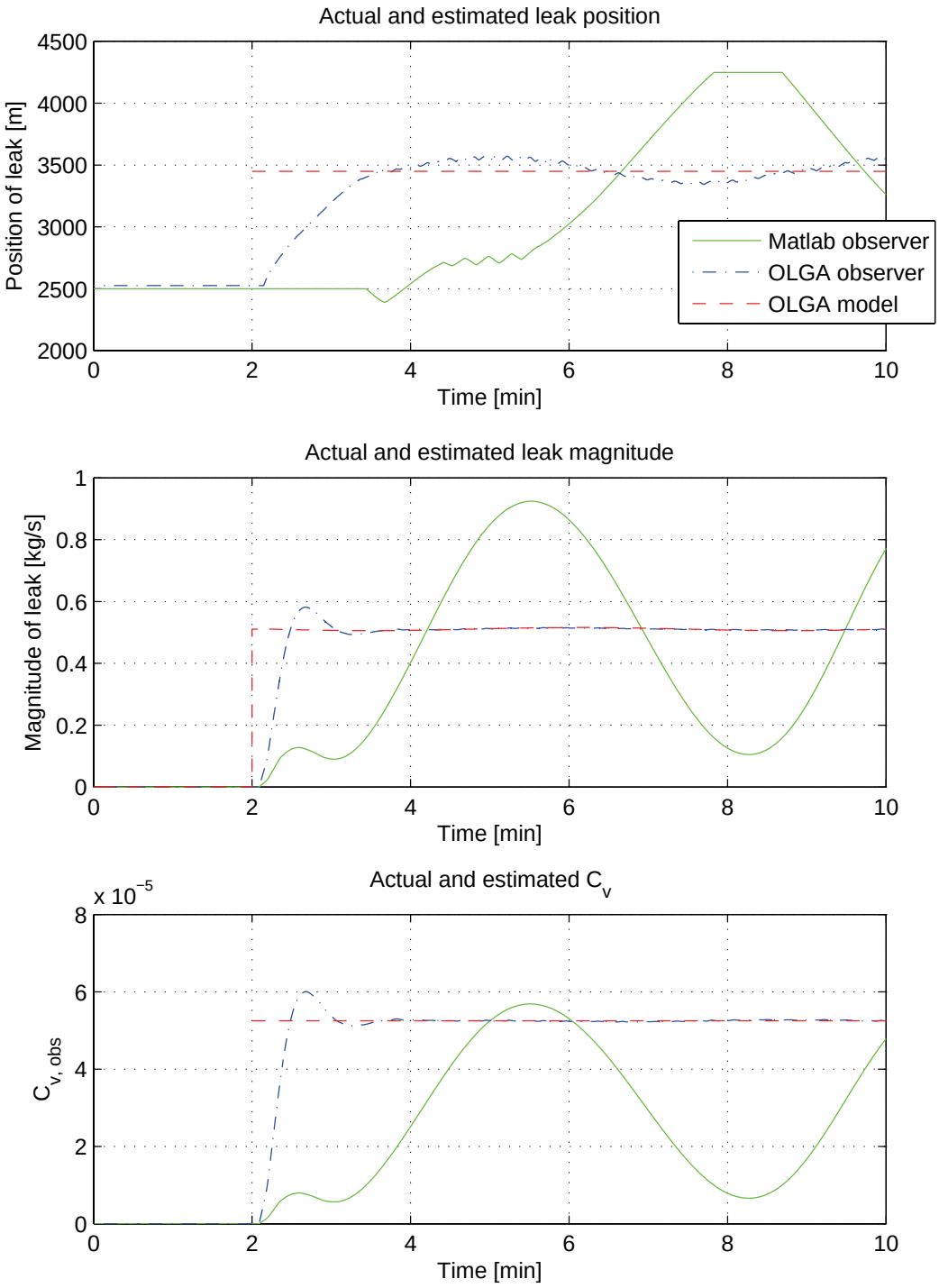

Figure 5.12: **Gas, sinusoid.** Estimates for a leak at 3450 m.

5.4.3 Shut down

In this subsection the production is shut down as the leak parameters C_v and x_l are estimated. Table 5.3 lists leak magnitudes and the estimated leak parameters can be seen in Figure 5.13-5.16. The estimated friction coefficient for each case can be seen in Figure B.5 and B.6.

Position		**Oil**	**Gas**
3450	Max	2.22 %	1.03 %
	Min	0.20 %	0.22 %

Table 5.3: Maximum leak magnitude in percent of initial mass rate at inlet.

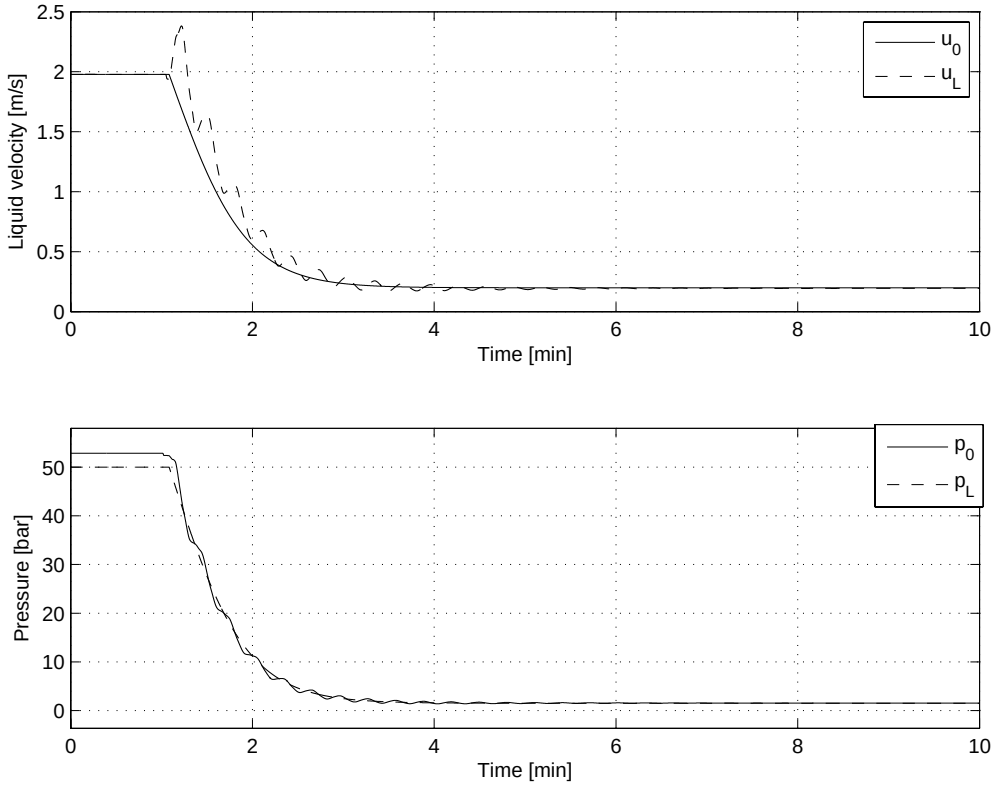

Figure 5.13: **Oil, shut down.** Measurements from OLGA of the boundaries with a leak at 1350 m.

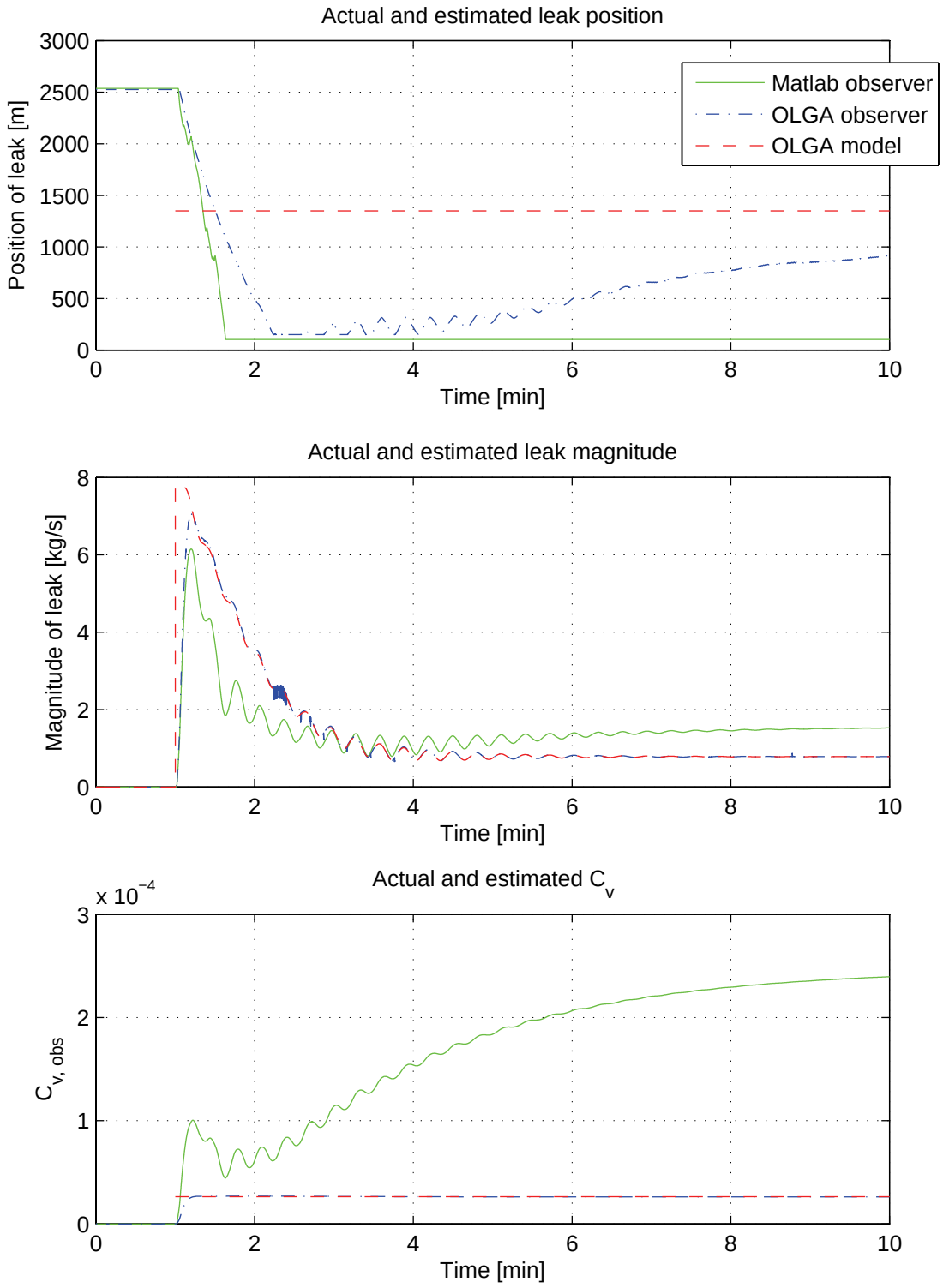

Figure 5.14: **Oil, shut down.** Estimates for a leak at 1350 m.

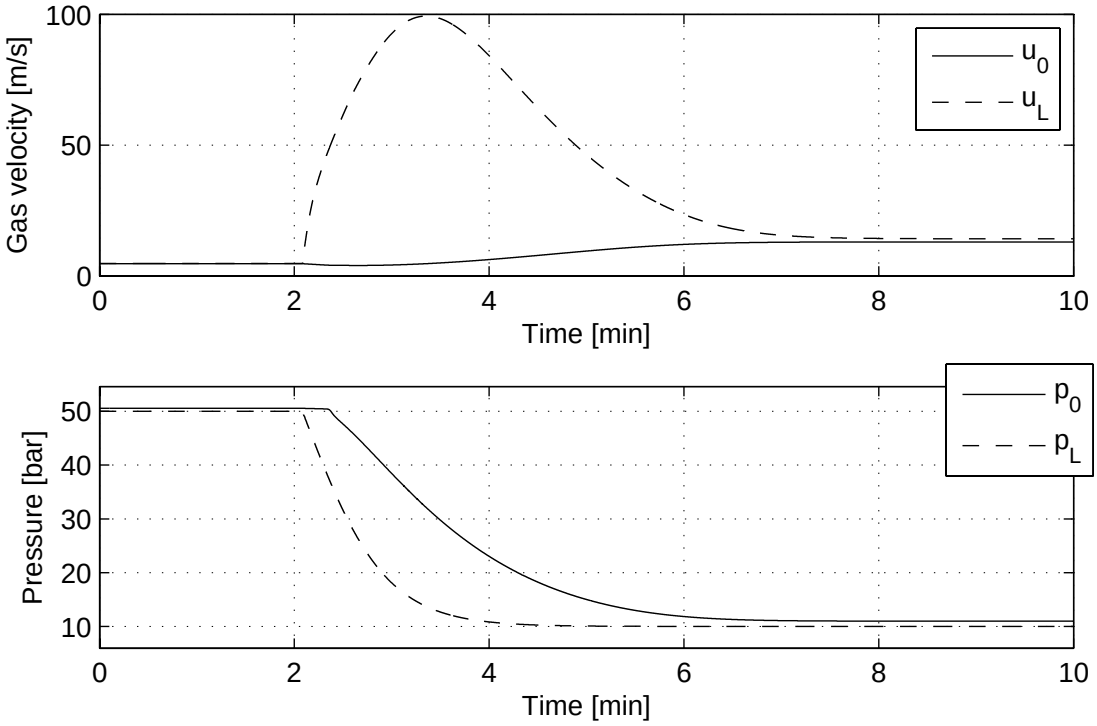

Figure 5.15: **Gas, shut down.** Measurements from OLGA of the boundaries with a leak at 1350 m.

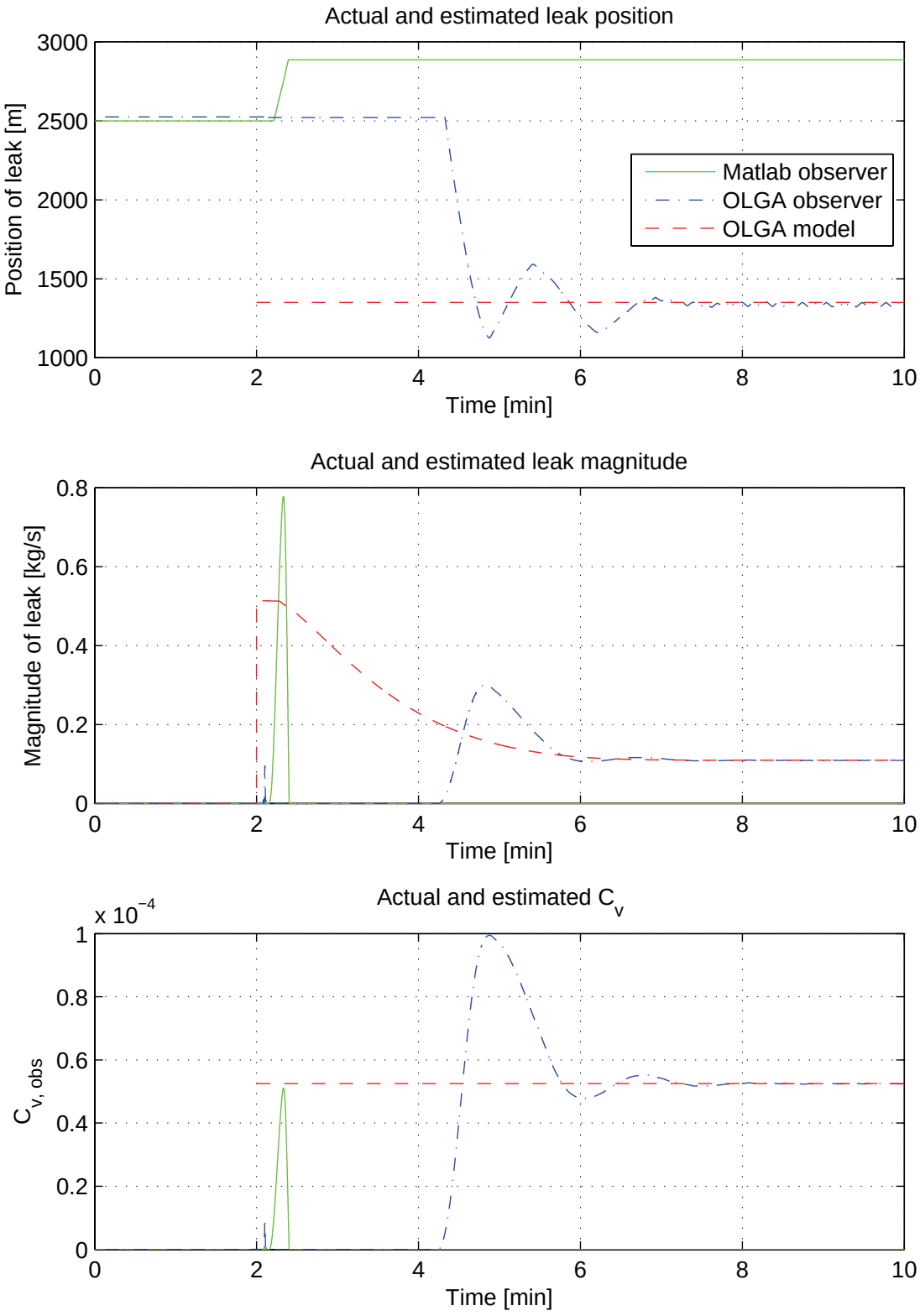

Figure 5.16: **Gas, shut down.** Estimates for a leak at 1350 m.

5.4.4 Summary

In Table 5.4 a summary of the simulations comparing the Matlab and OLGA observer are presented. The values listed under $\bar{\mathbf{x}}_{\mathbf{l},\text{dev}}$ refers to the mean of the deviation from the actual leak position. These values are computed by evaluating the expression in (4.34). Likewise the values listed under $\bar{\mathbf{w}}_{\mathbf{l},\text{dev}}$ refers to the evaluation of (4.35). The results in both of these columns are computed during the last 60 seconds of the simulations. The times of convergence, $\mathbf{t_c}$, arise from the evaluation of (4.36) with $M = 300$ m and a window of 30 seconds.

		Oil			Gas		
Case	**Observer**	$\mathbf{t_c}$	$\bar{\mathbf{x}}_{\mathbf{l},\text{dev}}$ [m]	$\bar{\mathbf{w}}_{\mathbf{l},\text{dev}}$ [g/s]	$\mathbf{t_c}$	$\bar{\mathbf{x}}_{\mathbf{l},\text{dev}}$ [m]	$\bar{\mathbf{w}}_{\mathbf{l},\text{dev}}$ [g/s]
850, Stationary	Matlab	2	56	-2	4	280	-14
	OLGA	2	11	1	4	8	0
4650, Stationary	Matlab	2	26	-2	5	87	-14
	OLGA	2	-7	0	4	7	0
1350, Shut down	Matlab	-	1247	-730	-	-1536	109
	OLGA	-	471	0	4	14	0
3450, Sinusoid	Matlab	-	194	96	10	-177	-10
	OLGA	2	156	-60	3	-63	-1

Table 5.4: Summary of the results for the comparison of the Matlab and OLGA observer.

5.5 Simulations with gas and temperature dynamics

In the previous section neither the models or observers took temperature dynamics into account. The following results in this section presents results with the energy equation incorporated in the simulations for both the model and the observer.

The Figures 5.17-5.22 presents estimated parameters and the boundaries for gas flow through a horizontal pipeline, as specified in Table A.3, with temperature dynamics turned on. The observer is an exact copy of the model and is initialized with the same values. The tuning of the update laws can be found in A.5. Leak magnitude is presented in percent of the initial mass flow in the Table 5.5 and a summary of the simulations can be seen in Table 5.6. The mean value of the deviations in this table are computed with $T = 3$ minutes and the time of convergence is evaluated with a window of 30 seconds and $M = 500$ meters.

	1550 m, stationary	750 m, sinusoid	3850 m, shut down
max	0.51 %	0.41 %	0.40 %
min	0.51 %	0.40 %	0.16 %

Table 5.5: Maximum and minimum of leak magnitude in percent of the initial mass flow.

	1550 m, stationary	750 m, sinusoid	3850 m, shut down
$\bar{x}_{l,\text{dev}}$[m]	1	229	11
$\bar{w}_{l,\text{dev}}$[g/s]	0	-6	0
t_c [min]	3	9	9

Table 5.6: Summary table, leakage with gas flow and temperature dynamics.

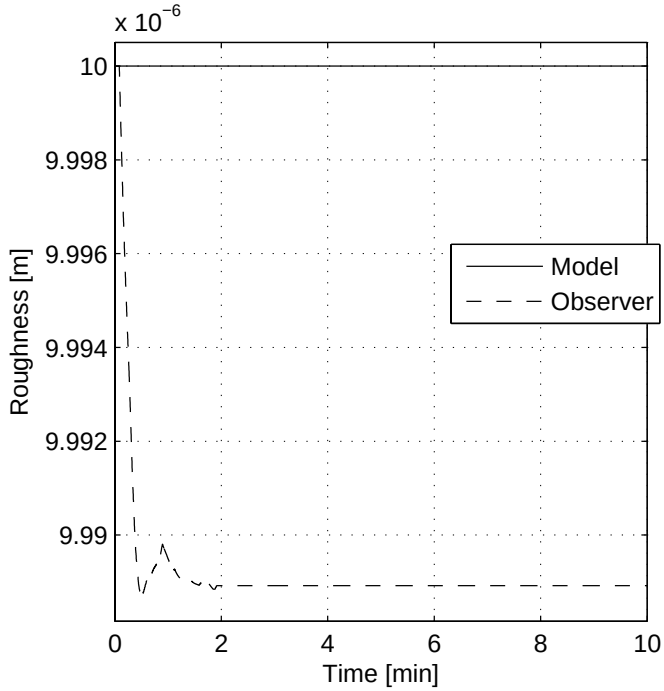

Figure 5.17: **Gas, stationary.** Estimation of roughness for an observer with temperature dynamics turned on. The estimation is turned off after 2 minutes due to the occurrence of a leak.

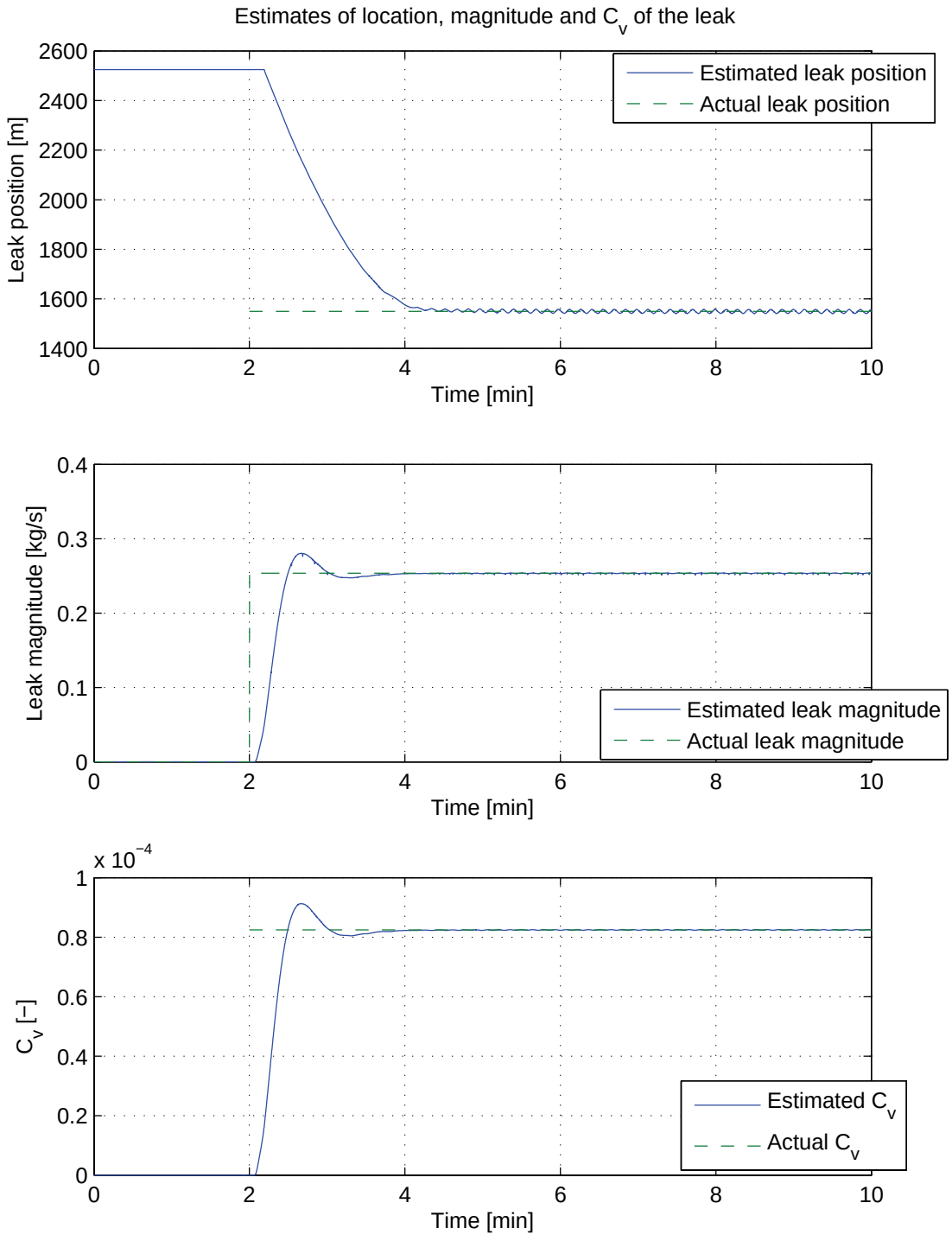

Figure 5.18: **Gas, stationary.** Estimates for a leak at 1550 m.

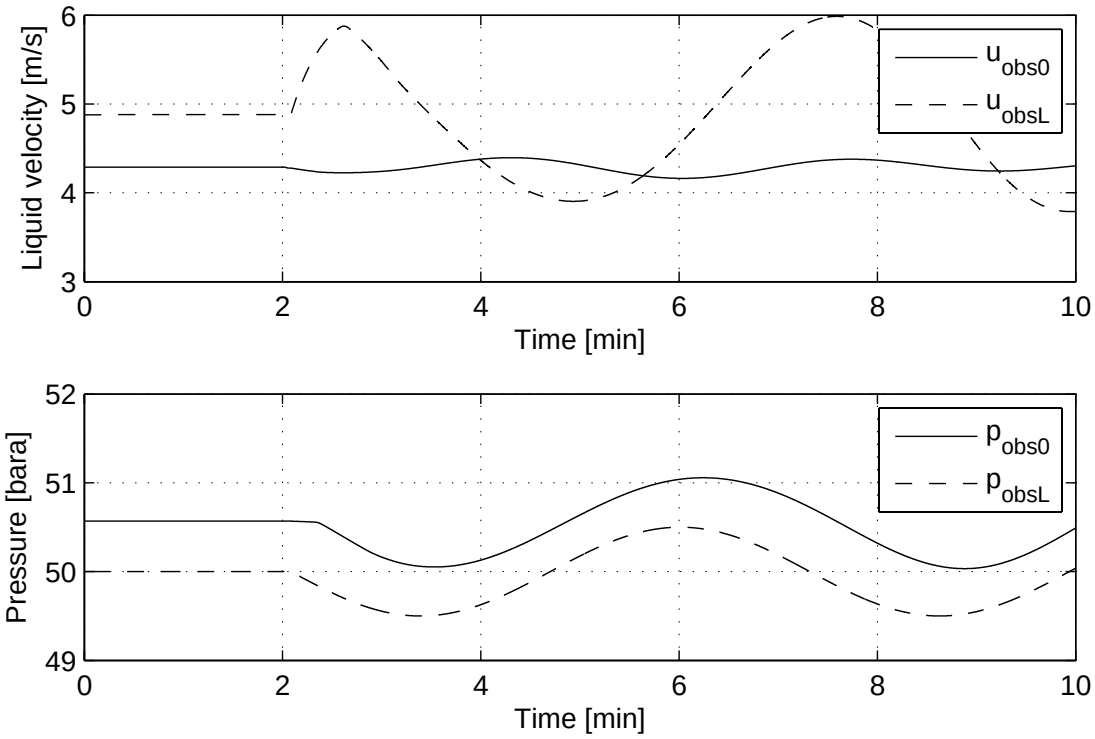

Figure 5.19: **Gas, sinusoid.** Sinusoidal varying boundaries for a leak at 750 m.

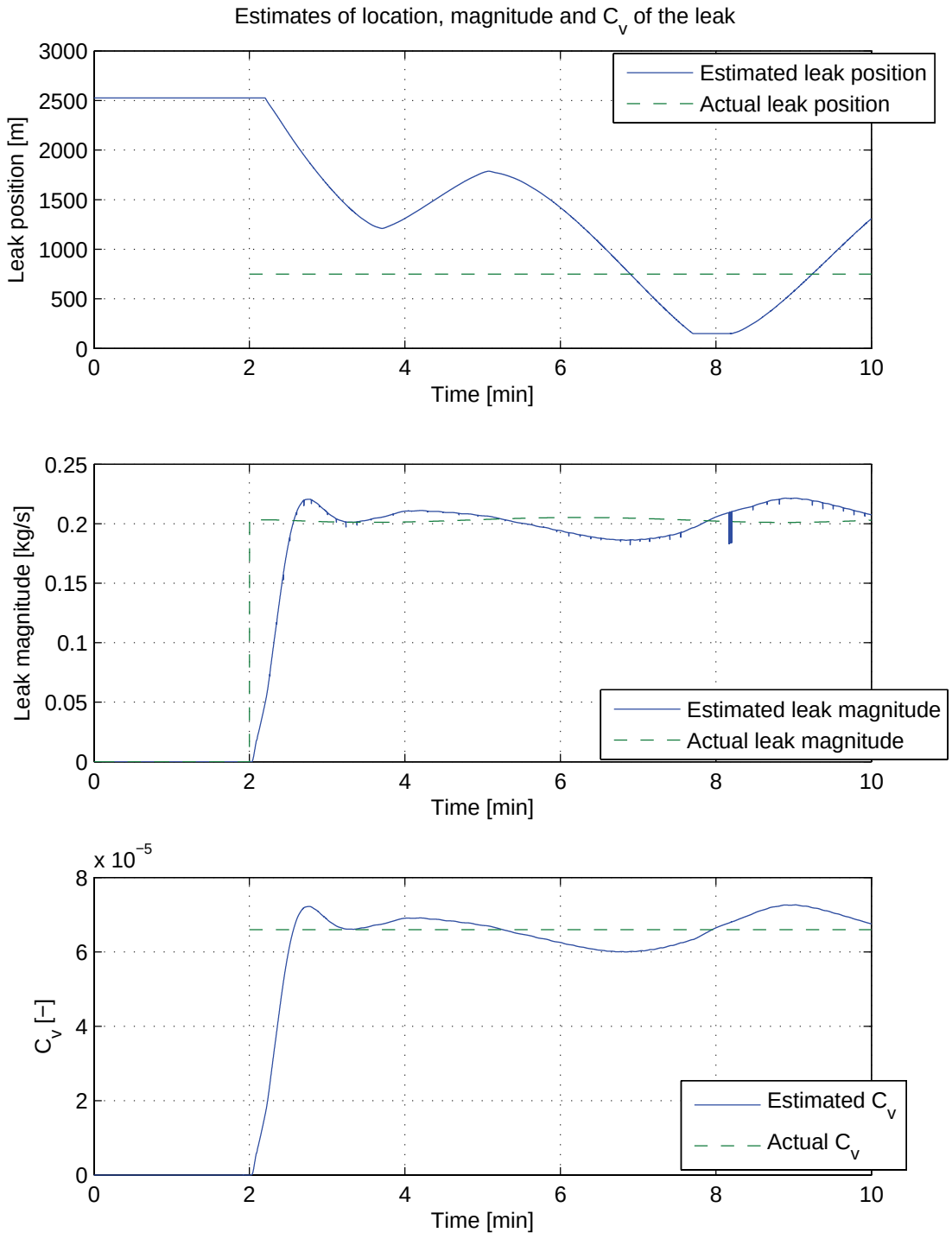

Figure 5.20: **Gas, sinusoid.** Estimates for a leak at 750 m.

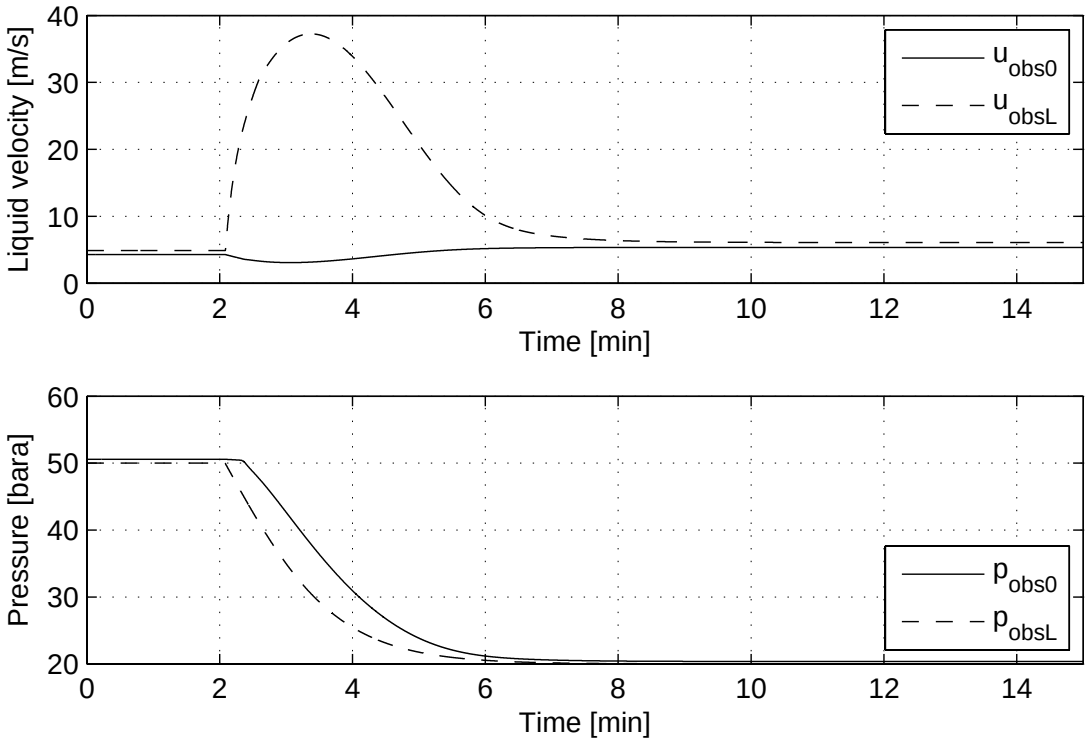

Figure 5.21: **Gas, shut down.** The boundaries during a shut down for a leak at 3850 m.

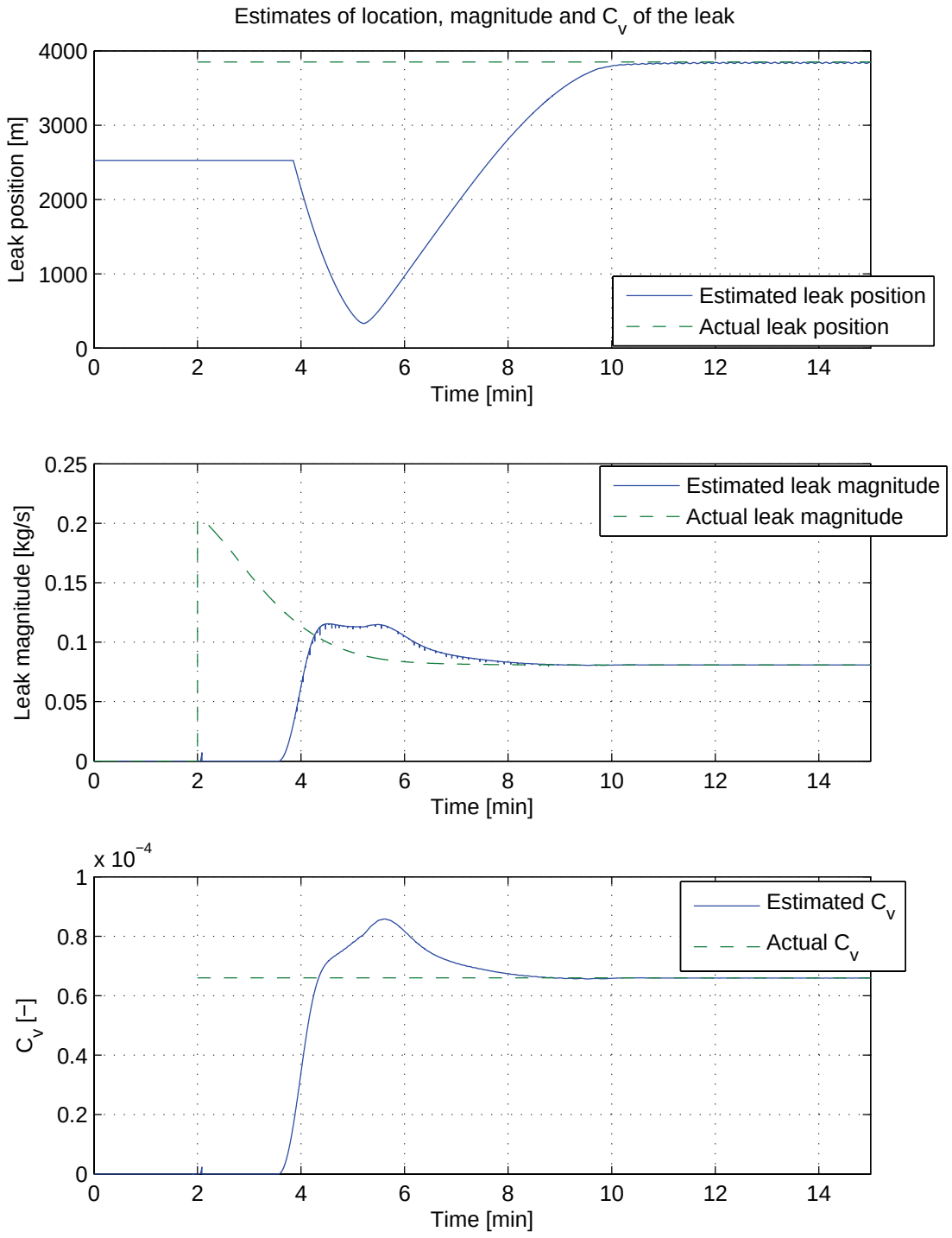

Figure 5.22: **Gas, shut down.** Estimates for a leak at 3850 m.

5.6 Multiple observers

In this section the OLGA observer is tested with a pipeline with a difference in altitude, which in fact is the pipeline between the Troll field in the North Sea and the mainland. Parameters for this pipeline, named Tor 1, is shown in Table A.4 and a plot of the profile can be seen in Figure 5.23. All simulations presented in this section were conducted with stationary flow of oil. The observer is an exact copy of the model and was initialized with the same values as listed in Table A.4. Temperature dynamics was turned on for all simulations and adaption of the friction coefficient turned off.

The following results shows the use of multiple observers with different starting point for the estimated leak position, different tuning of the update law and different backpressure at the leaks along the pipeline. In Figure 5.23 the location of the leaks and starting point of each observer are sketched. The observers are denoted observer 1 through 7, where in the four first observers the backpressure are dependent on the depth. The three last are initialized with a backpressure of 1 atm at every leak. The tuning and exact starting point for each of the observers can be found in Table 5.7 and Table 5.8. Table 5.9-5.14 show a summary for each of the observers where $\bar{x}_{l,\text{dev}}$ refers to mean of the deviation of the actual leak position in meters, $\bar{w}_{l,\text{dev}}$ is mean of the deviation from the actual leak magnitude in grams per second, w_l % denotes the minimum of the actual leak magnitude in percent of the initial mass rate at the inlet, and t_c is the time of convergence in minutes. For the calculation of the mean of the deviations $T = 3$ minutes, for the calculation of t_c $M = 1000$ meters and the length of the window was 30 seconds.

Observer	1	2	3	4
κ_x	2000	500	300	300
κ_u	$5 \cdot 10^{-3}$	$2 \cdot 10^{-2}$	$5 \cdot 10^{-2}$	$2 \cdot 10^{-2}$
k_0	0	0	0	0
k_L	0	0	0	0
starting point for $\hat{x}_l$	43230	50000	70000	80000

Table 5.7: Tuning and starting point of leak for the observers with ambient pressure depending on depth.

Observer	5	6	7
κ_x	500	600	600
κ_u	$2 \cdot 10^{-3}$	$7 \cdot 10^{-3}$	$7 \cdot 10^{-3}$
k_0	0	0	0
k_L	0	0	0
starting point for $\hat{x}_l$	50000	70000	80000

Table 5.8: Tuning and starting point of leak for the observers with uniform backpressure at each leak.

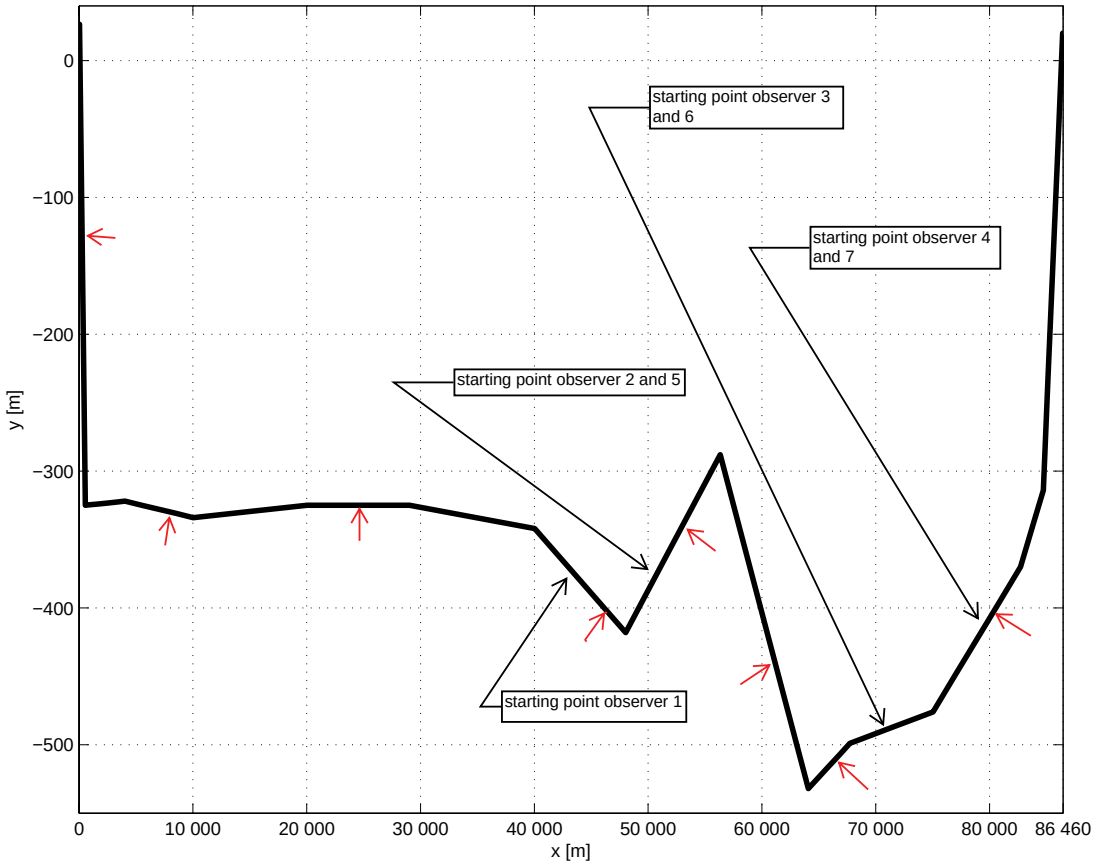

Figure 5.23: Profile of the Tor 1 pipeline with point of leaks marked with arrows and observer starting points marked with callout boxes.

		Position of leak [m]							
$\mathbf{C_v}$		292	7751	23645	46624	52766	61316	66474	81454
$1.65 \cdot 10^{-5}$	$\bar{x}_{l,\text{dev}}$	-266	27	56	-1	29	-548	3394	-2936
	$\bar{w}_{l,\text{dev}}$	-8	3	1	2	1	30	-39	113
	w_l %	1.39	1.24	1.11	0.89	0.79	0.73	0.54	0.25
	t_c	5	5	4	3	5	14	-	-
$8.25 \cdot 10^{-5}$	$\bar{x}_{l,\text{dev}}$	-297	323	75	157	25	2494	4687	-2936
	$\bar{w}_{l,\text{dev}}$	-41	24	13	4	8	-673	-3014	379
	w_l %	6.68	5.92	5.34	4.32	3.83	3.55	2.63	1.22
	t_c	3	8	5	15	5	14	-	-
$1.65 \cdot 10^{-4}$	$\bar{x}_{l,\text{dev}}$	-309	253	182	79	57	1453	9267	-2936
	$\bar{w}_{l,\text{dev}}$	-87	-22	-5	-8	-8	-591	-6190	713
	w_l %	12.72	11.25	10.2	8.32	7.39	6.9	5.1	2.4
	t_c	2	6	5	-	15	14	-	-

Table 5.9: **Observer 1.** Summary of simulations.

		Position of leak [m]	
$\mathbf{C_v}$		46624	52766
$1.65 \cdot 10^{-5}$	$\bar{x}_{l,\text{dev}}$	15	26
	$\bar{w}_{l,\text{dev}}$	5	7
	w_l %	0.89	0.79
	t_c	6	6
$8.25 \cdot 10^{-5}$	$\bar{x}_{l,\text{dev}}$	-25	-23
	$\bar{w}_{l,\text{dev}}$	19	28
	w_l %	4.32	3.83
	t_c	6	5
$1.65 \cdot 10^{-4}$	$\bar{x}_{l,\text{dev}}$	-14	-26
	$\bar{w}_{l,\text{dev}}$	29	45
	w_l %	8.32	7.39
	t_c	6	7

Table 5.10: **Observer 2.** Summary of simulations.

		Position of leak [m]	
$\mathbf{C_v}$		46624	52766
$1.65 \cdot 10^{-5}$	$\bar{x}_{l,\text{dev}}$	20	18
	$\bar{w}_{l,\text{dev}}$	1	1
	w_l %	0.89	0.79
	t_c	7	6
$8.25 \cdot 10^{-5}$	$\bar{x}_{l,\text{dev}}$	-20	3
	$\bar{w}_{l,\text{dev}}$	4	-1
	w_l %	4.32	3.83
	t_c	6	7
$1.65 \cdot 10^{-4}$	$\bar{x}_{l,\text{dev}}$	25	0
	$\bar{w}_{l,\text{dev}}$	4	-2
	w_l %	8.32	7.39
	t_c	5	7

Table 5.11: **Observer 5.** Summary of simulations.

		Position of leak [m]	
$\mathbf{C_v}$		61316	66474
$1.65 \cdot 10^{-5}$	$\bar{x}_{l,\text{dev}}$	-1618	-249
	$\bar{w}_{l,\text{dev}}$	-4	-1
	w_l %	0.73	0.54
	t_c	-	10
$8.25 \cdot 10^{-5}$	$\bar{x}_{l,\text{dev}}$	-55	-34
	$\bar{w}_{l,\text{dev}}$	2	-29
	w_l %	3.55	2.63
	t_c	9	7
$1.65 \cdot 10^{-4}$	$\bar{x}_{l,\text{dev}}$	54	54
	$\bar{w}_{l,\text{dev}}$	26	89
	w_l %	6.9	5.1
	t_c	6	7

Table 5.12: **Observer 3.** Summary of simulations.

		Position of leak [m]	
$\mathbf{C_v}$		61316	66474
$1.65 \cdot 10^{-5}$	$\bar{x}_{l,\text{dev}}$	26	-13
	$\bar{w}_{l,\text{dev}}$	0	2
	w_l %	0.73	0.54
	t_c	10	8
$8.25 \cdot 10^{-5}$	$\bar{x}_{l,\text{dev}}$	-22	-157
	$\bar{w}_{l,\text{dev}}$	6	18
	w_l %	3.55	2.63
	t_c	6	5
$1.65 \cdot 10^{-4}$	$\bar{x}_{l,\text{dev}}$	-30	-369
	$\bar{w}_{l,\text{dev}}$	8	58
	w_l %	6.9	5.1
	t_c	5	9

Table 5.13: **Observer 6.** Summary of simulations.

		Position of leak [m]	
$\mathbf{C_v}$		66474	81454
$1.65 \cdot 10^{-5}$	$\bar{x}_{l,\text{dev}}$	-6049	-923
	$\bar{w}_{l,\text{dev}}$	-12	4
	w_l %	0.54	0.25
	t_c	-	9
$8.25 \cdot 10^{-5}$	$\bar{x}_{l,\text{dev}}$	-1101	-1894
	$\bar{w}_{l,\text{dev}}$	-34	-58
	w_l %	2.63	1.22
	t_c	14	-
$1.65 \cdot 10^{-4}$	$\bar{x}_{l,\text{dev}}$	-391	-2046
	$\bar{w}_{l,\text{dev}}$	-110	129
	w_l %	5.10	2.40
	t_c	12	-

Table 5.14: **Observer 4.** Summary of simulations.

		Position of leak [m]	
$\mathbf{C_v}$		66474	81454
$1.65 \cdot 10^{-5}$	$\bar{x}_{l,\text{dev}}$	-1003	18
	$\bar{w}_{l,\text{dev}}$	-7	1
	w_l %	0.54	0.25
	t_c	14	4
$8.25 \cdot 10^{-5}$	$\bar{x}_{l,\text{dev}}$	23	277
	$\bar{w}_{l,\text{dev}}$	-4	-25
	w_l %	2.63	1.22
	t_c	8	8
$1.65 \cdot 10^{-4}$	$\bar{x}_{l,\text{dev}}$	-286	882
	$\bar{w}_{l,\text{dev}}$	75	-97
	w_l %	5.10	2.40
	t_c	10	-

Table 5.15: **Observer 7.** Summary of simulations.

5.6.1 Comments

Table 5.9 contains results for all of the points of leak to illustrate the need for multiple observers, while the other tables only deals with the leaks nearby.

5.7 Robustness

The method of leak detection presented in this report is based on measurements from the inlet and outlet of the pipeline. These measurements will have errors due to noise, biases, drifting etc. Also, in crude pipelines, effects such as wax deposition will affect the measurements and contribute to modelling error in the observer. The observer should preferably have the possibility to compensate for errors caused by biases and drifting by tuning a selection of appropriate parameters.

The simulations in this section were conducted with the model of the Tor 1 pipeline, depicted in Figure 5.23, carrying oil. The point of leak were chosen to be at 36643 meters which is in an area with a slight inclination. Previous simulations have showed that the observer has been able to efficiently locate and quantify leaks in this region. The initial point of leak in the observer is 43230 m for all of the simulations and the tuning can be seen in Table A.6.

Both the model and observer are initialized with the values from Table A.4 and the flow is stationary.

5.7.1 Biased measurements

In this subsection the effect of biased measurements from the model during leak detection is studied. The measurements of velocity, pressure and temperature are each added a bias, but only one at a time which leaves out the effect of cross-correlations. The biases are added at both the inlet and outlet measurements for pressure and mass rate. The temperature bias is added at the inlet. The measurements are expected to have biases according to Table 5.16.

Mass rate	Pressure	Temperature
±1.0 % of range	±0.1 bar	±0.1 °C

Table 5.16: The expected biases of the measured signals from the model.

The range of the multiphase meter is assumed to be twice the initial mass rate at the inlet, namely 200 kg/s.

The Tables 5.17, 5.19, 5.21 and 5.23 contain the summary from the results of a robustness study where the measured mass rate, pressure and temperature from the model are added a constant bias one at a time. In these cases there were no estimation of roughness prior to the event of a leak. Whereas in Table 5.18, 5.20, 5.22 and 5.24 adaptation of the roughness was carried out ahead of the occurrence of the leak and then turned off.

The uppermost row shows the bias and the leftmost column the leak magnitude in percent of the initial mass rate. The denomination for the listed values are: $\bar{x}_{l,\text{dev}}$,

meters; $\bar{w}_{l,\text{dev}}$, gram per second; t_c, minutes. The mean of the deviation from the exact values are computed with $T = 3$ minutes. t_c is evaluated with a window of 30 second and $M = 1000$ meters. The duration of the simulations were 15 minutes and Δt_{obs} was 0.1 seconds.

		-0.125 %	-0.063 %	0 %	0.063 %	0.125 %
0.20 %	$\bar{x}_{l,\text{dev}}$	-33240	-5897	134	16639	30502
	$\bar{w}_{l,\text{dev}}$	13	-1	0	2	7
	t_c	-	-	5	-	-
0.50 %	$\bar{x}_{l,\text{dev}}$	-2854	-6364	46	6657	13142
	$\bar{w}_{l,\text{dev}}$	-2	-1	0	1	2
	t_c	-	-	3	-	-
0.99 %	$\bar{x}_{l,\text{dev}}$	-6459	-3173	6	3263	6635
	$\bar{w}_{l,\text{dev}}$	-1	-1	0	1	2
	t_c	-	-	4	-	-

Table 5.17: A small bias added to the mass rate without estimation of roughness.

		-0.125 %	-0.063 %	0 %	0.063 %	0.125 %
0.20 %	$\bar{x}_{l,\text{dev}}$	-32	7	38	85	83
	$\bar{w}_{l,\text{dev}}$	-1	1	1	2	2
	t_c	6	6	6	5	5
0.50 %	$\bar{x}_{l,\text{dev}}$	-50	-16	12	27	55
	$\bar{w}_{l,\text{dev}}$	-2	-1	0	1	2
	t_c	6	3	3	3	3
0.99 %	$\bar{x}_{l,\text{dev}}$	-45	-29	-10	8	20
	$\bar{w}_{l,\text{dev}}$	-2	-1	1	2	2
	t_c	4	4	4	4	4

Table 5.18: A small bias added to the mass rate with estimation of roughness.

		-1.0 %	-0.5 %	0 %	0.5 %	1.0 %
0.20 %	$\bar{x}_{l,\text{dev}}$	-47747	-47747	38	36555	36555
	$\bar{w}_{l,\text{dev}}$	34	46	1	4	6
	t_c	-	-	6	-	-
0.50 %	$\bar{x}_{l,\text{dev}}$	-47747	-47747	12	36555	36555
	$\bar{w}_{l,\text{dev}}$	93	133	0	9	11
	t_c	-	-	3	-	-
0.99 %	$\bar{x}_{l,\text{dev}}$	-47747	-47747	-10	27024	36555
	$\bar{w}_{l,\text{dev}}$	204	-5	1	8	19
	t_c	-	-	4	-	-

Table 5.19: A relatively large bias added to the mass rate without estimation of roughness.

		-1.0 %	-0.5 %	0 %	0.5 %	1.0 %
0.20 %	$\bar{x}_{l,\text{dev}}$	-943	-502	134	346	987
	$\bar{w}_{l,\text{dev}}$	-13	-7	0	6	12
	t_c	14	6	5	5	14
0.50 %	$\bar{x}_{l,\text{dev}}$	-675	-264	46	192	650
	$\bar{w}_{l,\text{dev}}$	-15	-7	0	7	12
	t_c	7	6	3	3	3
0.99 %	$\bar{x}_{l,\text{dev}}$	-512	-222	6	163	469
	$\bar{w}_{l,\text{dev}}$	-14	-7	0	7	12
	t_c	7	6	4	4	4

Table 5.20: A relatively large bias added to the mass rate with estimation of roughness.

		-0.10 bar	-0.05 bar	0 bar	0.05 bar	0.10 bar
0.20 %	$\bar{x}_{l,\text{dev}}$	-3136	-493	134	1983	3564
	$\bar{w}_{l,\text{dev}}$	1	1	0	-1	-1
	t_c	-	-	5	-	-
0.50 %	$\bar{x}_{l,\text{dev}}$	-201	-648	46	808	1381
	$\bar{w}_{l,\text{dev}}$	1	1	0	-1	-1
	t_c	-	6	3	3	-
0.99 %	$\bar{x}_{l,\text{dev}}$	-686	-259	6	326	752
	$\bar{w}_{l,\text{dev}}$	1	1	0	0	-1
	t_c	7	6	4	4	10

Table 5.21: Perturbing pressure without estimation of the roughness.

		-0.10 bar	-0.05 bar	0 bar	0.05 bar	0.10 bar
0.20 %	$\bar{x}_{l,\mathrm{dev}}$	82	53	38	109	-15
	$\bar{w}_{l,\mathrm{dev}}$	3	3	1	2	-1
	t_c	5	5	6	6	7
0.50 %	$\bar{x}_{l,\mathrm{dev}}$	-10	-4	12	5	-13
	$\bar{w}_{l,\mathrm{dev}}$	1	1	0	-1	-1
	t_c	3	3	3	3	3
0.99 %	$\bar{x}_{l,\mathrm{dev}}$	-27	-25	-10	-4	5
	$\bar{w}_{l,\mathrm{dev}}$	2	1	1	0	-1
	t_c	4	4	4	4	4

Table 5.22: Perturbing pressure with estimation of roughness.

		-0.10 °C	-0.05 °C	0 °C	0.05 °C	0.10 °C
0.20 %	$\bar{x}_{l,\mathrm{dev}}$	-264	54	134	530	852
	$\bar{w}_{l,\mathrm{dev}}$	-1	2	0	0	0
	t_c	6	5	5	5	5
0.50 %	$\bar{x}_{l,\mathrm{dev}}$	-88	-8	46	148	243
	$\bar{w}_{l,\mathrm{dev}}$	-1	-1	0	1	1
	t_c	3	3	3	3	3
0.99 %	$\bar{x}_{l,\mathrm{dev}}$	-58	-25	6	53	93
	$\bar{w}_{l,\mathrm{dev}}$	-1	-1	0	1	1
	t_c	4	4	4	4	4

Table 5.23: Perturbing temperature without estimation of roughness.

		-0.10 °C	-0.05 °C	0 °C	0.05 °C	0.10 °C
0.20 %	$\bar{x}_{l,\mathrm{dev}}$	-20	15	38	73	104
	$\bar{w}_{l,\mathrm{dev}}$	-1	1	1	1	1
	t_c	5	5	6	6	6
0.50 %	$\bar{x}_{l,\mathrm{dev}}$	-9	1	12	26	37
	$\bar{w}_{l,\mathrm{dev}}$	-1	0	0	0	1
	t_c	3	3	3	6	6
0.99 %	$\bar{x}_{l,\mathrm{dev}}$	-30	-21	-10	15	14
	$\bar{w}_{l,\mathrm{dev}}$	0	0	1	1	1
	t_c	4	4	4	4	4

Table 5.24: Perturbing temperature with estimation of roughness.

5.7.2 Difference in grid size

The OLGA model of the Tor 1 pipeline, with specifications from Table A.4 used to produce input data to the observer, consists of 16 pipes and 100 segments. In this section the new OLGA model of the same pipeline is constructed. This model has the same pipeline profile, but each pipe is divided into shorter segments so the total number of segments sums up to 198. The OLGA observer however is unchanged with the purpose to induce a modelling error. Both the observer and the model are as specified in Table A.4, except for the number of sections which is specified above.

Three different observers have are tested with the data from the new model. These are denoted observer A, B and C. Observer A has no adaption of roughness and the backpressure is set to 1 atm for every leak along the pipeline. Observer B is similar to A, except for having adaption of roughness prior to the occurrence of the leak. Observer C has backpressure at each leak depending on the depth and adaption of roughness prior to the occurrence of the leak. The tuning of the observers are the same and can be seen in Table A.7. The starting point of the leak is at the middle of the pipeline at 43230 meters. Two plots of the results of the simulations are presented in Figure 5.24 and Figure 5.25. A summary is shown in Table 5.25 where the mean of the deviation from the exact values are computed with $T = 3$ minutes. t_c is evaluated with a window of 30 second and $M = 1000$ meters. The duration of the simulations were 15 minutes and Δt_{obs} was 0.1 seconds. In the leftmost column the mass rate of the leakage in percent of initial mass rate at the inlet is listed at the respective position.

Leak position		Observer A	Observer B	Observer C
23884 m, $w_l = 3.35\%$	$\bar{x}_{l,\text{dev}}$[m]	-566	-100	-29
	$\bar{w}_{l,\text{dev}}$[g/s]	-26	-26	-12
	t_c [min]	8	8	7
51774 m, $w_l = 5.67\%$	$\bar{x}_{l,\text{dev}}$[m]	-160	67	-46
	$\bar{w}_{l,\text{dev}}$[g/s]	-23	-24	-8
	t_c [min]	9	7	6
61102 m, $w_l = 1.49\%$	$\bar{x}_{l,\text{dev}}$[m]	-614	73	-386
	$\bar{w}_{l,\text{dev}}$[g/s]	-12	-11	40
	t_c [min]	8	9	11
65790 m, $w_l = 1.15\%$	$\bar{x}_{l,\text{dev}}$[m]	-471	467	3443
	$\bar{w}_{l,\text{dev}}$[g/s]	-22	-20	-284
	t_c [min]	-	9	-

Table 5.25: Summary table for the comparison of various observers with model error.

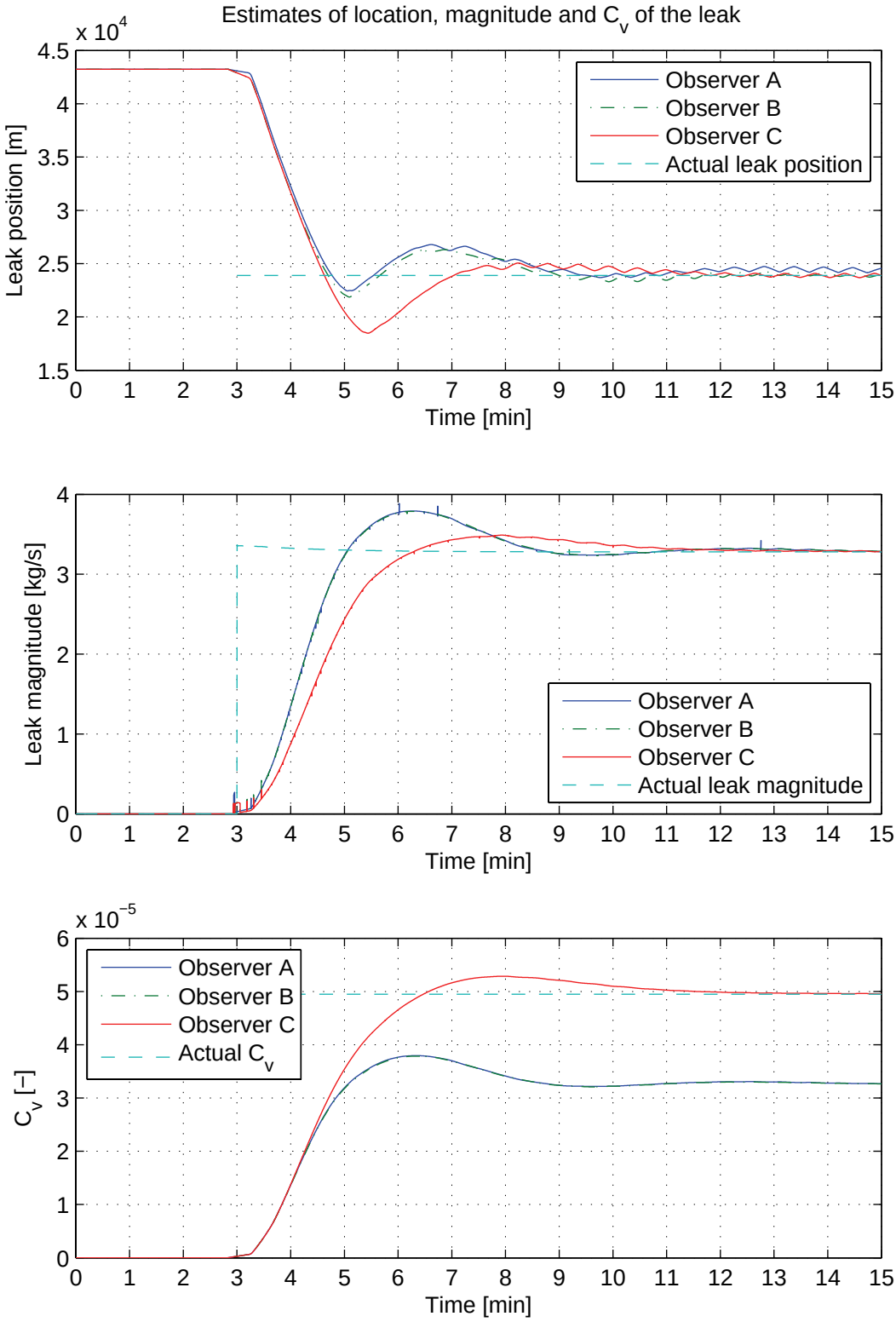

Figure 5.24: **Oil, stationary.** Estimates for a leak at 23884 m. The leak magnitude is 3.3 % of the mass rate at the inlet

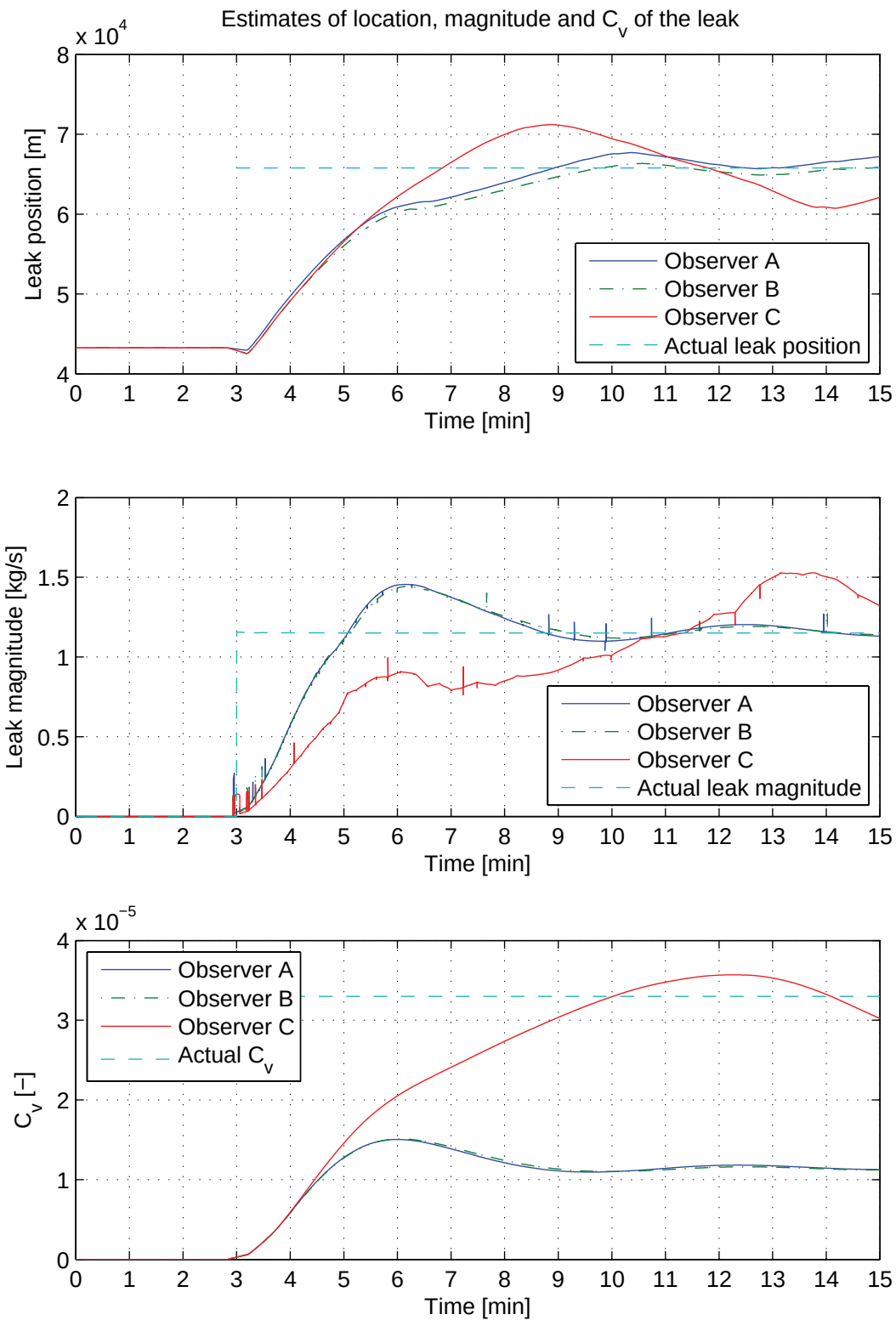

Figure 5.25: **Oil, stationary.** Estimates for a leak at 65790 m. The leak magnitude is 1.2 % of the mass rate at the inlet

5.8 Time-varying boundaries

During operation the mass flow through the pipeline will change with changes in production. Also, controlling the pressure in the separator with the topside choke will affect the pressure and the flow in the pipeline. It is therefore vital that the observer is capable of locating and quantifying a leakage under these conditions. It is also more likely for a pipeline to burst when the rate of production is changed, especially during start up.

The observer is designed to handle time-varying boundary conditions, but there will always be a slight delay of the convergence in terms of p and u when the boundaries are changing. This delay affects the estimates of the leak parameters and may cause them to drift off until the flow is fairly stationary.

In the following three cases are presented, namely shut down, start up and sinusoidal varying boundaries. The shut down is not a complete shut down since the leak needs to actually be present in order to be detected. The rate of the shut down is also restricted by the range of the tab-file which OLGA uses as look-up table for density, viscosity and such. The results from the shut down case are presented in Figure 5.26-5.28. Figure 5.29-5.31 treat a leak occurring during a start up and Figure 5.32-5.34 deals with sinusoidal varying boundaries while there is a leak. All cases concern the Tor 1 pipeline carrying oil.

The model data were produced with an OLGA model as specified in Table A.4. The observers tuning and starting points can be seen in Table A.8. The observers have uniform backpressure at each leak of 1 atm but is otherwise an exact copy of the model. Δt_{obs} is 0.1 s and no adaption of roughness is carried out. The magnitudes of the leaks can be seen in Table 5.26 and a summary of the simulations are shown in Table 5.27 where t_c is evaluated with $M = 1000$ m and a window of 30 s, and the deviations from the mean values are computed during the last 3 minutes of the simulations.

	21644 m, shut down	5758 m, start up	5758 m, sinusoid
max	2.29 %	2.56 %	2.79 %
min	1.20 %	1.88 %	2.21 %

Table 5.26: Maximum and minimum of leak magnitude in percent of the initial mass flow.

	21644 m, shut down	5758 m, start up	5758 m, sinusoid
$\bar{x}_{l,\text{dev}}$[m]	-50	-19	243
$\bar{w}_{l,\text{dev}}$[g/s]	-3	12	-83
t_c [min]	7	-	-

Table 5.27: Summary table, leakage with gas flow with temperature dynamics.

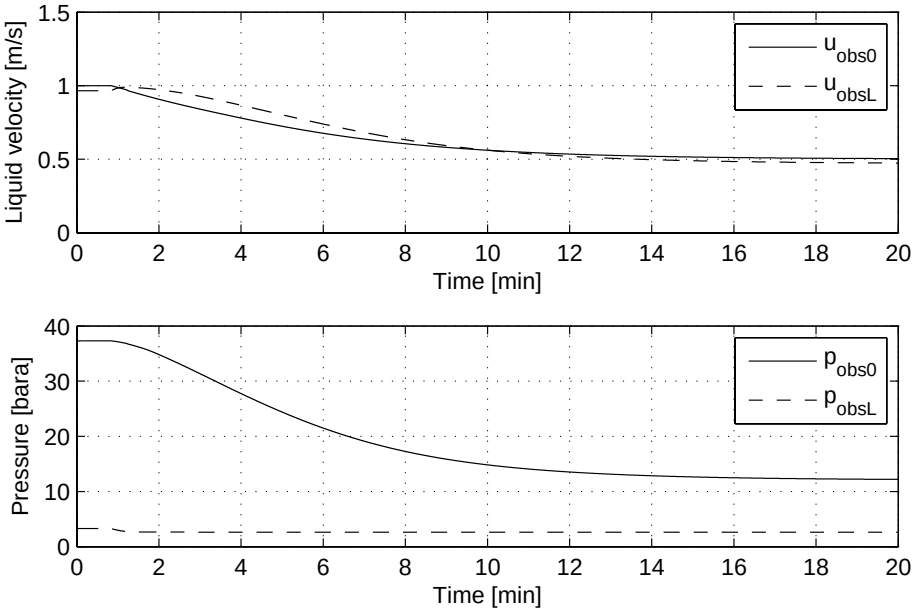

Figure 5.26: **Oil, shut down.** Observer boundaries during a shut down with a leak at 21664 m.

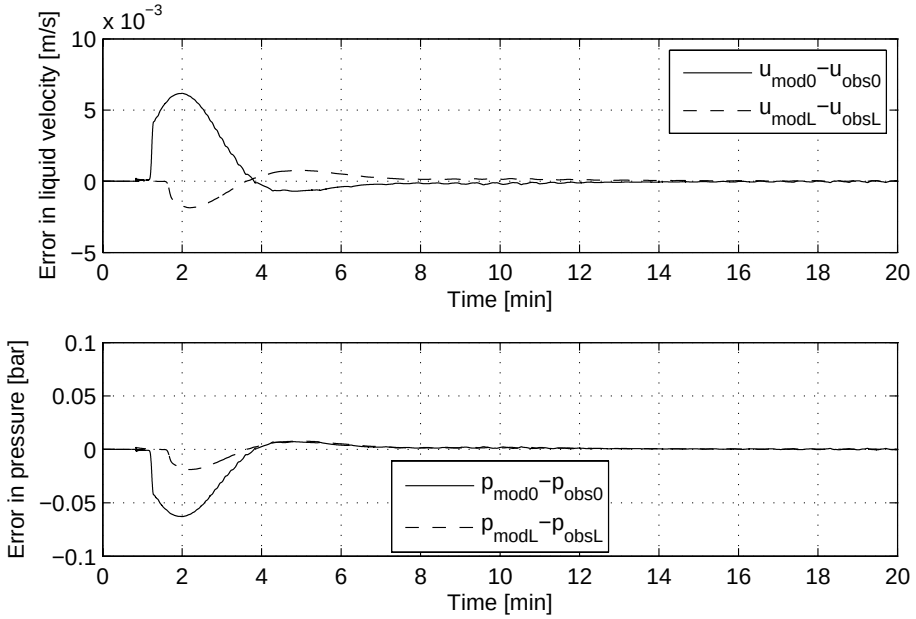

Figure 5.27: **Oil, shut down.** Observer error during a shut down with a leak at 21664 m.

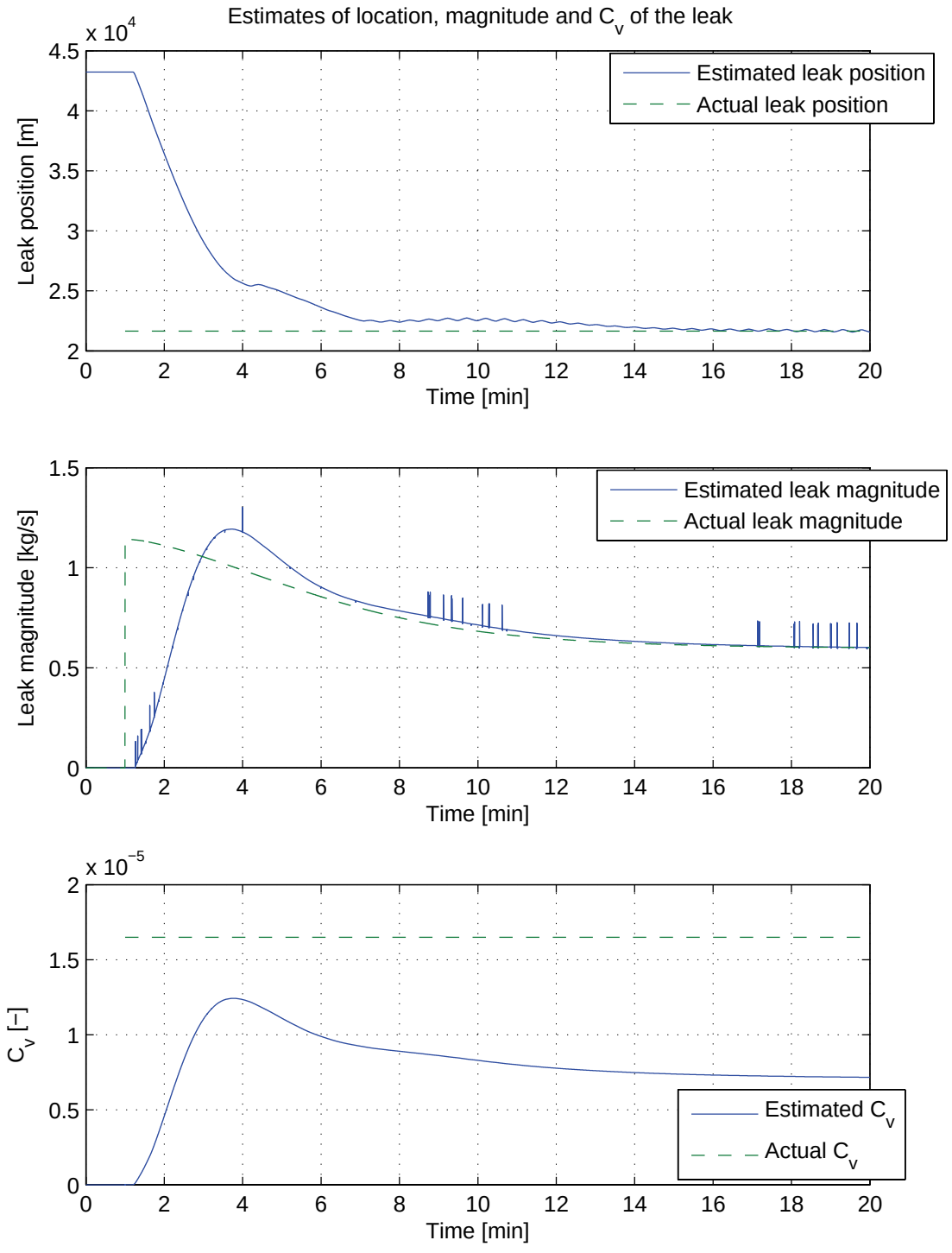

Figure 5.28: **Oil, shut down.** Estimates during a shut down with a leak at 21664 m.

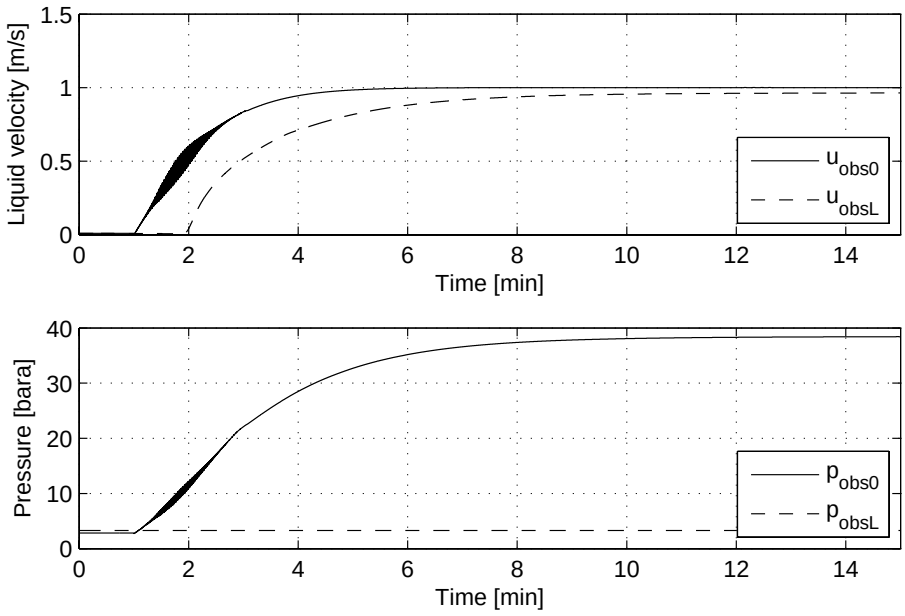

Figure 5.29: **Oil, start up.** Observer boundaries during a start up with a leak at 5758 m.

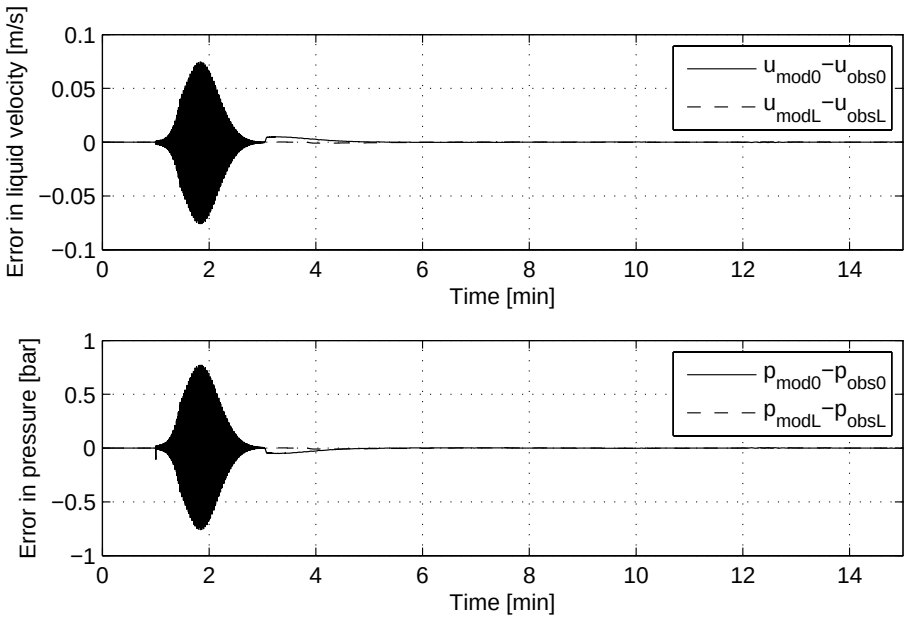

Figure 5.30: **Oil, start up.** Observer error during a start up with a leak at 5758 m.

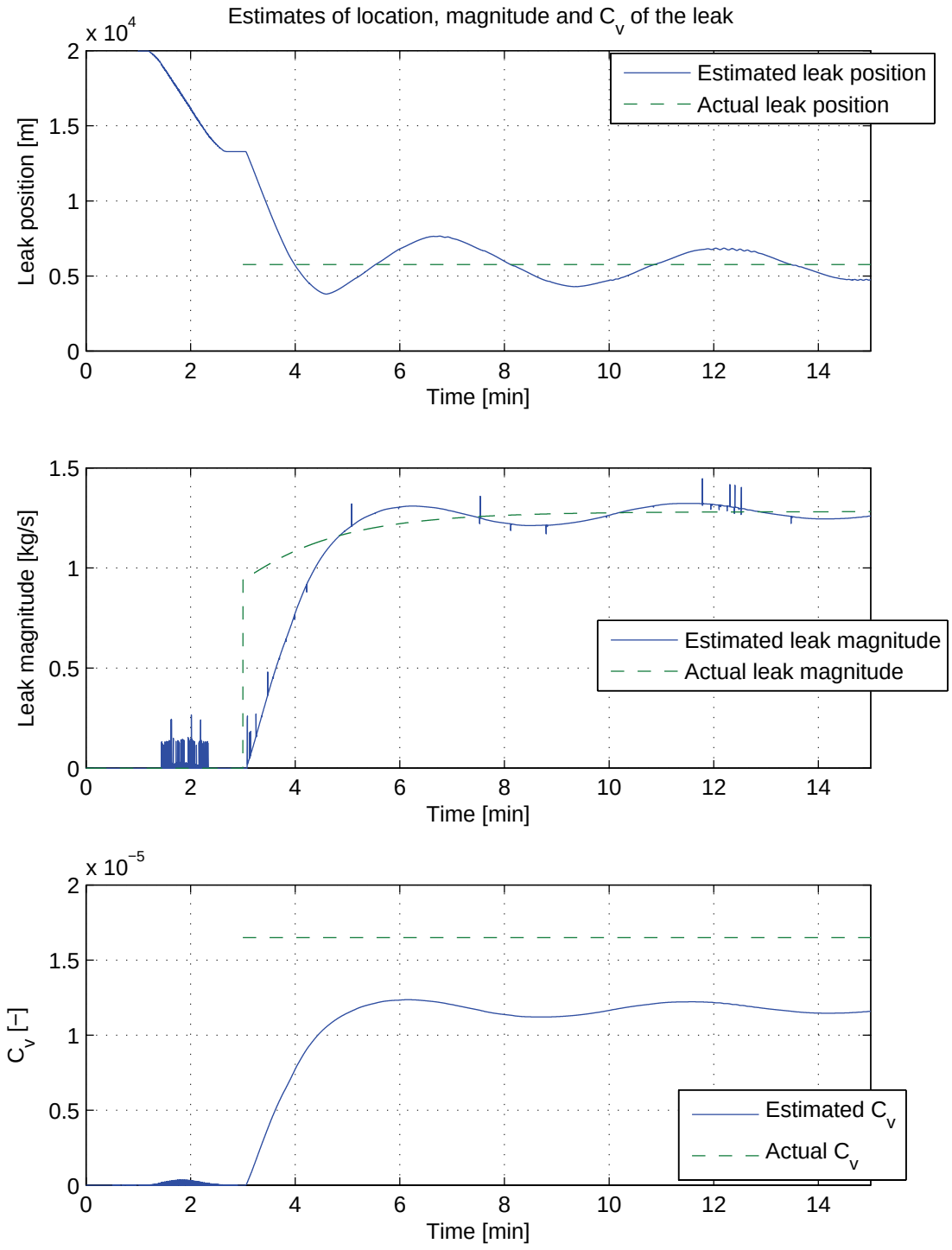

Figure 5.31: **Oil, start up.** Estimates during a start up with a leak at 5758 m.

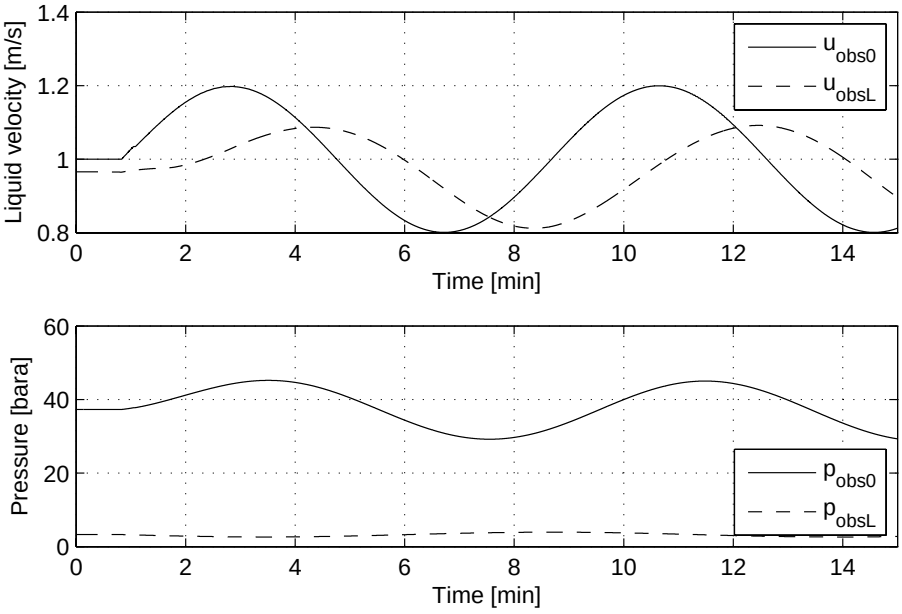

Figure 5.32: **Oil, sinusoid.** Observer boundaries varying as sinusoids with a leak at 5758 m.

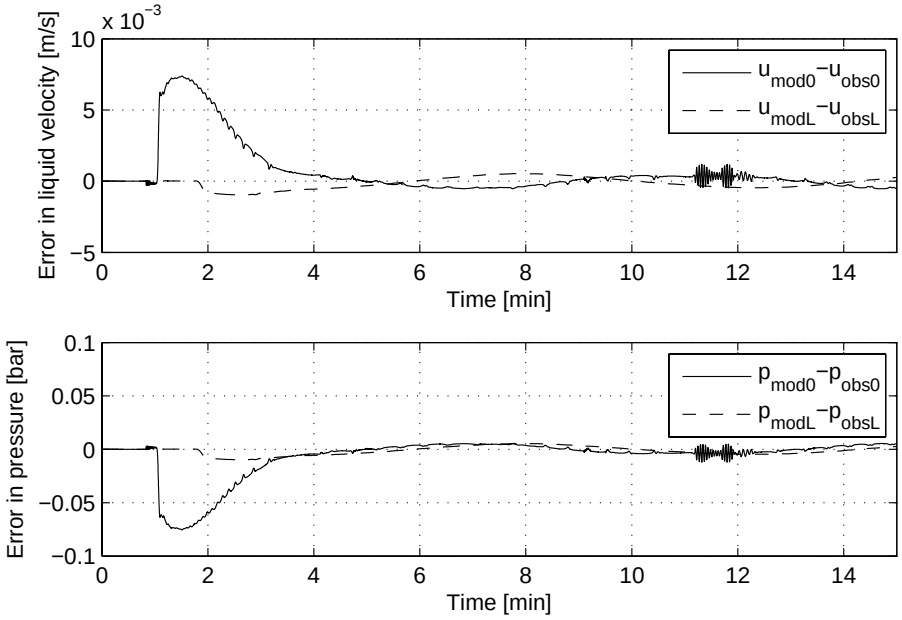

Figure 5.33: **Oil, sinusoid.** Observer error with a leak at 5758 m.

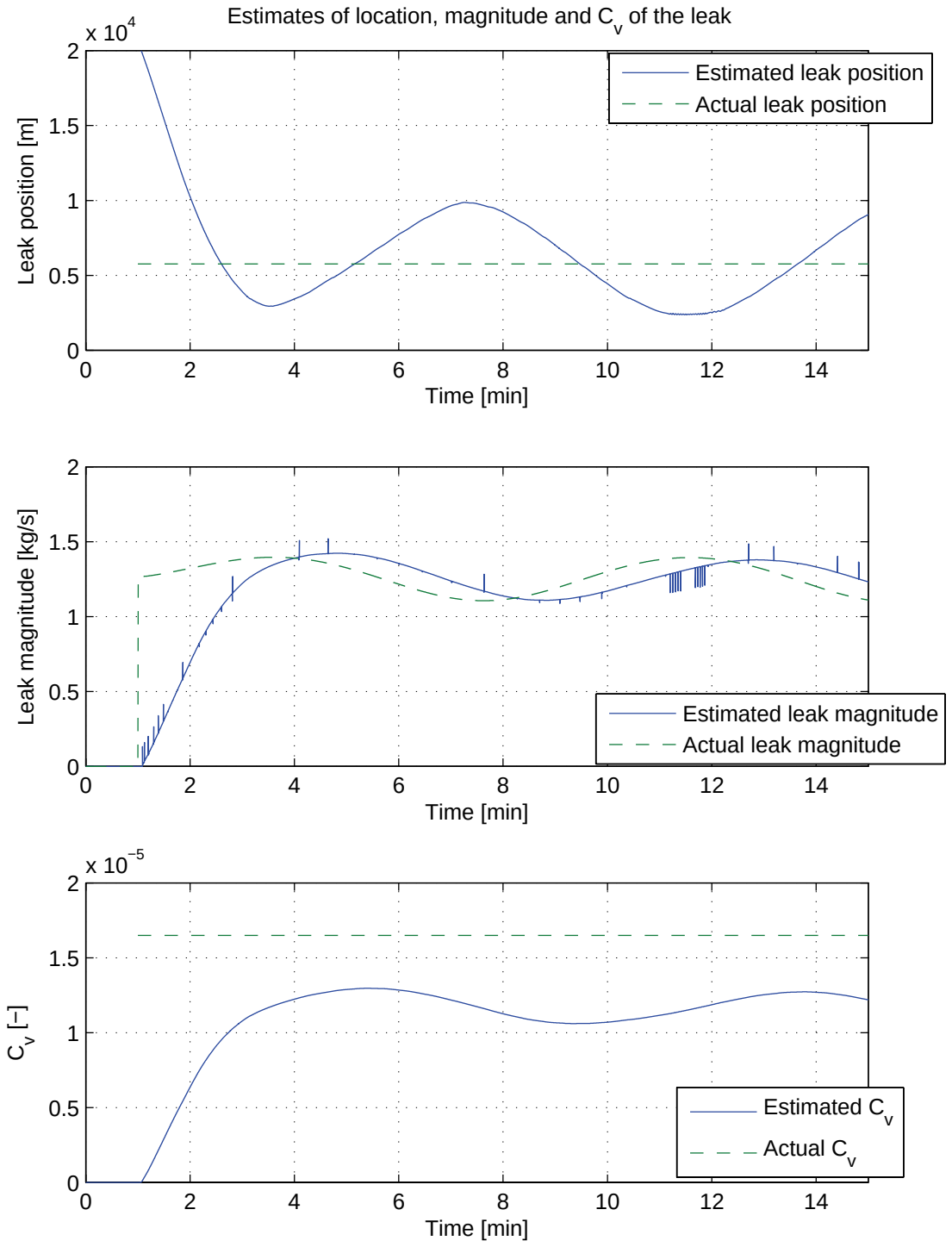

Figure 5.34: **Oil, sinusoid.** Estimates for sinusoidal varying boundary conditions with a leak at 5758 m.

5.9 Estimation of mass rate

In this section two different ways of estimating the leak magnitude is compared. One observer estimates the control signal $\hat{u}_s$ which is multiplied with $\hat{C}_d A_{\text{opening}}$ to give $\hat{C}_v$. The other estimates the leak mass rate w_l directly as specified in Section 4.6.

The test was conducted with the model of the Tor 1 pipeline with temperature dynamics turned on. Adaption of roughness was done prior to the leakage at 67387 meters. The flow was stationary during the period of the simulations which were 20 minutes. Maximum leak magnitude in percent of mass rate at the inlet was 3.1%. Δt_{obs} was 0.1 seconds. Tuning of the observer can be found in Table A.9. The starting point of the observer was at the middle of the pipeline, namely 43230 m.

The estimates are shown in Figure 5.35.

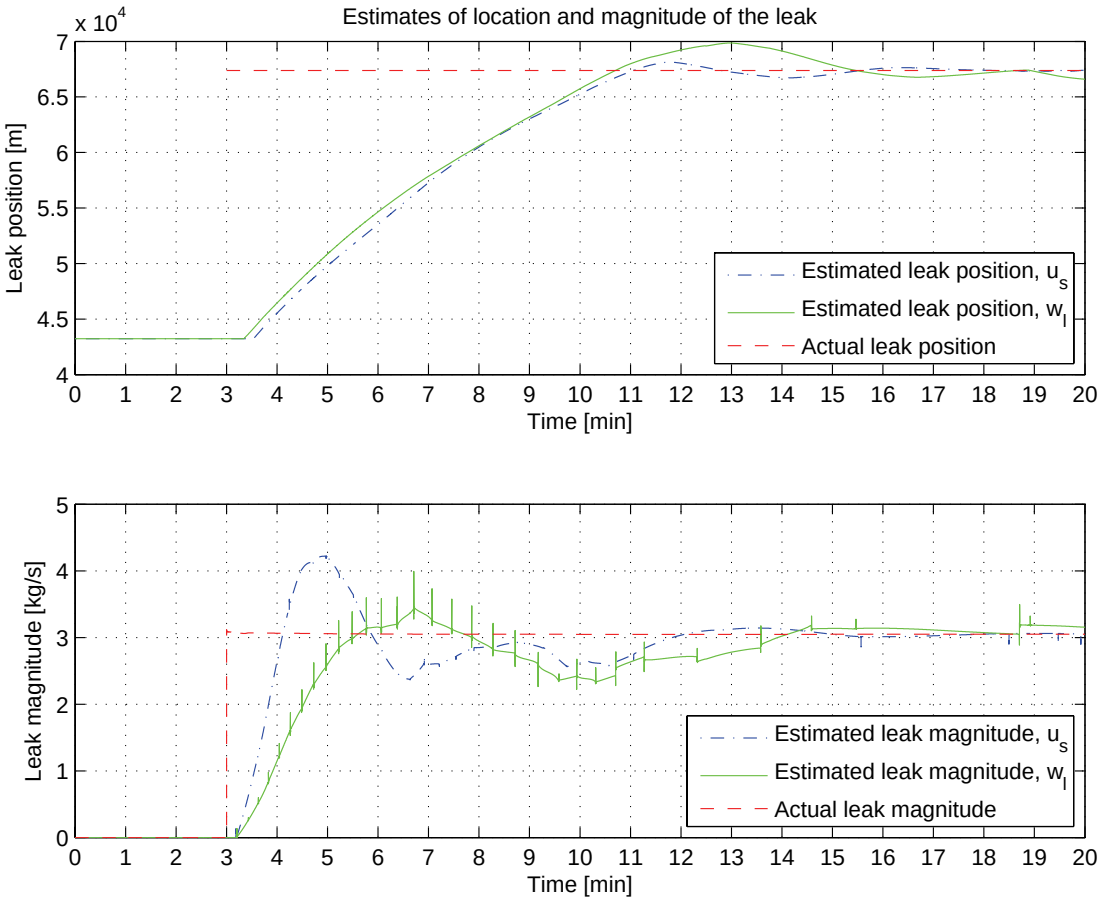

Figure 5.35: **Oil, stationary.** Comparison of estimations of $\hat{C}_v$ and $\hat{w}_l$.

5.10 Tor 1 carrying gas

In this section a plot of the estimated leak parameters for a case with gas flow in the Tor 1 pipeline is presented. Both the model and observer were initialized with the values in Table A.4 and are also as specified in this table. The tuning of the observer can be found in Table A.10. The starting point of the observer is at 10000 m and the leak magnitude is 11% of the mass rate at the inlet.

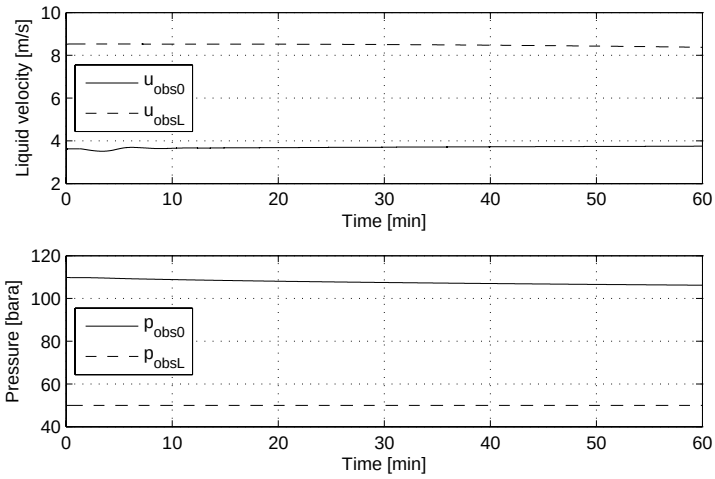

Figure 5.36: **Gas, stationary.** The boundaries of the observer for a leak at 8709 m.

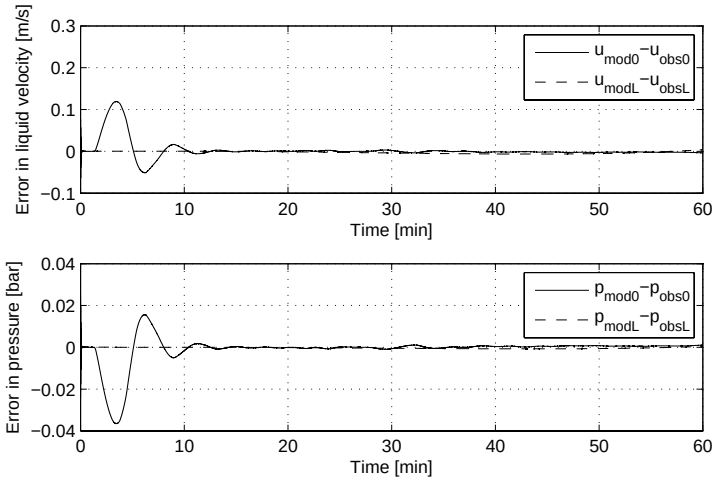

Figure 5.37: **Gas, stationary.** Observer error with gas flow and a leak at 8709 m.

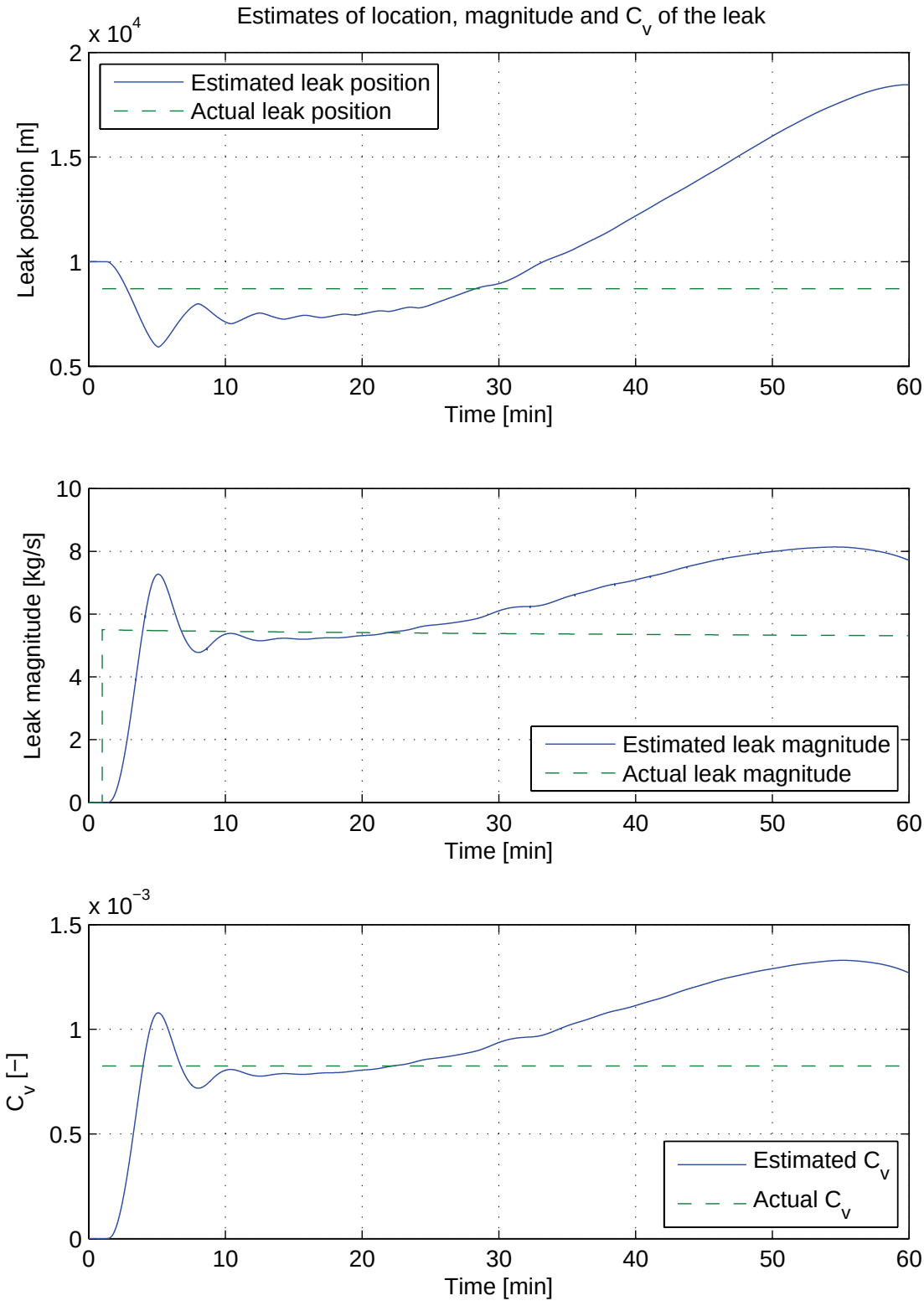

Figure 5.38: **Gas, stationary.** A failed attempt to locate a leak at 8709 m.

5.11 Discussion

Simulations in this chapter have covered a wide range of cases with different types of observers, pipelines and production rates which will be discussed in this section. The $\mathcal{L}_2$-norm of the observer error was the first result presented which showed that even though there are no formal proof for this type of convergence with the OLGA observer, employing output injection induces the favorable convergence properties as seen with the Matlab observer in (Hauge, 2006). The most vital property, being the ability to converge in terms of p and u in the time it takes a pressure wave to travel back and forth through the pipeline, is kept up. This also worked flawlessly for observers monitoring pipelines with varying altitude carrying oil and straight pipelines carrying gas.

Adaption of a friction coefficient was introduced to handle modelling errors and this method was tested with an OLGA observer monitoring an OLGA model. Simulations, where the observer was an exact copy of the model, revealed that the estimated roughness did not match the one of the model. This must have been caused by a dissemblance in differential pressure and velocity through the pipeline between the observer and model. This deviation might originate from the extrapolation of the pressure at the outlet when producing model data, or maybe through the conversion of velocity to mass rate at the inlet.

Adjusting the roughness of the pipeline by adaptation had positive effects for the cases with biases and model errors. The tolerance of the observer regarding biases was rather poor, driving the estimate of $\hat{x}_l$ to wrong values, but this was coped with by estimation of the roughness prior to the leak. There is a problem with estimating the roughness concurrently with the adaption of the leak parameters because all three update laws will respond to a change in the observer error at inlet and outlet. For instance, if all of the three parameters $\hat{u}_s$, $\hat{x}_l$ and ζ are estimated concurrently, which one will react when a small leak occurs? This will of course be affected by the tuning of each of the update laws, but even though the adaption of roughness is slower than the adaption of magnitude, there is no guarantee that the estimated value of the magnitude will converge to the correct value. Most likely the adaption of roughness would corrupt the detection. This can be solved simply by running two observers simultaneously where one adapts roughness and the other the leak parameters. The roughness estimated in the former observer, let's denote it observer R, is set in the latter, observer L, until it signalizes that a leak might have occurred, and then the adaption of roughness is turned off. By setting the adapted roughness from observer R to observer L once in a while, for instance once a day instead of every time step, the chance for an interaction between the estimates would be minimal. This would be possible because of the different time scale between a change in roughness and a pipeline burst.

The equation used to model the leakage did not prove to be an exact copy of the one used in OLGA, but it was seemingly good enough for this purpose. For the cases with stationary flow, there was only a multiplicative constant that distinguished the unknown

valve equation from the one used in this work. For the case with time-varying boundaries there was a minor difference from the former case mentioned due to ripples in the plot of the ratio. These ripples were small compared to the ratio and would most likely not affect the adaption of C_v noticeably. Simulations covering a wide range of cases have shown that the modelling is sufficiently accurate, and can also be said to be robust due to its simplicity. Comparing a simulation of the estimation of mass rate to another with estimation of C_v, demonstrated the benefits of the latter scheme. With only one case supporting this claim, more effort could have been spent on tuning and testing with adaption of w_l to get a broader set of results, but this type of research was not the scope of this thesis and was therefore neglected.

The method of distributing the leakage over two nodes showed not to be as well suited as expected since it was in need of a uniform grid to keep $f_{l,1}$ and $f_{l,2}$ positive or zero for all possible leak positions. This problem was dealt with by using logic which kept the two leakages positive under all circumstances. There is a possible problem with this solution which could occur when the leakage in the observer is supposed to be shared over two nodes but is only present in one node. This could restrain the adaption of the position since the seemingly continuous movement of the leakage stops. But this issue has never emerged during simulations, most likely because the observer is excited through the nonlinearity in the update law for the position adaption.

The work done in (Hauge, 2006) involved an observer written in Matlab which was tested with a model also written in Matlab. It was therefore desirable to test this observer with data produced with a state of the art computational fluid dynamics simulator, namely OLGA. Comparing the estimates for the Matlab observer with the ones from the OLGA observer indicated that the OLGA observer was superior in all cases, but the Matlab observer performed decently for the cases with stationary flow in pipelines carrying oil. This justifies the simplifications made during the mathematical modelling, but the lack of an energy equation makes the Matlab model to simple for practical use.

Since OLGA supports simulations with temperature dynamics, new tests with gas flow in a straight pipeline was conducted. Incorporating temperature as a factor during simulations with gas flow, adds a realistic flavor that earlier has been missing. These tests showed that for a straight pipe, employing output injection worked and a small leak of gas could be detected during stationary flow with great accuracy. For the cases with sinusoidal varying boundary conditions the position estimate was not very accurate, but at least the location was narrowed down to the first half of the pipeline. As for the case with shut down, it takes about two minutes for the observer to respond to the leak. This is most likely due to the reduction in pressure at the outlet causing a drastic increase in velocity, which again causes the estimated magnitude to be negative during this time span. When the flow has settled, both magnitude and position are correctly estimated within 6 minutes.

Unfortunately, applying output injection to an observer, not initialized with the exact same values as the model, monitoring the Tor 1 pipeline carrying gas, resulted in the

pressure exceeding the values bounded by the tab-file which is used as look-up table for fluid properties. For this case the mass rate at the inlet in the observer deviated with -1 kg/s from the model during initialization. The reason for the sudden increase in pressure is not certain, but could have been caused by wrong modelling of the gas flow in the mathematical model since it neither does incorporate the effect of gravity or temperature. This could result in the wrong boundary conditions for the observer employing output injection. The results mentioned above have been omitted due to not being very descriptive. Another case with the Tor 1 pipeline carrying gas was also tested, but in this case the observer was initialized with the exact same boundaries as the model. This worked out fine even with $k_0 = k_L = 0$, which is maximum observer gain, but the observer was not capable of locating any leaks. It seems as if the signature left in the measurements of velocity and pressure by the leak is too weak for it to be located, even though the magnitude of the leakage is rather large. There might also be a chance that the leakage affects the boundaries of the model with such impact that they no longer can be called stationary.

As seen in the section dealing with time-varying boundary conditions, some problems emerged when locating the leakage. First off, when applying sinusoidal boundary conditions, the position estimate fluctuated with approximately the same period as the liquid velocity at the inlet. This is due to the observer not being able to track the boundaries of the observer without a slight delay. This delay results in an error which again affects the estimated leak parameters. By inspecting the plots of $\hat{x}_l$ and the leak magnitude for the start up and shut down cases, it is clear that the position estimate does not converge until the boundaries reach a steady state. Another issue also arises with time-varying boundary conditions, namely: for what leak magnitude should the observer signalize a leak? With the observer lagging behind the model there might be a chance that the error is sufficiently large to affect the estimated magnitude of the leak and result in a false alarm.

With the Tor 1 pipeline carrying oil, multiple observers were used to locate and quantify leakages. It was shown that the multiple observers with different tuning and starting point would induce greater certainty for the estimates. Also, introducing observers where the backpressure was the same for each of the leaks along the pipeline, proved to be more effective than the intuitive setup with ambient pressure dependent on the sea depth. The positive effects with uniform backpressure trigger the thought of setting the backpressure at each leak to a constant value depending on the pressure inside the pipe. The result would be that the differential pressure over all of the leaks along the pipeline would be approximately the same, and this might cause the estimated leak parameters to converge more rapidly in areas with steep inclinations of the pipeline.

The weak spot of the model-based observer presented in this thesis is its sensitivity to biased and drifting measurements which causes vast errors in the position estimate. The estimated magnitude of the leak, on the other hand, is relatively robust to these kinds of error, but this is of less importance than the position. Adaption of roughness prior to the leakage compensates for the differences between the observer and model causing

erroneous estimates, but this was only tested for cases with one biased measurement at a time. Even though the following problem was not encountered in this work, there could be cases where the adaption of roughness is not sufficient to compensate for biases and drifting. In such cases it might be possible to utilize the built-in support in the OLGAMatlabToolbox to adjust the pipeline diameter in the OLGA observer. This could most likely be done in a similar manner as with the pipeline roughness by using the same update law with a slower tuning.

5.11.1 Future work

It would be interesting to conduct a rigorous study of robustness with measurements from operational pipelines, but this is of course difficult since leaks seldom occurs and not can be induced. Instead it would be desirable to carry out experiments with a scaled test rig to see if the benefits of the model-based observer would still be applicable.

There has not been established any proofs of convergence for the update laws, but numerous simulations indicate that the estimated values will converge to the correct value with stationary boundary conditions. These proofs are vital for the acceptance of the adaptive, model-based observer in the engineering communities, and this is why future work should focus on laying such a theoretical foundation. There are neither any proofs showing that output injection will work with time-varying boundary conditions or that output injection should work with the OLGA observer with a pipeline following the seabed and incorporating temperature dynamics.

Since the OLGA observer works with one-phase flow of both oil and gas in straight, horizontal pipelines, it is not unthinkable that it might work for two-phase flow. It would most likely require modification of the observer presented in this thesis. This could be modifications such as a new valve equation and different boundary conditions.

Another interesting aspect of the observer which can be investigated, is whether running multiple simulations with the same set of data while resetting the starting point of $\hat{x}_l$ and $\hat{u}_s$ to best ones available between the simulations will improve precision. The best ones in this context would be the ones which are obtained last. If this procedure seems to work, it might be possible to locate leaks during fast shut downs where the leakage disappears after a short period of time.

Chapter 6

Conclusions

The adaptive Luenberger-type observer presented in this thesis employs OLGA as its computational fluid dynamics simulator which is a state of the art simulator for one-, two- and three-phase flow. The OLGA observer is manipulated through Matlab which make it possible to make use of output injection in form of boundary conditions, control the magnitude and position of the estimated leakage and adapt roughness to compensate for model errors and biased measurements. The OLGA observer has numerous advantages over its predecessor, i.e. the observer constructed with Matlab in (Hauge, 2006), among which the incorporation of temperature dynamics, the support for pipelines with difference in altitude, no need for uniform grid and that it is widely used by oil companies are the most important ones.

Setting up an OLGA observer is time consuming, especially if there is no OLGA model which can be used as a basis. The observer bases its estimates on measurements of pressure, velocity and temperature from the inlet and pressure and velocity from the outlet. These measurements are usually available for newer pipelines and can easily be logged or low-pass filtered and fed directly to the observer. If data are logged, it is possible to run simulations repeatedly after a leak has been detected, but not located. This makes it possible to use the observer after the pipeline has been shut down.

Simulations with a straight, horizontal pipeline showed that the OLGA observer was superior to the Matlab observer constructed in (Hauge, 2006) with both oil and gas flow, and without any temperature dynamics. The OLGA observer was also tested with small leakages in a straight, horizontal pipeline carrying gas, where temperature dynamics was turned on. This yielded promising results.

An observer for an actual pipeline was also constructed in OLGA and tests were carried out with data from an existing OLGA model provided by Statoil. These tests revealed the need for multiple observers along long pipelines with difference in height. Beneficial effects for observers with uniform backpressure at each leak were also shown.

Numerous simulations with biased inputs to the observer identified a need for some kind

of internal compensation to take care of the position estimate which was highly affected by the incorrect measurements. This problem was fixed by adapting the roughness ahead of the occurrence of the leak and keeping it constant during localization and quantification. The estimated magnitude did not suffer from the same sensitivity to biased measurements as the position estimate.

Simulations conducted with time-varying boundary conditions showed that the observer was capable of detecting leaks in cases such as start up, shut down and with sinusoidal varying boundary conditions.

OLGA proved to be well suited for the task as fluid simulator for the model-based observer. It has the essential features such as controllable leaks, sources and pressure nodes, and an interface which makes it possible to manipulate them through Matlab.

References

O. M. Aamo, J. Salvesen, and B. A. Foss. Observer design using boundary injections for pipeline monitoring and leak detection. 2005. Accepted for the Adchem 2006 Conference held at Gramado, Brazil, April 2-5 2006.

L. Billmann and R. Isermann. Leak detection methods for pipelines. *Automatica*, 23: 381–385, 1987.

H. E. Emara-Shabaik, A. E. Khulief, and I. Hussaini. A non-linear multiple-model state estimation scheme for pipeline leak detection and isolation. *Journal of Systems and Control Engineering*, 216:497–512, 2002.

J. Feng, H Zhang, and D. Liu. Applications of fuzzy decision-making in pipeline leak localization. In *Proceedings of IEEE International Conference on Fuzzy Systems, 2004*, volume 2, pages 599–603, 2004.

E. Hauge. Leak detection for oil and gas pipelines with time varying boundary conditions. Technical report, NTNU, 2006.

R. Hu, H. Ye, G. Wang, and C. Lu. Leak detection in pipelines based on PCA. In *Proceedings of the 8th IEEE International Conference on Control, Automation, Robotics and Vision, 2004*, volume 3, pages 1985–1989, 2004.

W. Ming and W. Wei-qiang. Application of wavelet to detect pipeline leak point. In *Proceedings of the sixth International Conference on Intelligent Systems Design and Applications*, 2006.

C. R. Nilssen. Leak detection for oil and gas pipelines by parameter and state estimation. Master's thesis, NTNU, 2006.

OLGA User Manual, version 5. Scandpower Petroleum Technology, a.

Users's Manual OLGA - Matlab toolbox, version 1.01. Scandpower Petroleum Technology, b.

J. A. Schetz and A. E. Fuhs. *Fundamentals of Fluid Mechanics*, volume 1 of *Handbook of fluid dynamics and fluid machinery.* John Wiley and Sons, 1996.

C. Verde. Multi-leak detection and isolation in fluid pipelines. *Control Engineering Practice*, 9:467–472, 2001.

F. M. White. *Fluid Mechanics*. McGraw-Hill, fifth edition, 2003.

Appendix A

Simulation parameters

A.1 Matlab observer

Description	Parameter	Oil	Gas
Length of pipeline	L	5075 m	5075 m
Diameter of pipeline	D	20 in	20 in
Reference pressure	p_{ref}	50 bara	50 bara
Ambient pressure	p^{amb}	1 atm	1 atm
Reference density	ρ_{ref}	873 kg/m^3	52.7 kg/m^3
Reference viscosity	μ_{ref}	$6.1 \cdot 10^{-3}$ Pa·s	$1.2 \cdot 10^{-5}$ Pa·s
Speed of sound	c	1169 m/s	308 m/s
Bulk modulus	K	$1.87 \cdot 10^9$ Pa	$1.01 \cdot 10^5$
Number of nodes	N	100	100

Table A.1: Pipeline and fluid parameters for the Matlab observer for a horizontal pipeline.

Description	Oil	Gas
κ_x	350	35
κ_C	$2 \cdot 10^{-4}$	$7 \cdot 10^{-6}$
κ_Δ	0.01	$4 \cdot 10^{-4}$
γ	4	4
k_0	0	0
k_L	0	0

Table A.2: Tuning parameters for the Matlab observer.

A.2 OLGA models

A.2.1 Straight pipe

Description	Oil	Gas
Length of pipeline	5100 m	5100 m
Diameter of pipeline	20 in	20 in
Roughness	$1 \cdot 10^{-5}$ m	$1 \cdot 10^{-5}$ m
Pressure at outlet	50 bara	50 bara
Mass rate at inlet	350 kg/s	50 kg/s
Differential pressure	3.74 bar	0.56 bar
Ambient pressure	1 atm	1 atm
Temperature at inlet	70 °C	70 °C
Temperature at outlet	25 °C	25 °C
Ambient temperature	4 °C	4 °C
Number of sections	52	52

Table A.3: Pipeline parameters for the OLGA model without inclinations.

A.2.2 Tor

Description	Oil	Gas
Length of pipeline	86460 m	86460 m
Diameter of pipeline	31.8 cm	31.8 cm
Roughness	$1.05 \cdot 10^{-3}$ m	$1.05 \cdot 10^{-3}$ m
Pressure at outlet	3.29 bara	50 bara
Mass rate at inlet	100.6 kg/s	50 kg/s
Differential pressure	34.0 bar	59.8 bar
Temperature at inlet	45.9 °C	45.9 °C
Temperature at outlet	7.8 °C	7.8 °C
Ambient temperature	7 °C - 7.5 °C	7 °C - 7.5 °C
Number of sections	100	100

Table A.4: Pipeline parameters for the OLGA model of the Tor pipeline.

A.3 OLGA observers

A.3.1 Straight pipe

Description	Oil	Gas
κ_u	0.1	$7 \cdot 10^{-2}$
κ_x	500	100
κ_f	100	0.2
γ	2.5	2.5
k_0	0	0
k_L	0	0

Table A.5: Tuning for the straight pipe OLGA observer.

A.3.2 Tor

Description	Value
κ_x	1500
κ_u	$7 \cdot 10^{-3}$
κ_f	0 / 0.5
γ	2
k_0	0
k_L	0

Table A.6: Tuning of update laws for the robustness study.

Description	Value
κ_x	1500
κ_u	$5 \cdot 10^{-3}$
κ_f	0 / 0.5
γ	2
k_0	0
k_L	0

Table A.7: Tuning of update laws for the cases with model error.

Description	Shut down	Start up	Sinusoid
κ_x	1500	1500	1500
κ_u	$5 \cdot 10^{-3}$	$1 \cdot 10^{-2}$	$5 \cdot 10^{-3}$
κ_f	0	0	0
γ	2	2	2
k_0	0	0	0
k_L	0	0	0
Starting point [m]	43230	20000	20000

Table A.8: Tuning of update laws for the cases with time-varying boundaries.

Description	Value
κ_x	500
κ_u	0.1
κ_w	100
κ_f	1
γ	2.5
k_0	0
k_L	0

Table A.9: Observer parameters for estimation of C_v vs w_l.

Description	Value
κ_x	50
κ_u	0.02
γ	2.5
k_0	0
k_L	0

Table A.10: Observer parameters for estimation during gas flow with the Tor 1 pipeline.

Appendix B

Additional plots

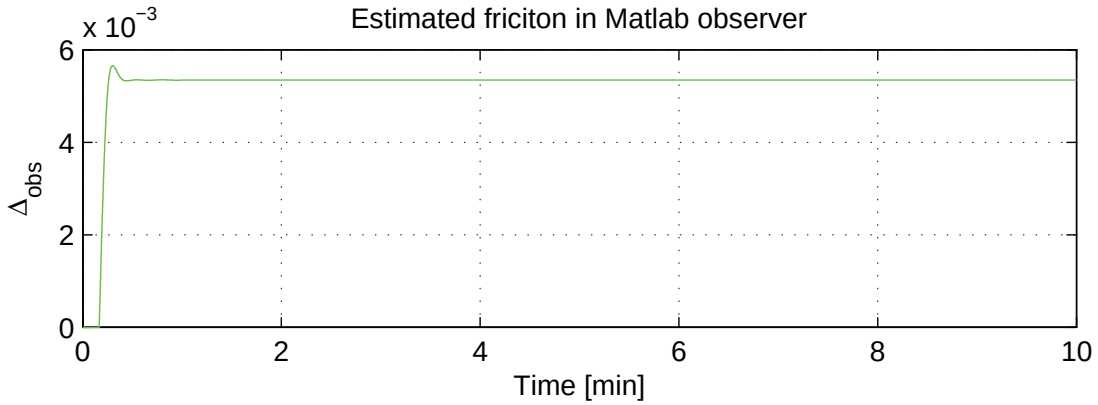

Figure B.1: **Oil, stationary.** Estimates of the friction coefficient, $\hat{\Delta}$, for leaks at both 850 m and 4650 m.

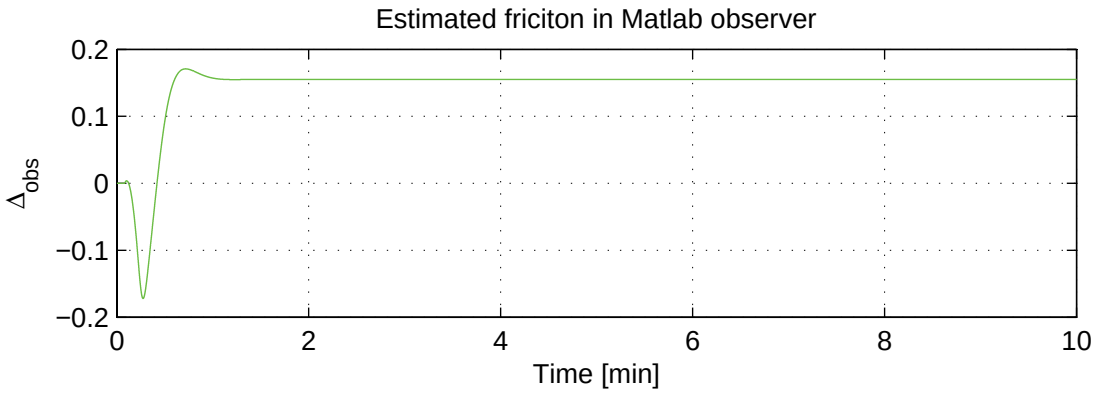

Figure B.2: **Gas, stationary.** Estimates of the friction coefficient, $\hat{\Delta}$, for leaks at both 850 m and 4650 m.

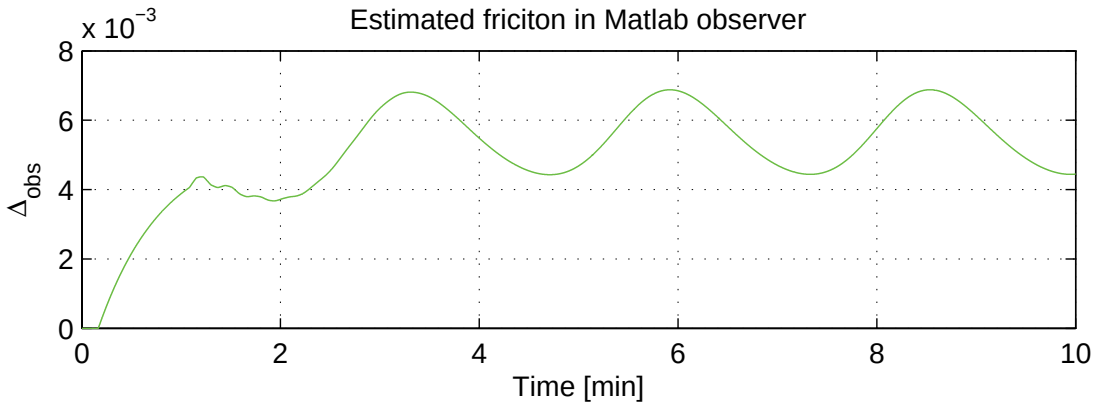

Figure B.3: **Oil, sinusoid.** Estimates of the friction coefficient, $\hat{\Delta}$, for a leak a leak at 3450 m.

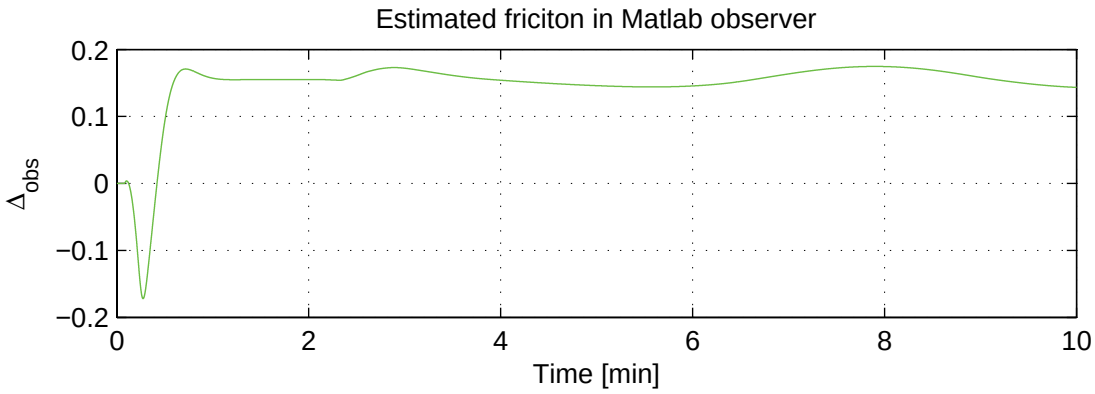

Figure B.4: **Gas, sinusoid.** Estimates of the friction coefficient, $\hat{\Delta}$, for a leak at 3450 m.

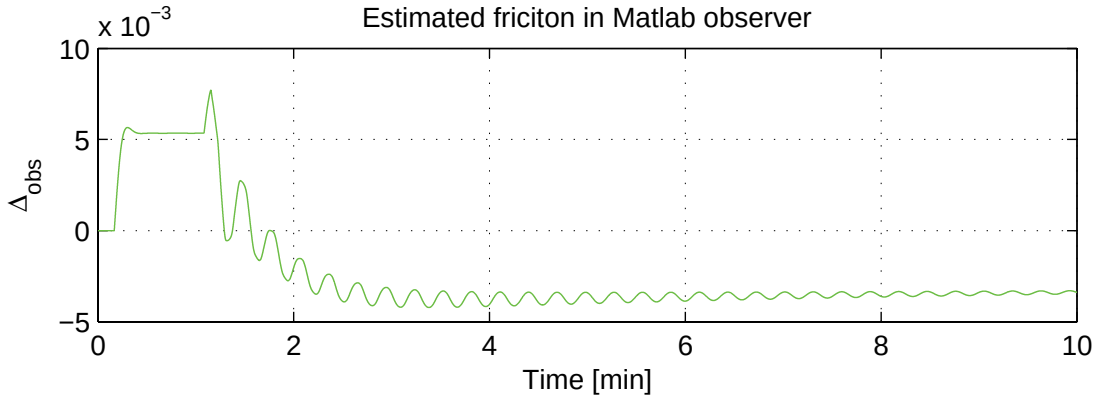

Figure B.5: **Oil, shut down.** Estimates of the friction coefficient, $\hat{\Delta}$, for a leak at 1350 m.

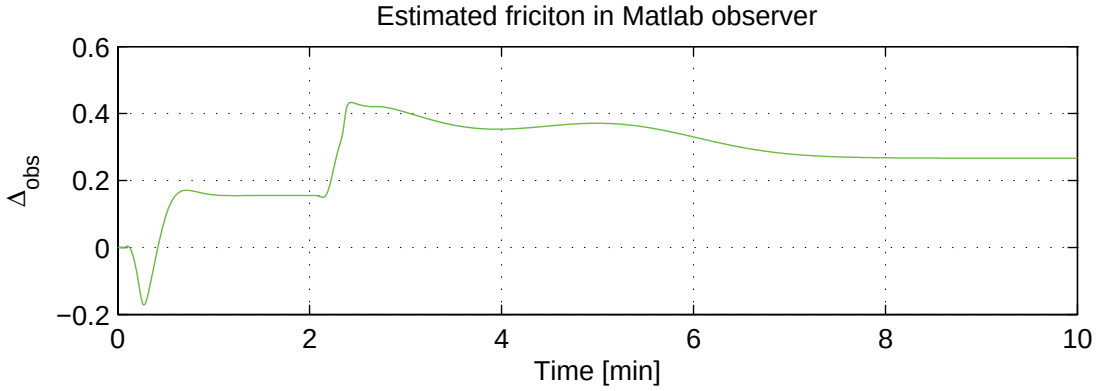

Figure B.6: **Gas, shut down.** Estimates of the friction coefficient, $\hat{\Delta}$, for a leak at 1350 m.

Appendix C

Proof

C.1 Uniform grid size for positive leak distribution

In Section 4.2 the following equation were presented:

$$\begin{bmatrix} f_{l,1} \\ f_{l,2} \end{bmatrix} = G_l^{-1} \begin{bmatrix} w_l \\ w_l \end{bmatrix},$$

where

$$G_l = \begin{bmatrix} \frac{\Delta x_0 + \Delta x_1}{2} & \frac{\Delta x_1 + \Delta x_2}{2} \\ \Delta x_0 + 2(x_l - x_1) - \frac{(x_l - x_1)^2}{\Delta x_1} & \frac{(x_l - x_1)^2}{\Delta x_1} \end{bmatrix}.$$

In the following it will be proved that an uniform grid is necessary to keep $f_{l,1} \geq 0$ and $f_{l,2} \geq 0$ for $w_l > 0$ and $x_l \in [\Delta x_0,\, L - \Delta x_N]$ (the leak can not occur between the first and second node or the last but one and last node).

First of all, lets introduce $\Delta x_l = x_l - x_1$ so G_l can be rewritten as

$$G_l = \begin{bmatrix} \frac{\Delta x_0 + \Delta x_1}{2} & \frac{\Delta x_1 + \Delta x_2}{2} \\ \Delta x_0 + 2\Delta x_l - \frac{\Delta x_l^2}{\Delta x_1} & \frac{\Delta x_l^2}{\Delta x_1} \end{bmatrix}. \tag{C.1}$$

By taking the inverse of G_l the following inequalities emerge

$$(G_{l,11}^{-1} + G_{l,12}^{-1}) w_l \geq 0 \Rightarrow G_{l,11}^{-1} + G_{l,12}^{-1} \geq 0 \tag{C.2}$$

$$(G_{l,21}^{-1} + G_{l,22}^{-1}) w_l \geq 0 \Rightarrow G_{l,21}^{-1} + G_{l,22}^{-1} \geq 0 \tag{C.3}$$

due to $w_l > 0$. Taking the inverse of a 2×2 matrix is easy and reveals the following inequalities

$$\frac{1}{|G_l|}(G_{l,22} - G_{l,12}) \geq 0 \tag{C.4}$$

$$\frac{1}{|G_l|}(G_{l,11} - G_{l,21}) \geq 0. \tag{C.5}$$

Now lets see if it is possible to say anything about the sign of $|G_l|$.

$$|G_l| = G_{l,11}G_{l,22} - G_{l,21}G_{l,12} \tag{C.6}$$

$$\begin{aligned}
&= \frac{\Delta x_0 + \Delta x_1}{2}\frac{\Delta x_l^2}{\Delta x_1} - (\Delta x_0 + 2\Delta x_l - \frac{\Delta x_l^2}{\Delta x_1})\frac{\Delta x_1 + \Delta x_2}{2} \\
&= \frac{\Delta x_l^2(\Delta x_0 + \Delta x_1)}{2\Delta x_1} - \frac{\Delta x_0(\Delta x_1 + \Delta x_2)}{2} \\
&- \frac{2\Delta x_l(\Delta x_1 + \Delta x_2)}{2} + \frac{\Delta x_l^2(\Delta x_1 + \Delta x_2)}{2\Delta x_1} \\
&= \frac{\Delta x_l^2(\Delta x_0 + \Delta x_1) - \Delta x_0\Delta x_l^2 - \Delta x_0\Delta x_1\Delta x_2 - 2\Delta x_l\Delta x_1^2}{2\Delta x_1} \\
&- \frac{2\Delta x_l\Delta x_1\Delta x_2 + \Delta x_l^2(\Delta x_1 + \Delta x_2)}{2\Delta x_1}
\end{aligned} \tag{C.7}$$

where $\Delta x_i > 0$ for $i = 0, 1, 2$. Suspecting that $|G_l|$ is negative one can write

$$\Delta x_l^2(\Delta x_0 + 2\Delta x_1 + \Delta x_2) \overset{?}{<} \Delta x_1^2(\Delta x_0 + 2\Delta x_l) + \Delta x_0\Delta x_1\Delta x_2 + 2\Delta x_l\Delta x_1\Delta x_2 \tag{C.8}$$

Knowing that $\Delta x_l \leq \Delta x_1$ then $\Delta x_l^2\Delta x_0 \leq \Delta x_1^2\Delta x_0$ and these terms can be ruled out. This leaves

$$\Delta x_l^2(2\Delta x_1 + \Delta x_2) \overset{?}{<} 2\Delta x_1^2\Delta x_l + \Delta x_0\Delta x_1\Delta x_2 + 2\Delta x_l\Delta x_1\Delta x_2 \tag{C.9}$$

where $\Delta x_l^2\Delta x_2 < 2\Delta x_l\Delta x_1\Delta x_2$ since $\Delta x_l < \Delta x_1$. Cutting out these two terms gives

$$2\Delta x_l^2\Delta x_1 \overset{?}{<} 2\Delta x_1^2\Delta x_l + \Delta x_0\Delta x_1\Delta x_2 \tag{C.10}$$

which in fact is true due to

$$2\Delta x_l^2\Delta x_1 < 2\Delta x_1\Delta x_1\Delta x_l, \quad \Delta x_1\Delta x_l > \Delta x_l^2 \tag{C.11}$$

and

$$\Delta x_0\Delta x_1\Delta x_2 > 0. \tag{C.12}$$

So $|G_l| < 0$ for $\Delta x_i > 0$ for $i = 0, 1, 2$ and $0 \leq \Delta x_l \leq \Delta x_1$.

Knowing that $|G_l|$ is negative, it is necessary that

$$G_{l,22} - G_{l,12} \leq 0 \tag{C.13}$$

$$G_{l,11} - G_{l,21} \leq 0. \tag{C.14}$$

Starting off with $G_{l,22} - G_{l,12} \leq 0$:

$$\begin{aligned}
\frac{\Delta x_l^2}{\Delta x_1} - \frac{\Delta x_1 + \Delta x_2}{2} &\leq 0 \\
&\Downarrow \\
2\Delta x_l^2 - \Delta x_1^2 - \Delta x_1\Delta x_2 &\leq 0 \\
2\Delta x_l^2 &\leq \Delta x_1^2 + \Delta x_1\Delta x_2
\end{aligned} \tag{C.15}$$

where the term on the left hand side would reach its maximum value for $\Delta x_l = \Delta x_1$. Inserting this gives

$$\begin{aligned} 2\Delta x_1^2 &\leq \Delta x_1^2 + \Delta x_1 \Delta x_2 \\ \Delta x_1^2 &\leq \Delta x_1 \Delta x_2 \\ \Delta x_1 &\leq \Delta x_2. \end{aligned} \tag{C.16}$$

Now lets evaluate $G_{l,11} - G_{l,21} \leq 0$

$$\begin{aligned} \Delta x_1(\Delta x_0 + \Delta x_1) - 2\Delta x_0 \Delta x_1 - 2\Delta x_l \Delta x_1 + 2\Delta x_l^2 &\leq 0 \\ \Delta x_1(\Delta x_0 + \Delta x_1) + 2\Delta x_l^2 &\leq 2\Delta x_1(\Delta x_0 + \Delta x_l). \end{aligned} \tag{C.17}$$

The left hand side of the inequality above will reach its maximum value for $\Delta x_l = \Delta x_1$ which gives

$$\begin{aligned} \Delta x_1(\Delta x_0 + \Delta x_1) + 2\Delta x_1^2 &\leq 2\Delta x_1^2 + 2\Delta x_0 \Delta x_1 \\ \Delta x_1 + \Delta x_0 \Delta x_1 &\leq 2\Delta x_0 \Delta x_1 \\ \Delta x_1^2 &\leq \Delta x_0 \Delta x_1 \\ \Delta x_1 &\leq \Delta x_0. \end{aligned} \tag{C.18}$$

So in order to keep $f_{l,1}$ and $f_{l,2}$ positive it is necessary that $\Delta x_1 \leq \Delta x_0$ and $\Delta x_1 \leq \Delta x_2$. Remembering that $x_l \in [\Delta x_0,\ L - \Delta x_N]$ leaves out no other choice than $\Delta x_i = \Delta x_{i+1}$ for $i = 1, \cdots, N-2$ i.e. the grid must be uniform between the second and last but one node. As for the first and last section, $\Delta x_0 \geq \Delta x_i$ and $\Delta x_N \geq \Delta x_i$ for $i = 1, \cdots, N-1$.

Appendix D

Article

The first of the following articles was accepted for oral presentation at the 7^{th} IFAC Symposium on Nonlinear Control Systems 22-24 August, 2007 in Pretoria, South Africa. The second one is a draft which will be submitted to SPE Journal.

MODEL BASED PIPELINE MONITORING WITH LEAK DETECTION

Espen Hauge* **Ole Morten Aamo*,[1]** **John-Morten Godhavn** **

**Department of Engineering Cybernetics, Norwegian University of Science and Technology, Trondheim, Norway*
***R&D, Statoil ASA, Trondheim, Norway*

Abstract: We design a leak detection system consisting of an adaptive Luenberger-type observer based on a set of two coupled one dimensional first order nonlinear hyperbolic partial differential equations governing the flow dynamics. It is assumed that measurements are only available at the inlet and outlet of the pipe, and output injection is applied in the form of boundary conditions. Heuristic update laws for adaptation of the friction coefficient and leak parameters are given, and simulations demonstrate their ability to detect, quantify and locate leaks. Particular attention is given to time-varying boundary conditions, such as during pipeline shut-down. A scenario consisting of leak detection followed by pipeline shut-down during which the leak is accurately quantified and located is successfully simulated for both liquid and gas systems.

Keywords: Partial differential equations; Observers; Adaptive systems; Pipeline leaks

1. INTRODUCTION

Transportation of fluids in pipelines requires monitoring to detect malfunctioning such as leaks. In the petroleum industry, leaks from pipelines may potentially cause environmental damage, as well as economic loss. These are motivating factors, along with requirements from environmental authorities, for developing efficient leak detection systems. While some leak detection methods are hardware-based, relying on physical equipment being installed along the pipeline, the focus of this paper is on software-based methods that work for cases with limited instrumentation. In fact, instrumentation in the petroleum industry is usually limited to the inlet and outlet of pipelines, only. This calls for sophisticated signal processing methods to obtain reliable detection of leaks. Some software-based leak detection methods perform statistical analysis on measurements (black box), while others incorporate models based on physical principles. Our method falls into the latter category, in that we will use a dynamic model of the pipe flow based on a set of two coupled hyperbolic partial differential equations.

There have been numerous studies on model based leak detection. We mention here the most relevant ones with regard to our work. Based on a discretized pipe flow model, Billman and Isermann (1987) designed an observer with friction adaptation. In the event of a leak, the outputs from the observer differs from the measurements, and this is exploited in a correlation technique that detects, quantifies and locates the leak. Verde (2001) used a bank of observers, computed by the method for fault detection and isolation developed by Hou and Müller (1994). The underlying model is a linearized, discretized pipe flow model on a grid of N nodes. The observers are designed in

[1] Corresponding author: aamo@ntnu.no

such a way that all but one will react to a leak. Which one of the N observers that does not react to the leak depends on the position of the leak, and this is the mechanism by which the leak is located. The outputs of the remaining observers are used for quantifying the leak. The bank of observers are computed using the recursive numerical procedure suggested by Hou and Müller (1994), however it was shown in Salvesen (2005) that due to the simple structure of the discretized model, the observers may be written explicitly. This is important, because it removes the need for recomputing the bank of observers when the operating point of the pipeline is changed. Verde (2004) also proposed a nonlinear version, using an extremely coarse discretization grid.

Several companies offer commercial solutions to pipeline monitoring with leak detection. Fantoft (2005) uses a transient model approach in conjunction with the commercial pipeline simulator OLGA2000, while EFA Technologies (1987, 1990, 1991) uses an event detection method that looks for signatures of no-leak to leak transitions in the measurements.

The detection method of Verde (2001) using a bank of observers, can potentially detect multiple leaks. However, multiple simultaneous leaks is an unlikely event, so the complex structure of a bank of N observers seems unnecessary. Aamo et al. (2006) instead employed ideas from adaptive control, treating the magnitude and location of a single point leak as constant unknown parameters in an adaptive Luenberger-type observer based on a set of two coupled one dimensional first order nonlinear hyperbolic partial differential equations. Heuristic update laws for adaptation of the friction coefficient, magnitude of the leak and position of the leak were suggested. In the present paper, we continue the development of our leak detection system by greatly improving the leak detection performance under time-varying boundary conditions. This is achieved by remodelling the leak. A comprehensive simulation study demonstrates the leak detection system for both liquid and gas systems.

2. MATHEMATICAL MODEL

For liquid flow in a pipe we have the mass conservation

$$\frac{\partial p}{\partial t} + u\frac{\partial p}{\partial x} + \rho c^2 \frac{\partial u}{\partial x} = 0, \tag{1}$$

and the momentum conservation (ignoring friction for now)

$$\frac{\partial u}{\partial t} + u\frac{\partial u}{\partial x} + \frac{1}{\rho}\frac{\partial p}{\partial x} = 0, \tag{2}$$

for $(x,t) \in (0,L) \times (0,\infty)$, and where $u(x,t)$ is flow velocity, $p(x,t)$ is pressure, and $\rho(x,t)$ is density. The relation between pressure and density is modelled as (Nieckele et al. (2001))

$$\rho(x,t) = \rho_{ref} + \frac{p(x,t) - p_{ref}}{c^2}, \tag{3}$$

where ρ_{ref} is a reference density at reference pressure p_{ref}, and c is the speed of sound in the fluid. Equation (1)–(2) also describes gas flow in a pipe, simply by replacing (3) with the ideal gas law. Under the conditions we consider, we assume c is sufficiently large to ensure $\rho > 0$. Defining $k = c^2\rho_{ref} - p_{ref}$ and substituting (3) into (1)–(2) we obtain

$$\frac{\partial p}{\partial t} + u\frac{\partial p}{\partial x} + (k+p)\frac{\partial u}{\partial x} = 0, \tag{4}$$

$$\frac{\partial u}{\partial t} + \frac{c^2}{k+p}\frac{\partial p}{\partial x} + u\frac{\partial u}{\partial x} = 0. \tag{5}$$

The boundary conditions are

$$u(0,t) = u_0(t), \tag{6}$$

$$p(L,t) = p_L(t). \tag{7}$$

3. OBSERVER DESIGN

In reality, input signals to pipelines are usually choke openings at the inlet and outlet. Here, we instead view $u_0(t)$ and $p_L(t)$ in (6)–(7) as inputs to the process, and the remaining boundary quantities $p_0(t) = p(0,t)$ and $u_L(t) = u(L,t)$ as process measurements. Aamo et al. (2006) showed that a Luenberger-type observer consisiting of a copy of (4)–(5) and the boundary injections

$$\hat{u}(0,t) = u_0(t) + c\frac{1-k_0}{1+k_0}\ln\left(\frac{k+p_0(t)}{k+\hat{p}(0,t)}\right), \tag{8}$$

$$\hat{p}(L,t) = (k+p_L(t)) \times \exp\left(\frac{k_L - 1}{c(1+k_L)}\left(u_L(t) - \hat{u}(L,t)\right)\right) - k. \tag{9}$$

has favorable convergence properties for $|k_0| \leq 1$ and $|k_L| < 1$ when compared to a plain copy of the plant, that is $\hat{u}(0,t) = u_0(t)$ and $p(L,t) = p_L(t)$. Figure 1 shows the observer error in terms of evolution in time of the $L_2(0,L)$ norm of $u(x,t) - \hat{u}(x,t)$ and $p(x,t) - \hat{p}(x,t)$ for the cases with and without output injection. Notice that when $k_0 = 1$ and $k_L = 1$, (8)–(9) reduces to the plain copy.

4. ADAPTATION OF FRICTION COEFFICIENT

Adding friction to the model (4)–(5), we have the mass balance

$$\frac{\partial p}{\partial t} + u\frac{\partial p}{\partial x} + (k+p)\frac{\partial u}{\partial x} = 0, \tag{10}$$

and momentum conservation

$$\frac{\partial u}{\partial t} + u\frac{\partial u}{\partial x} + \frac{c^2}{k+p}\frac{\partial p}{\partial x} = -(1+\Delta)\frac{f}{2}\frac{|u|\,u}{D}, \tag{11}$$

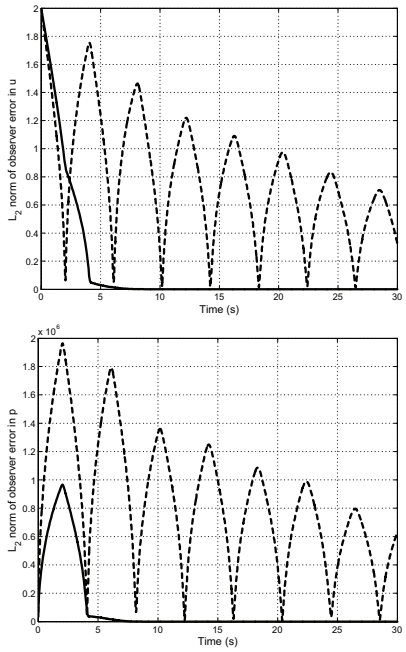

Fig. 1. Observer error with (solid) and without (dashed) output injection.

where D is the pipe diameter, and Δ is considered an unknown constant that accounts for uncertainty in the friction coefficient f, which is given by Schetz and Fuhs (1996) as

$$\frac{1}{\sqrt{f}} = -1.8\log_{10}\left[\left(\frac{\epsilon/D}{3.7}\right)^{1.11} + \frac{6.9}{\mathrm{Re}_d}\right]. \quad (12)$$

ϵ/D is the pipe relative roughness, Re_d is the Reynolds number defined as

$$\mathrm{Re}_d = \frac{\rho u D}{\mu}, \quad (13)$$

and μ is the fluid viscosity. The observer is then

$$\frac{\partial \hat{p}}{\partial t} + \hat{u}\frac{\partial \hat{p}}{\partial x} + (k+\hat{p})\frac{\partial \hat{u}}{\partial x} = 0, \quad (14)$$

$$\frac{\partial \hat{u}}{\partial t} + \hat{u}\frac{\partial \hat{u}}{\partial x} + \frac{c^2}{k+\hat{p}}\frac{\partial \hat{p}}{\partial x} = -\left(1+\hat{\Delta}\right)\frac{\hat{f}}{2}\frac{|\hat{u}|\,\hat{u}}{D}, \quad (15)$$

which incorporates an estimate $\hat{\Delta}$ of Δ, and with boundary conditions (8)–(9). Consider the heuristic parameter update law

$$\dot{\hat{\Delta}} = -\kappa_\Delta\left(\varphi_1 + \varphi_2\right), \quad (16)$$

where κ_Δ is a strictly positive constant, and

$$\varphi_1 = u(0) - \hat{u}(0) + c\,\ln\left(\frac{k+\hat{p}(0)}{k+p(0)}\right), \quad (17)$$

$$\varphi_2 = u(L) - \hat{u}(L) + c\,\ln\left(\frac{k+p(L)}{k+\hat{p}(L)}\right). \quad (18)$$

Figure 2 shows the evolution of $\Delta - \hat{\Delta}$ when the initial friction in the observer is twice that of the plant.

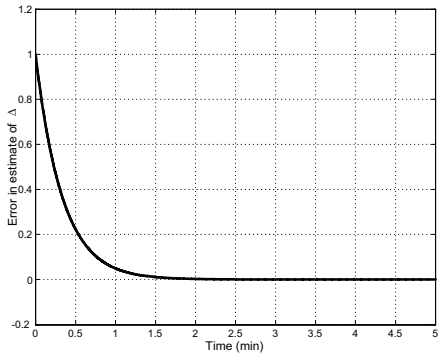

Fig. 2. Error in estimated friction factor, that is $\Delta - \hat{\Delta}$.

5. LEAK DETECTION

Adding a leak to the model (10)–(11), with $\Delta = 0$, we have the mass balance

$$\frac{\partial p}{\partial t} + u\frac{\partial p}{\partial x} + (k+p)\frac{\partial u}{\partial x} = -\frac{c^2}{A}f_l(x,t), \quad (19)$$

and the momentum conservation

$$\frac{\partial u}{\partial t} + u\frac{\partial u}{\partial x} + \frac{c^2}{k+p}\frac{\partial p}{\partial x} = -\frac{f}{2}\frac{|u|\,u}{D} + \frac{1}{A}\frac{c^2}{k+p}uf_l(x,t), \quad (20)$$

where A is the pipe cross sectional area. Assuming a point leak occuring at $t = t_l$, we select $f_l(x,t)$ as

$$f_l(x,t) = w_l\delta(x - x_l)\,H(t - t_l), \quad (21)$$

where w_l and x_l are the magnitude of the leak and position of the leak, respectively, δ denotes the Dirac distribution, and H denotes the Heaviside step function. Aamo et al. (2006) treated w_l as a constant which led to poor leak localization performance for time-varying boundary conditions. In practice, the boundary conditions will most likely be time-varying since the logical thing to do as soon as a leak is detected, is to start shutting down the pipeline. In this case, the leak magnitude will vary during the shut-down, violating the assumption that w_l be constant. To overcome this problem, we propose to model the point leakage rate according to the valve equation

$$w_l(t) = C_v\sqrt{\rho(x_l,t)\left(p(x_l,t) - p_{amb}\right)}, \quad (22)$$

where C_v is a discharge coefficient and p_{amb} is the ambient pressure on the exterior of the pipe. While p_{amb} is assumed known, C_v is an unknown constant to be estimated by the leak detection system. The observer now becomes

$$\frac{\partial \hat{p}}{\partial t} + \hat{u}\frac{\partial \hat{p}}{\partial x} + (k+\hat{p})\frac{\partial \hat{u}}{\partial x} = -\frac{c\hat{C}_v}{A}\sqrt{(k+\hat{p}(\hat{x}_l))\left(\hat{p}(\hat{x}_l) - p_{amb}\right)}\delta(x - \hat{x}_l), \quad (23)$$

$$\frac{\partial \hat{u}}{\partial t} + \hat{u}\frac{\partial \hat{u}}{\partial x} + \frac{c^2}{k+\hat{p}}\frac{\partial \hat{p}}{\partial x} = -\frac{\hat{f}}{2}\frac{|\hat{u}|\,\hat{u}}{D}$$

$$+\frac{c\hat{C}_v}{A}\hat{u}\sqrt{\frac{\hat{p}\left(\hat{x}_l\right)-p_{amb}}{k+\hat{p}\left(\hat{x}_l\right)}}\delta\left(x-\hat{x}_l\right), \quad (24)$$

which incorporates estimates of the leak discharge coefficient and position, $\hat{C}_v$, $\hat{x}_l$. We consider the heuristic parameter update laws

$$\dot{\hat{C}}_v = \kappa_C\left(\varphi_1-\varphi_2\right), \quad (25)$$

$$\dot{\hat{x}}_l = -\kappa_x\left(\varphi_1+\varphi_2\right)\left|\varphi_1+\varphi_2\right|^{\frac{1}{\gamma}-1}, \quad (26)$$

where φ_1 and φ_2 are given in (17)–(18), and κ_C, κ_x and γ are strictly positive constants. The update laws (25)–(26) are derived from those in (Aamo et al. 2006) taking the new leakage model (22) into account.

6. SIMULATION RESULTS

A comprehensive simulation study has been carried out for a 5 km long pipeline with a diameter of 20 inches, varying the many parameters in the process model and observer. Due to page constraints, we report here on selected key results. The parameters used are summarized in Tables 1 and 3 for the oil and gas cases, respectively. Tuning parameters for the leak parameter update laws are given in Tables 2 and 4. The most probable scenario in practice, is the one where the pipeline is shut down as a consequence of detecting a leak. This leaves a limited time window for quantifying and locating the leak. A partial shut-down of the pipeline carrying oil is simulated by reducing the velocity at the inlet to 10 percent of its initial value and the pressure at the outlet to 30 percent of its initial value over a period of 3 minutes. An illustration of the performance of the leak detection system with these boundary conditions can be seen in Figure 3. The leak is very quickly detected, as shown by the steep increase in the magnitude-of-leak estimate immediately following the time when the leak occurs. An accurate estimate of the leak magnitude is obtained within a few seconds, while localization takes several minutes. Figure 4 shows the corresponding results for the gas case, where the velocity at the inlet was decreased to 10 percent of its initial value and the outlet pressure to 30 percent of its initial value over a period of 11 minutes. Due to the compressibility of gas, giving a lower speed of sound, there is a longer time-lag before the leak is detected (a few seconds). Accurate estimates of the leak magnitude and position are obtained in about a minute. The position of the leak shows some oscillatory behaviour, which is related to grid-size and tuning, and may be removed by filtering.

To further demonstrate the leak detection capabilities under time-varying boundary conditions, sinusoid perturbations were applied to both ends of the pipeline carrying oil. The sinusoids are meant to represent the varying production rate set at the

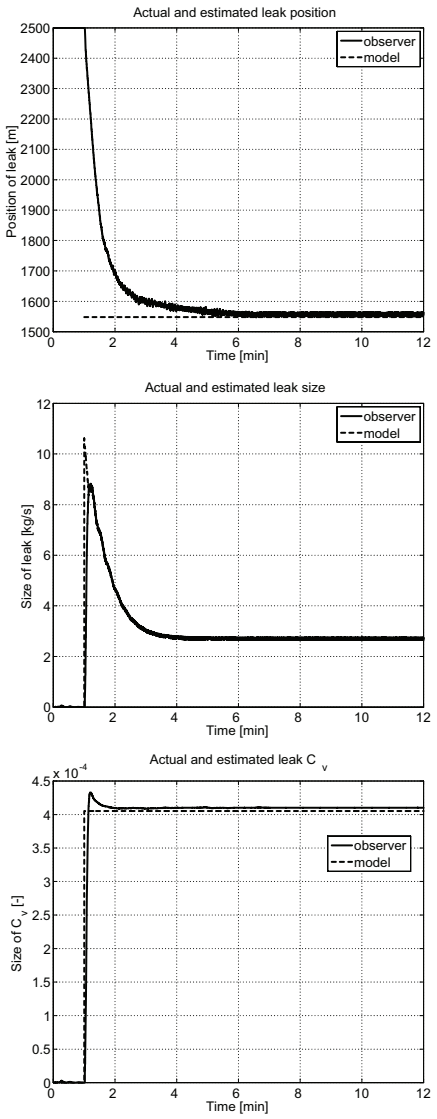

Fig. 3. **Oil, shut-down.** Estimates for a leak at 1548 m of with $C_v = 4.05 \cdot 10^{-4}$.

inlet and the choking at the outlet. The velocity perturbation at the inlet has an amplitude of 25 percent of the initial value and a period of 3 minutes. The pressure perturbation at the outlet has an amplitude of 10 percent of the initial value and a period of 2 minutes. Figure 5 shows that leak detection and quantification performs very well under these boundary conditions, while localization suffers some oscillations at the frequency of the perturbation.

Finally, we present a case showing the important effect of the chosen boundary injections, that is, it compares results for $k_0 = k_L = 0$ (*with* boundary injection) with results for $k_0 = k_L = 1$ (*without* boundary injection). Here, the boundary conditions of the process model, u_0 and p_L, are assumed to vary randomly (low-pass filtered, however), while a leak occurs at 1548 m with $C_v = 2.55 \cdot 10^{-4}$. The amplitude of the input

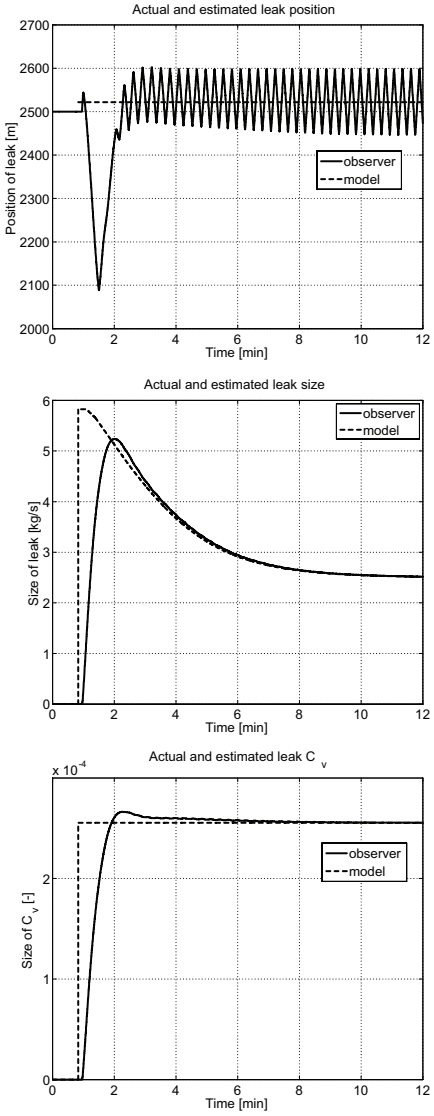

Fig. 4. **Gas, shut-down.** Estimates for a leak at 1548 m with $C_v = 2.55 \cdot 10^{-4}$.

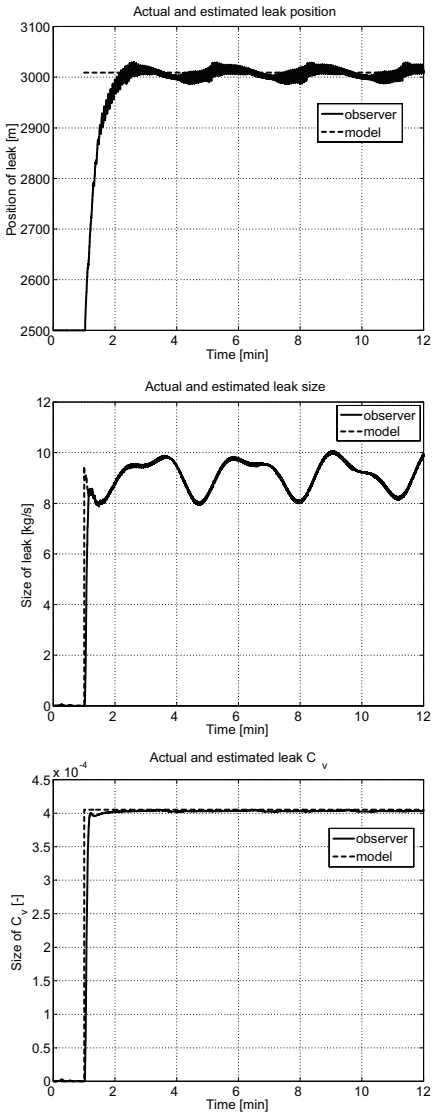

Fig. 5. **Oil, sinusoid.** Estimates for a leak at 3009 m of with $C_v = 4.05 \cdot 10^{-4}$.

velocity varies within 10 percent of the initial value, and the output pressure varies within 0.7 percent of the initial value. Figure 6 clearly shows the crucial effect of output injection, as well as the leak detection capability under randomly varying input.

7. CONCLUDING REMARKS

We have designed a leak detection system for pipelines consisting of an adaptive Luenberger-type observer and heuristic update laws for the parameters characterizing a point leak. The only available process information is flow velocity and pressure at the inlet and outlet of the pipe. Simulations demonstrate accurate quantification and localization of the leak under transient operation of the pipeline, such as for instance during shut-down. Current work focuses on replacing the simple model presented in this paper with a state-of-the-art fluid flow simulator and incorporating

Parameter	Value
L	5000 m
D	20 in
p_{ref}	$5 \cdot 10^5$ Pa
p_{amb}	101325 Pa
p_{initial}	101325 Pa
u_{initial}	2 m/s
$\bar{u} = u_0$	2 m/s
$\bar{p} = p_L$	$5 \cdot 10^5$ Pa
ρ_{ref}	870 kg/m^3
w_{in}	353 kg/s
μ_{ref}	$1.04 \cdot 10^{-1}$ Pa·s
c	1227 m/s
K	$1.31 \cdot 10^9$ Pa

Table 1. Pipeline and fluid parameters for oil.

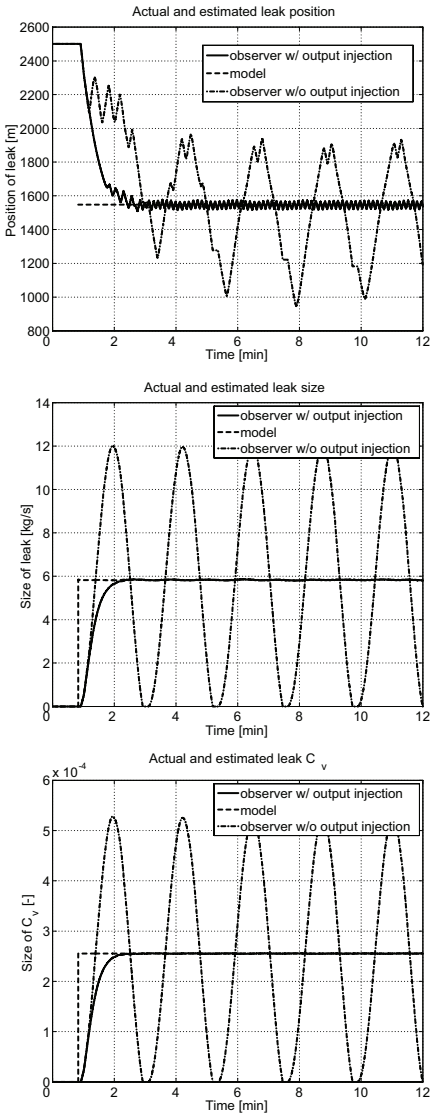

Fig. 6. **Gas, random.** Leak detection with and without output injection.

Parameter	Value
κ_c	$8.12 \cdot 10^{-4}$
κ_x	100
γ	4

Table 2. Tuning parameters for oil.

Parameter	Value
L	5000 m
D	20 in
p_{ref}	0 Pa
p_{amb}	101325 Pa
p_{initial}	5016390 Pa
u_{initial}	4 m/s
$\bar{u} = u_0$	4 m/s
$\bar{p} = p_L$	5016390 Pa
ρ_{ref}	52.67 kg/m^3
w_{in}	43 kg/s
μ_{ref}	$1.20 \cdot 10^{-5}$ Pa·s
c	308 m/s

Table 3. Pipeline and fluid parameters for gas.

Parameter	Value
κ_c	$8.12 \cdot 10^{-4}$
κ_x	35
γ	4

Table 4. Tuning parameters for gas.

the presented boundary conditions and parameter update laws into it. The increased accuracy of the flow calculations provided by such a simulator is expected to improve the leak detection capability described in this paper even further.

ACKNOWLEDGEMENTS

We gratefully acknowledge the support from the Gas Technology Center at NTNU, Statoil, and the Norwegian Research Council.

REFERENCES

O.M. Aamo, J. Salvesen, and B.A. Foss, "Observer design using boundary injections for pipeline monitoring and leak detection," *Proceedings of the 2006 International Symposium on Advanced Control of Chemical Processes,* Gramado, Brazil, April 2-5, 2006.

L. Billmann and R. Isermann, "Leak detection methods for pipelines," *Automatica*, vol. 23, no. 3, pp. 381–385, 1987.

EFA Technologies, Inc., "Events at a leak," Technical paper available from EFA on request, 1987.

EFA Technologies, Inc., "Effect of pressure measurement resolution on PPA leak detection," Technical paper available from EFA on request, 1990.

EFA Technologies, Inc., "PPA event suppression capability," Technical paper available from EFA on request, 1991.

Fantoft, "D-SPICE overview: Production management systems," Fantoft Process Technologies, 2005.

M. Hou and P. Müller, "Fault detection and isolation observers," *International Journal of Control*, vol. 60, no. 5, pp. 827–846, 1994.

A.O. Nieckele, A.M.B. Brage, and L.F.A. Azevedo, "Transient pig motion through gas and liquid pipelines," *Journal of Energy Resources Technology*, vol. 123, no. 4, 2001.

J. Salvesen, *Leak Detection by Estimation in an Oil Pipeline*, MSc Thesis, NTNU, 2005.

J.A. Schetz and A.E. Fuhs, *Handbook of Fluid Dynamics and Fluid Machinery, Volume 1, Fundamentals of Fluid Mechanics*, John Wiley & Sons, 1996.

C. Verde, "Multi-leak detection and isolation in fluid pipelines," *Control Engineering Practice*, vol. 9, pp. 673–682, 2001.

C. Verde, "Minimal order nonlinear observer for leak detection," *Journal of Dynamic Systems, Measurement and Control*, vol. 126, pp. 467–472, 2004.

SPE Paper Number ?

Advanced leak detection in oil and gas pipelines using a nonlinear observer and OLGA models

Espen Hauge, Ole Morten Aamo, and John-Morten Godhavn, Norwegian University of Science and Technology

Abstract

An adaptive Luenberger-type observer with the purpose of locating and quantifying leakages is presented. The observer only needs measurements of velocity and temperature at the inlet and pressure at the outlet to function. The beneficial effect of output injection in form of boundary conditions is used to ensure fast convergence of the observer error. Depending only on measurements from inlet and outlet makes it possible to use OLGA, which is a state of the art computational fluid dynamics simulator, to govern the one-phase fluid flow of the observer. The observer is tested with both a straight, horizontal pipeline and an actual, long pipeline with inclinations, and both simulations with oil and gas are carried out. In order to cope with modelling errors and biased measurements, estimation of roughness in the monitored pipeline is introduced.

1 Introduction

Leak detection based on dynamic modelling is a propitious approach in the special field of leak quantification and location. This article documents one of the first steps toward a new method of pipeline monitoring. A state of the art multiphase simulator is manipulated through Matlab to work as an adaptive Luenberger-type observer which uses measurements from the supervised pipeline as well as internal measurements. Since the only measurements fed into the observer are pressure from the outlet and velocity and temperature from the inlet, which in most cases already are available, the method can be used with most existing pipelines without extra instrumentation. Also, the computational fluid dynamics simulator, which is the backbone of the observer, is a widely used one,

namely OLGA[1]. Many existing pipelines have already been modeled in OLGA which can be exploited in the construction of the observer.

The benefits of a leak detection system able of locating the position of the leak are obviously of an environmental kind. But the economical aspect of it is also important. Another advantage of this kind of method would be that it under some circumstances can be used after a leak has been detected and the pipeline has been shut down. This is possible by logging the relevant measurements and running simulations with the observer with the stored model data. It is also be possible to have multiple observers with different tuning and starting point monitoring a pipeline during operation.

2 Mathematical Model

For liquid flow in a pipe we have the mass and momentum conservations

$$\frac{\partial p}{\partial t} + u\frac{\partial p}{\partial x} + \rho c^2 \frac{\partial u}{\partial x} = 0 \quad \text{.....(1)}$$

$$\frac{\partial u}{\partial t} + u\frac{\partial u}{\partial x} + \frac{1}{\rho}\frac{\partial p}{\partial x} = 0 \quad \text{.....(2)}$$

for $(x,t) \in [0, L] \times [0, \infty)$, and where $u(x,t)$ is flow velocity, $p(x,t)$ is pressure and L is the length of the pipeline. The density $\rho(x,t)$ is modelled as in Nieckele et al.[2]

$$\rho(x,t) = \rho_{ref} + \frac{p(x,t) - p_{ref}}{c^2} \quad \text{..... (3)}$$

where ρ_{ref} is a reference density at reference pressure p_{ref}, and c is the speed of sound in the fluid. Defining $k = c^2 \rho_{ref} - p_{ref}$ and substituting (3) into (1)-(2) gives us

$$\frac{\partial p}{\partial t} + u\frac{\partial p}{\partial x} + (k+p)\frac{\partial u}{\partial x} = 0 \quad \text{.....(4)}$$

$$\frac{\partial u}{\partial t} + \frac{c^2}{k+p}\frac{\partial p}{\partial x} + u\frac{\partial u}{\partial x} = 0 \quad \text{.....(5)}$$

The boundary conditions are

$$u(0,t) = u_0(t) \quad \text{.....(6)}$$

$$p(0,t) = p_L(t) \quad \text{.....(7)}$$

3 Observer design

In Aamo et al.[1] boundary injections for a Luenberger-type observer consisting of (4)-(5) were proven to induce exponential stability at the origin. These boundary injections were

$$\hat{u}(0) = u(0) + c\frac{1-k_0}{1+k_0}\ln\left(\frac{k+p(0)}{k+\hat{p}(0)}\right) \quad \text{.....(8)}$$

[1] OLGA is a multiphase computational fluid dynamics simulator developed by Sintef, IFE, Statoil and Scandpower Petroleum Technology.

$$\hat{p}(L) = \left(k + p(L)\right)$$

$$\times \exp\left(\frac{k_L - 1}{c(1+k_L)}\left(u(L) - \hat{u}(L)\right)\right) - k \quad \ldots\ldots\ldots(9)$$

where $|k_0| \le 1$ and $|k_L| < 1$. Setting $k_0 = k_L = 1$ reduces the observer to a plain open-loop observer with $\hat{u}(0) = u(0)$ and $\hat{p}(L) = p(L)$, and setting $k_0 = k_L = 0$ results in maximum observer gain and leads to favorable convergence properties as shown in the plot of the L_2-norm of observer error in **Fig. 1**.

The boundary conditions (8)-(9) are applied to an observer constructed with OLGA which is capable of quantifying and locating leaks along straight pipelines carrying either oil or gas, and pipelines with difference in altitude carrying oil. Using OLGA as the fluid simulator also enables temperature dynamics to be turned on during simulations, which makes this the first observer used for leak detection incorporating an energy equation known to the authors. The OLGA observer is based on an existing OLGA model. Leaks, which are process equipments in OLGA, are added to each segment of the pipeline. The leaks and the boundaries are controlled via Matlab and the interface provided by OLGAMatlabToolbox.

The leak parameters to be adapted are the coefficient of velocity of the leakage, C_v, and the position, x_l. Also, the roughness of the pipeline is adjusted adaptively by multiplying the current roughness in the observer with a factor, Δ, which is initially set to 1. The idea of adapting C_v instead of the magnitude of the leak directly, has been triggered by the fact that the leak magnitude will not be a constant during scenarios such as shut-downs and start-ups, but the C_v most likely will. We introduce the common valve equation

$$w_l = C_d u_s \frac{\pi}{4} D_l^{\,2} \sqrt{(p_l - p_{amb})\rho_l} \quad \ldots\ldots\ldots\ldots\ldots(10)$$

where: w_l is the magnitude of the leakage; C_d the discharge coefficient; D_l the diameter of the leakage; p_l the pressure inside the pipeline at the leak; p_{amb} the ambient pressure at the point of leak; ρ_l the density inside the pipeline at the leak. $u_s \in [0,1]$ is a control signal which governs the leak opening. By defining

$$C_v = C_d u_s \frac{\pi}{4} D_l^{\,2} \quad \text{.....(11)}$$

it is clear that we can now estimate C_v by adjusting u_s which is available for manipulation through the interface provided by the OLGAMatlabToolbox. C_d and D_l are set prior to the simulations in the input-file used by OLGA. The observer and model have similar values for these parameters throughout this article.

The update laws are heuristic and are based on the ones first proposed in Aamo et al.[1] Consider the following

$$\dot{\hat{u}}_s(t) = \kappa_u(\varphi_1 - \varphi_2) \quad \text{.....(12)}$$

$$\dot{\hat{x}}_l(t) = -\kappa_x(\varphi_1 + \varphi_2) \quad \text{.....(13)}$$

$$\dot{\hat{\Delta}}(t) = -\kappa_\Delta(\varphi_1 + \varphi_2)|\varphi_1 + \varphi_2|^{\frac{1}{\gamma}-1} \quad \text{.....(14)}$$

where

$$\varphi_1 = u(0,t) - \hat{u}(0,t) + c\ln\left(\frac{k + \hat{p}(0,t)}{k + p(0,t)}\right) \quad \text{.....(15)}$$

$$\varphi_1 = u(L,t) - \hat{u}(L,t) + c\ln\left(\frac{k + p(L,t)}{k + \hat{p}(L,t)}\right) \quad \text{.....(16)}$$

and $\kappa_u, \kappa_x, \kappa_\Delta$ and γ are strictly positive constants. Unfortunately there are no convergence proofs for any of the update laws, but they have been tested with numerous nominal simulations and never converged to wrong values. Note that it is not possible to estimate both roughness and the leak parameters concurrently in a single observer since adapting the roughness during the occurrence of a leakage would corrupt the leak estimates. This can be easily solved by running two observers simultaneously where one observer adapts roughness and the other observer estimates the leak parameters. The time scale of wax deposition and other factors which may affect the roughness of the pipeline are very slow compared with the effect of a leakage. So by setting the roughness estimated with the first observer to the observer used for leak detection once a day for instance, concurrent estimation of roughness and leak parameters is possible.

Measurements of the temperature *T(x,t)* is only available at the inlet of the model, i.e. only *T(0,t)* is available. This temperature is set directly to the inlet of the observer.

$$\hat{T}(0,t) = T(0,t) \quad \text{.....(17)}$$

4 Simulation results

A comprehensive simulation study has been conducted as part of a Master thesis at the Norwegian University of Science and Technology (NTNU). A few chosen results from this thesis are presented in this section. The observers are in all cases initialized with the same values as the model and temperature dynamics is turned on during all simulations.

In **Table 1** a straight, horizontal pipeline is defined, and the tuning of the corresponding observer is presented in **Table 4**. This observer is set to monitor the pipeline with the boundaries seen in **Fig. 2**. The leak occurs after one minute, simultaneously as the boundaries start to vary. This is supposed to resemble the effect which can be caused by controlling chokes at inlet and outlet. **Fig. 4** shows the estimated leak parameters. The effect of the sinusoidal boundary conditions is clearly visible, and none of the estimates converge to a certain value. But still it is possible to narrow down to an area where the leak has occurred. Estimation of the roughness was conducted prior to the leakage and then turned off so it would not interfere with the estimates of the leak parameters. A plot of the estimated roughness for this case can be seen in **Fig. 3**.

In **Table 2** parameters for a straight, horizontal pipeline carrying gas are presented. An OLGA observer was constructed to monitor this model and its tuning can be seen in **Table 5**. The estimates in **Fig. 5** show that it is possible to quantify and locate a leakage during stationary gas flow. The estimated friction is presented in **Fig. 6**.

In **Fig. 7** the boundaries for a model of an actual, long pipeline during start-up are showed. The profile for this pipeline is plotted in **Fig. 10**. The parameters for this pipeline are presented in **Table 3** and the tuning of the corresponding observer can be seen in **Table 6**. After 3 minutes a leak occurs which is detected by the observer. The estimated leak parameters are plotted in **Fig. 8**. Notice that the estimated C_v is lower than the actual. This is due to a modification done in the observer monitoring pipelines with inclinations. Instead of having ambient pressure in the observer at the position of the leak depending on the depth, it is set to 1 atm

even though the pipeline reaches depths down to 510 m. This modification has shown to be successful since the adaption of $\hat{C}_v$ is smoother. This can be explained by considering the following: while adapting $\hat{C}_v$, $\hat{x}_l$ is moving along the pipeline, possibly through an inclined part. With backpressure at each leak depending on the depth, the differential pressure over the leaks can vary vastly from one segment to another, which again will cause $\hat{C}_v$ to fluctuate when $\hat{x}_l$ passes through. This opposes the idea of estimating a constant parameter and is coped with by defining the ambient pressure in the observer as 1 atm at every leak.

The last case in this article involves biased measurements from the model and stationary boundary conditions. The pressure measurements from the inlet and outlet of the model are added a bias of -0.10 bar each. This error is coped with by estimating the roughness prior to the leakage, which magnitude is only 0.20 % of the mass rate at the inlet. The pipeline and tuning parameters are presented in **Table 3** and **Table 6**, respectively. The plot of estimates with and without adaption of roughness can be seen in **Fig. 9**.

5 Conclusions

The adaptive Luenberger-type observer presented in this article uses OLGA as its computational fluid dynamics simulator which is a state of the art simulator for one-, two- and three-phase flow. The OLGA observer is manipulated through Matlab which make it possible to make use of output injection in form of boundary conditions, control the magnitude and position of the estimated leakage and adapt roughness to compensate for model errors and biased measurements. The OLGA observer has numerous advantages over its predecessor, i.e. the observer constructed with Matlab in Aamo et al.[1], among which the incorporation of temperature dynamics, the support for pipelines with difference in altitude and that it is widely used by oil companies are the most important ones. It has also proved to work with time-varying boundary conditions for pipelines carrying oil.

Acknowledgements

We gratefully acknowledge the support from the Gas Technology Center at NTNU, Statoil, and the Norwegian Research Council.

Nomenclature

c	Speed of sound in the fluid, [L/t], m/s
C_d	Discharge coefficient of leakage, [-]
C_v	Valve constant for leak in the model, [L^2], m^2
$\hat{C}_v$	Valve constant for leak in the observer, [L^2], m^2
D_l	Diameter of leak opening, [L], m
$\hat{\Delta}$	Estimated factor which is used for adaption of roughness, [-]
γ	Tuning coefficient in update law for leak position, [-]
k_0	Tuning constant for the output injection at the outlet, [-]
k_L	Tuning constant for the output injection at the inlet, [-]
κ_Δ	Tuning coefficient in update law for roughness, [-]
κ_u	Tuning coefficient in update law for leak magnitude, [-]
κ_x	Tuning coefficient in update law for leak position, [-]
L	Length of pipeline, [L], m
p	Pressure in the model, [m/Lt^2], bara
$\hat{p}$	Pressure in the observer, [m/Lt^2], bara
p_{amb}	Ambient pressure, [m/Lt^2], atm
ρ	Density of the fluid in the model, [m/L^3], kg/m^3
ρ_l	Density of the fluid at the point of leak [m/L^3], kg/m^3
T	Temperature in model, [T], K
$\hat{T}$	Temperature in observer, [T], K
u	Velocity of fluid in the model, [L/t], m/s
$\hat{u}$	Velocity of fluid in the observer, [L/t], m/s
u_s	Control signal used to govern the leak opening in the model, [-]
$\hat{u}_s$	Estimated control signal used to govern the leak opening in the observer, [-]
w_l	Magnitude of leak, [m/t], kg/s
x_l	Actual leak position, [L], m
$\hat{x}_l$	Estimated leak position, [L], m

References

1. Aamo, O.M., Salvesen, J. and Foss, B.A.: *Observer design using boundary injections for pipeline monitoring and leak detection*, presented at the Adchem 2006 conference, Gamado, Brazil, April 2-5, 2006.
2. Nieckele, A.O., Brage, A.M.B. and Azevedo L.F.A.: *Transient pig motion through gas and liquid pipelines*, Journal of Energy Resources Technology, vol. **123**. no. 4, 2001.

SI Metric Conversion Factors

bar	×	1.0*	E+05	=	Pa
ft	×	3.048*	E-01	=	m
ft^2	×	9.290 304*	E-02	=	m^2
ft^3	×	2.831 685	E-02	=	m^3
°F		(°F+459.67)/1.8		=	K
lbm	×	4.535 924	E-01	=	kg

*Conversion factor is exact.

Table 1: Parameters for a straight, horizontal pipeline carrying oil.

Parameter	Value	Unit
ρ_{ref}	872	kg/m^3
c	1169	m/s
D	20	in
L	5100	m
N_{sec}	52	-
$p(0,L)$	50	bara
p_{amb}	1	atm
p_{ref}	50	bara
Roughness	1×10^{-5}	m
$T(0,0)$	343	K
$T(0,L)$	298	K
T_{amb}	277	K
$w(0,0)$	350	kg/s

Table 2: Parameters for a straight, horizontal pipeline carrying gas.

Parameter	Value	Unit
ρ_{ref}	100	kg/m^3
c	308	m/s
D	20	in
L	5100	m
N_{sec}	52	-
$p(0,L)$	50	bara
p_{amb}	1	atm
p_{ref}	110	bara
Roughness	1×10^{-5}	m
$T(0,0)$	343	K
$T(0,L)$	298	K
T_{amb}	277	K
$w(0,0)$	50	kg/s

Table 3: Parameters for a pipeline with inclinations carrying oil.

Parameter	Value	Unit
ρ_{ref}	872	kg/m^3
c	1169	m/s
D	12.5	in
L	86460	m
N_{sec}	100	-
$p(0,L)$	3.29	bara
p_{ref}	33	bara
Roughness	1.05×10^{-3}	m
$T(0,0)$	318.9	K
$T(0,L)$	280.8	K
T_{amb}	280.0-280.5	K
$w(0,0)$	100.6	kg/s

Table 4: Tuning of the observer corresponding with the pipeline defined in Table 1.

Parameter	Value	Unit
κ_u	7×10^{-3}	-
κ_x	200	-
κ_Δ	100	-
γ	2.5	-
k_0	0	-
k_L	0	-

Table 5: Tuning of the observer corresponding with the pipeline defined in Table 2

Parameter	Value	Unit
κ_u	7×10^{-2}	-
κ_x	100	-
κ_Δ	0.2	-
γ	2.5	-
k_0	0	-
k_L	0	-

Table 6: Tuning for the observer corresponding with the pipeline defined in Table 3

Parameter	Value	Unit
κ_u	7×10^{-3}	-
κ_x	1500	-
κ_Δ	0.5	-
γ	2	-
k_0	0	-
k_L	0	-

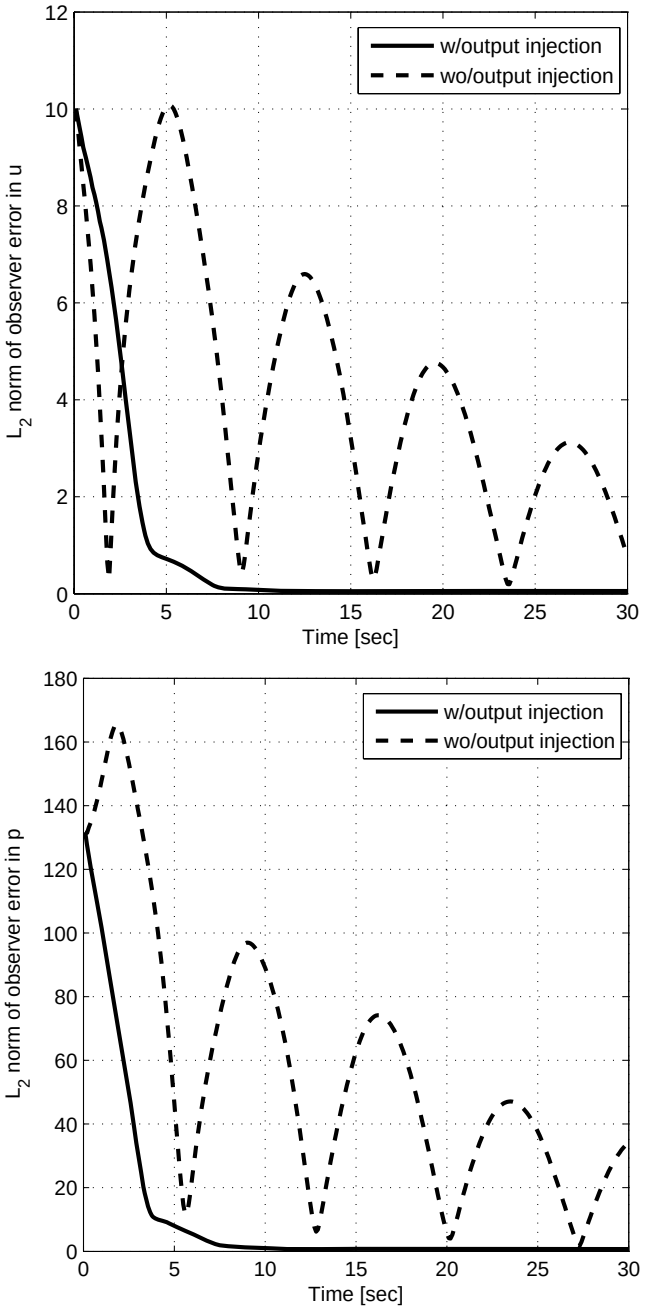

Fig. 1. Observer error with and without output injection.

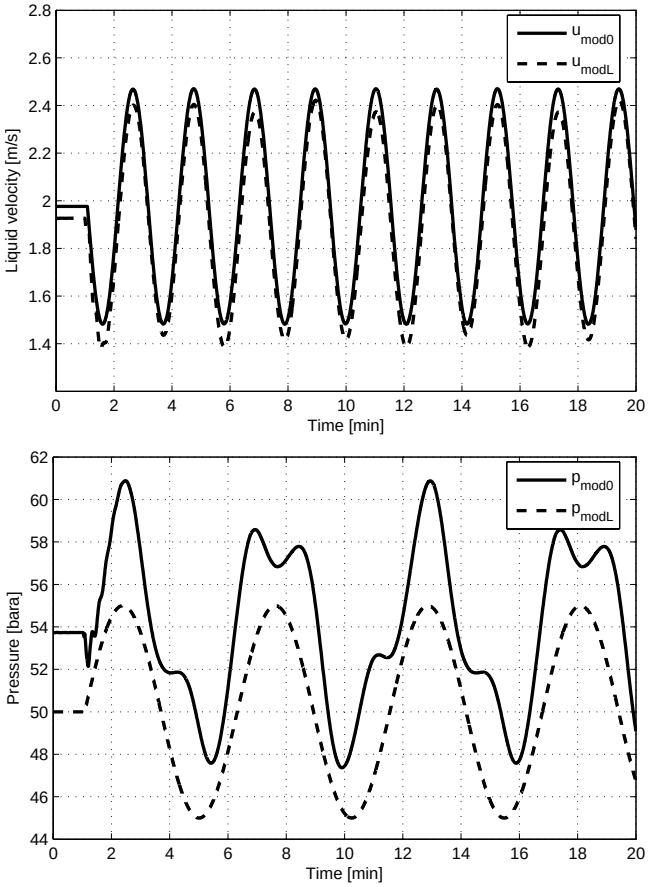

Fig. 2. Sinusoidal varying boundaries for straight horizontal pipeline carrying oil.

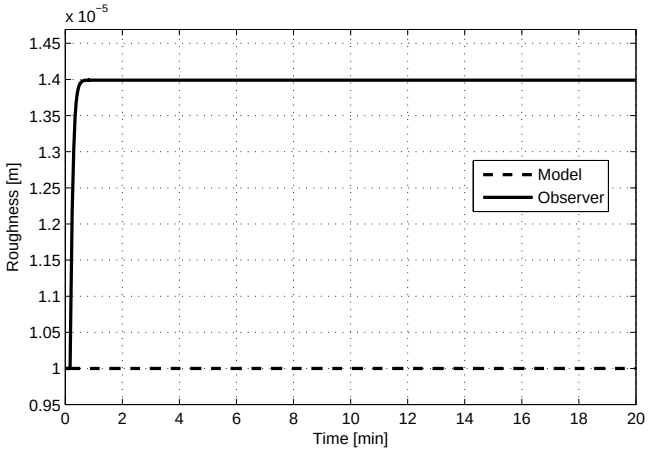

Fig. 3. The estimated roughness in a straight horizontal pipeline carrying oil. Adaption is turned off after 1 minute.

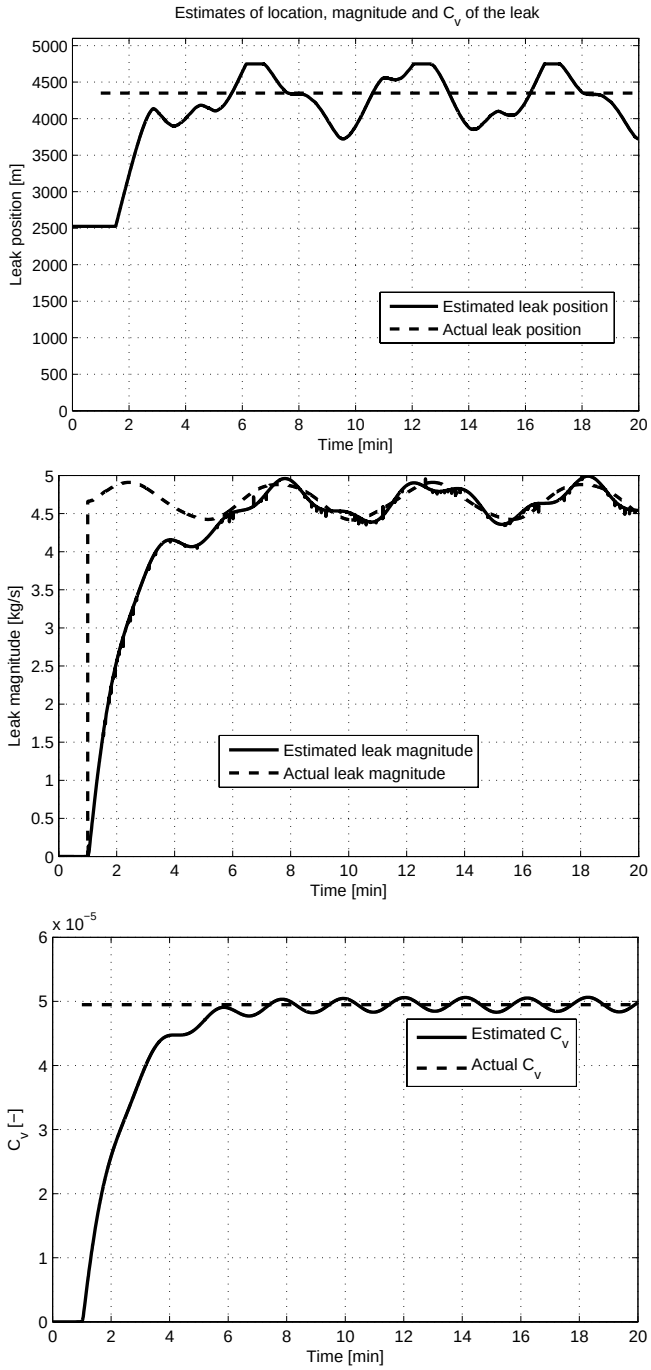

Fig. 4. Estimates for a leak at 4350 m in a 5100 m long pipeline carrying oil.

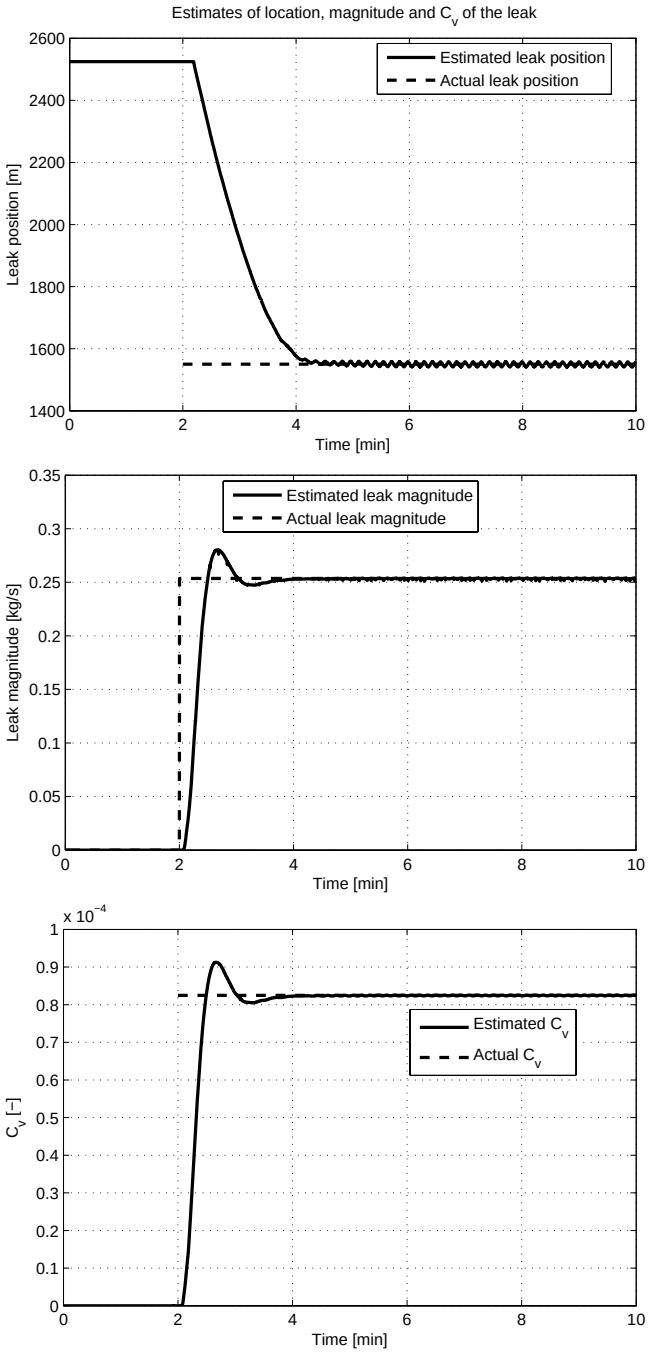

Fig. 5. Estimates for a leak at 1550 m in a 5100 m long pipeline carrying gas.

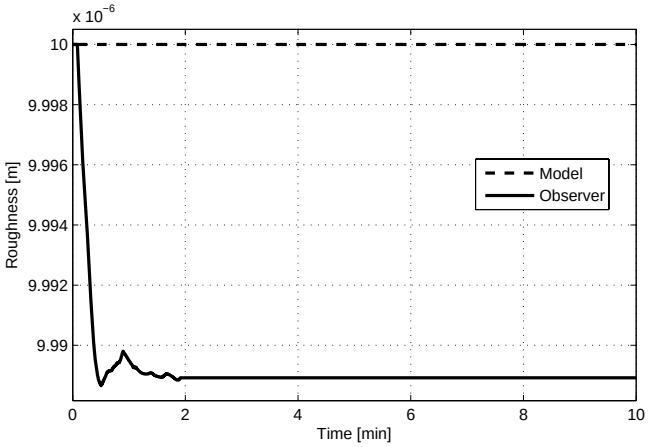

Fig. 6. The estimated roughness in a straight horizontal pipeline carrying gas. Adaption is turned off after 2 minutes.

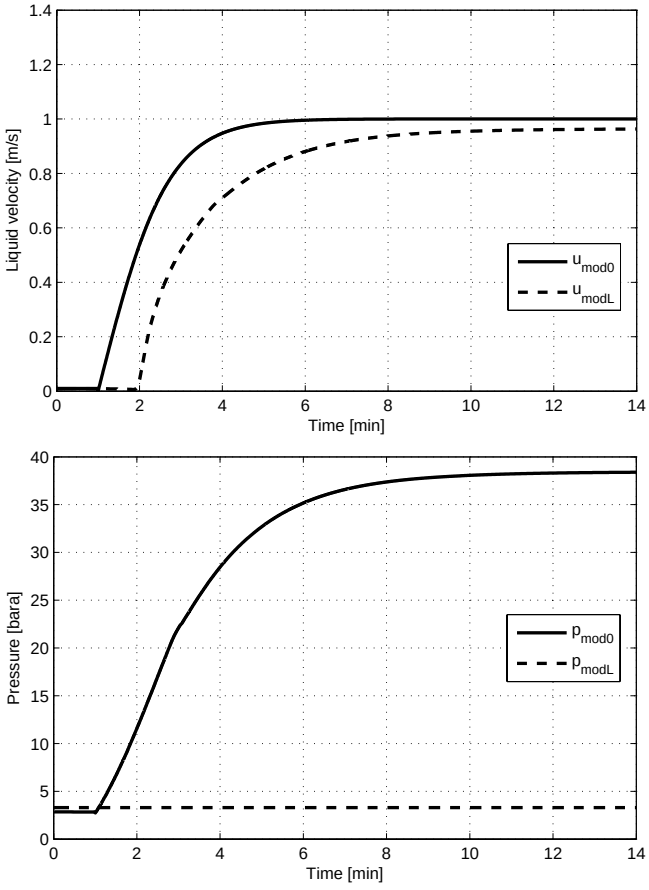

Fig. 7. The boundaries of the model during start up with a long pipeline with inclinations carrying oil.

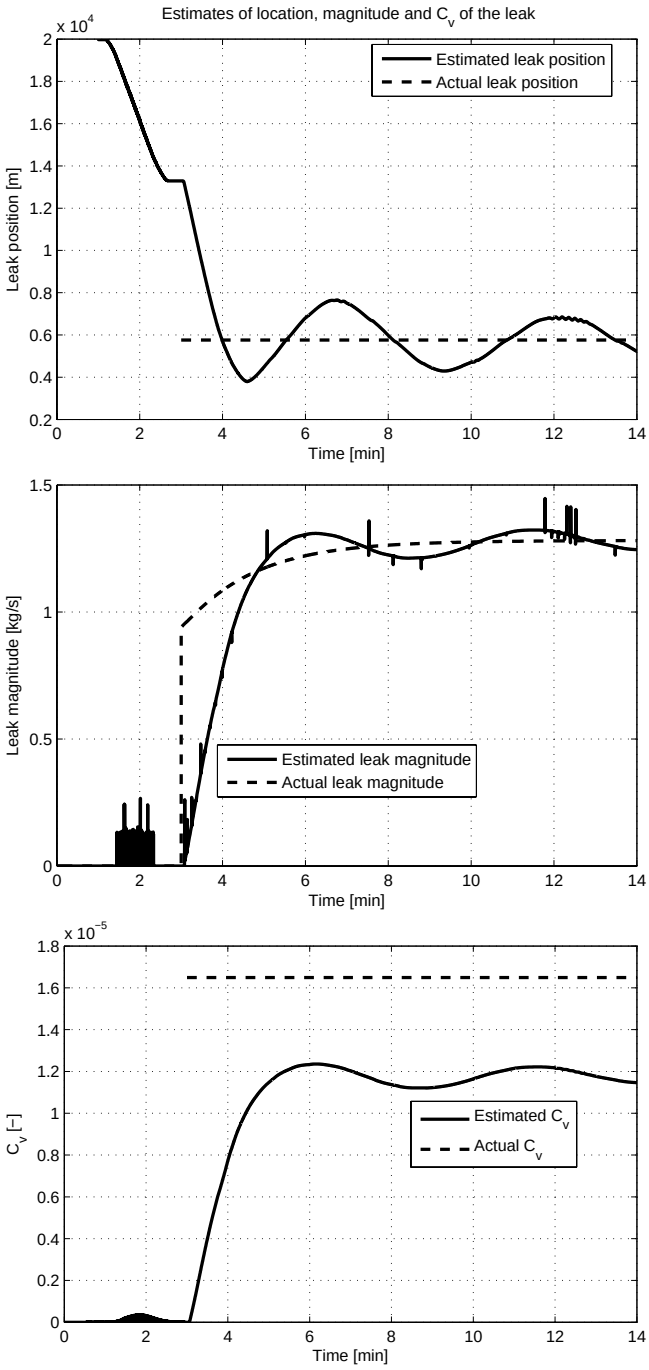

Fig. 8. Estimates for a leak at 5758 m with a long pipeline with inclinations carrying oil. The leakage occurs during start-up.

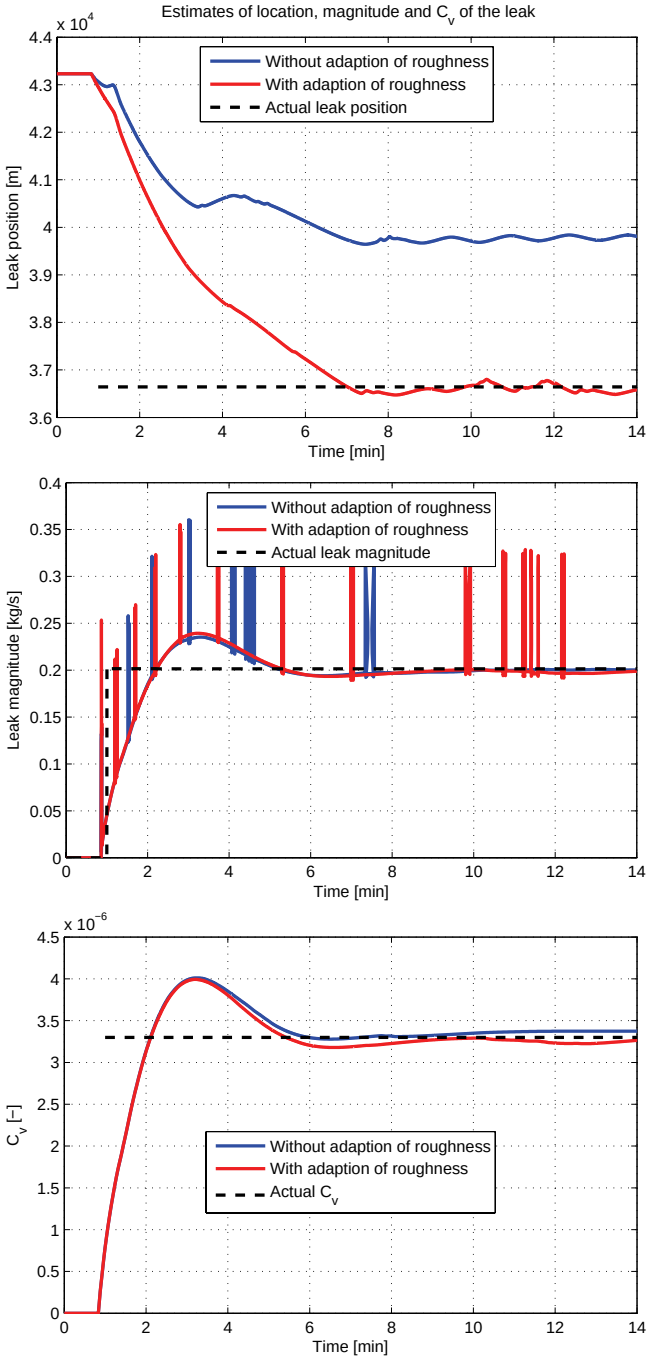

Fig. 9. Estimates with stationary boundaries and a leak occurring at 36643 m. The pressure measurements have a slight bias witch is compensated for by adaption of roughness. The pipeline carries oil and has inclinations.

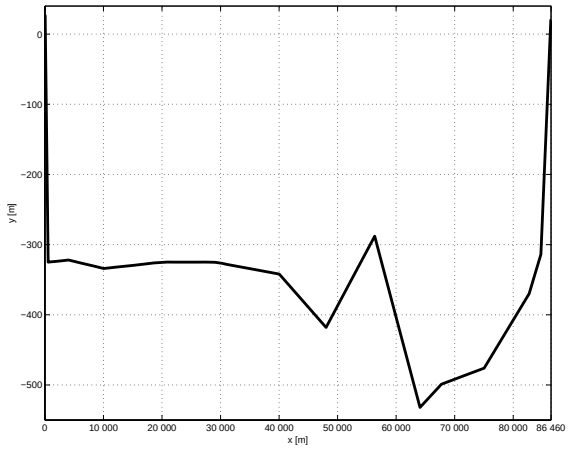

Fig. 10. Pipeline profile for the long pipeline with difference in altitude.